THE ROLE OF CD73 IN GLIOBLASTOMA PATHOGENESIS AND ANTI-GLIOBLASTOMA IMMUNE RESPONSE

A Dissertation

Presented to the Faculty of the Graduate School

of Cornell University

in Partial Fulfillment of the Requirements for the Degree of

Doctor of Philosophy

by

Angela Yan

May 2019

THE ROLE OF CD73 IN GLIOBLASTOMA PATHOGENESIS AND ANTI-GLIOBLASTOMA IMMUNE RESPONSE

Angela Yan, Ph.D.

Cornell University 2019

CD73 is a key enzyme in extracellular ATP metabolism; it converts AMP to extracellular adenosine. CD73 is involved in many cellular functions, including cell adhesion, cell proliferation, tumor invasion, and angiogenesis. Because of its enzymatic activity, CD73 is also a key immune regulator. CD73-generated extracellular adenosine signals through the A_{2A} adenosine receptor (AR) on leukocytes to attenuate inflammation and restore immune homeostasis. Because of these properties, CD73 is used by tumor cells to promote their pathogenesis and attenuate the host anti-tumor immune response. In this dissertation, we investigated the role of CD73 in glioblastoma (GB) pathogenesis and anti-GB immune response.

We implanted mouse GB cells in wild type (WT) and $CD73^{-/-}$ mice. We found that GB-bearing $CD73^{-/-}$ mice had reduced tumor size and invasiveness and decreased tumor vessel density compared with GB-bearing WT mice. To investigate whether host CD73 promoted GB invasiveness, we generated the CD73-FLK mice from the $CD73^{-/-}$ mice by enforcing CD73 expression on endothelial cells. GB-bearing CD73-FLK mice had the most invasive tumors compared with GB-bearing WT and $CD73^{-/-}$ mice, suggesting that the limited host CD73 on endothelial cells increased GB invasiveness. We also found a 20-fold upregulation of the A_{2B} AR in GB, which is rarely expressed in the central nervous system under physiological conditions and only upregulated during pathological conditions. Inhibition of A_{2B} AR signaling decreased the permeability glycoprotein (P-gp) and the multidrug resistance-associated protein 1

(MRP1) expression on mouse GB cells and made GB cells more susceptible to temozolomide-induced cell death. Additionally, we found that GB-bearing $CD73^{-/-}$ mice mounted a stronger inflammatory response to GB than GB-bearing WT mice. Compared with GB-bearing WT mice, GB-bearing $CD73^{-/-}$ mice had increased anti-inflammatory cytokine IL-10 and reduced pro-inflammatory cytokines TNF-α and IL-1β. Further, GB-infiltrating regulatory T cells and M2 microglia/macrophages were reduced in GB-bearing $CD73^{-/-}$ mice, whereas GB-infiltrating $CD8^{+}$ T cells were increased.

Together, these findings suggest that CD73 is used by GB to promote its pathogenesis through increasing GB angiogenesis, invasion, and chemoresistance. Our data also suggest that GB evades the host immune response by using CD73 to attenuate inflammatory responses. Therefore, targeting the CD73-AR axis presents great potentials for future GB therapeutic interventions.

BIOGRAPHICAL SKETCH

Angela attended National Hsinchu Girls' Senior High School in Hsinchu, Taiwan and earned a Bachelor of Science degree in microbiology and cell science at University of Florida in Gainesville, Florida. She entered the Biological and Biomedical Sciences Graduate Program at Cornell University in Ithaca, New York to pursue a Ph.D. degree in the field of immunology and infectious disease.

ACKNOWLEDGEMENTS

I would like to express my sincere gratitude to my advisor Dr. Margaret Bynoe for her guidance, motivation, enthusiasm, and for her continuous support throughout my time at Cornell. I am especially grateful for the time and energy she put into training and supervising me through this entire process. She truly is an exceptional mentor who cared for her students on both a professional and personal level. Without her guidance and support, this dissertation would not have been possible.

In addition to my advisor, I would like to thank the members of my Special Committee: Dr. Avery August, Dr. Brian Rudd, and Dr. Ted Clark, not only for their time but also for their insightful comments and intellectual contributions to my development as a scientist.

My sincere thanks also goes to our collaborators Dr. Linda Thompson, Dr. Andrew Miller, and Dr. Peter Canoll, who provided valuable comments and insights towards improving our manuscript.

A sincere thank you goes to Kate Kallal for her diligent proofreading of this dissertation.

I am also grateful to all the past and current members of the Bynoe lab for creating a fun and friendly work environment. Special thanks goes to Sudie Robinson, Dr. Luisa Torres, Dr. Dogeun Kim, and Dr. Leon Toussaint for all their help and support.

I would also like to thank Dr. Lu Huang for all his help and great advice and for being such a great friend.

Last, but not least, I would like to say a heartfelt thank you to all my friends and family. I am grateful for my parents for encouraging me to follow my dreams and for their

never-ending love and support. I would like to thank Szu-Yi Yang for helping me through the hard times in life and for always being there for me. I would also like to thank Po-Ya Hsu for always believing in me, cheering me on, and always being there for me through thick and thin.

TABLE OF CONTENTS

CHAPTER 1

Introduction

Significance

Glioblastoma multiforme (GB) is the most aggressive primary malignant brain tumor that affects humans. Current standard treatments for GB include surgical resection, chemotherapy with temozolomide (TMZ), and radiation therapy. GB is highly invasive and often infiltrates the surrounding non-neoplastic brain tissue. This makes complete surgical removal difficult and sometimes impossible. Incomplete GB resection leads to recurrence and reduced overall survival. Additionally, because the tumor is located in the central nervous system (CNS), surgical removal and chemotherapeutic drug delivery is extremely challenging. The blood-brain barrier (BBB) blocks chemotherapeutic drug delivery to the brain, and GB is resistant to chemotherapy (1). Therefore, GB patients have a very poor prognosis, with a median survival time of 18 months even with treatment.

CD73 and extracellular adenosine have been implicated in many types of cancers (2) and are key regulators in attenuating the immune response during inflammatory conditions (3). This dissertation focuses on the mechanism by which CD73 and adenosine/adenosine receptor pathway contribute to GB pathogenesis by promoting its growth, invasiveness, and chemoresistance, or by modulating the host immune response to GB.

Glioblastoma Multiforme

Epidemiology and Etiology

GB occurs mostly in elderly people with a median age at diagnosis of 64 (4). 90% of GB develops de novo (primary GB), while less than 10% progresses from a lower grade astrocytoma (5), also known as secondary GB. Unlike primary GB,

secondary GB is prevalent in young patients (4). 68% of primary GB patients have a short clinical history (from first symptoms to histological diagnosis) of less than 3 months, while secondary GB patients often have years of clinical history (5). The signs and symptoms of GB patients often differ based on the tumor size, growth rate, and location in the brain. GB symptoms generally arise from necrosis of the brain tissue, increased intracranial pressure, and/or its location in specific regions of the brain, which result in reduced or loss of brain functions (6, 7). Necrosis of the brain tissue often leads to cognitive impairments, loss of vision, hearing problems, and/or personality changes caused by cognitive impairments. Other GB symptoms include headaches, nausea, vomiting, memory loss, speech difficulties, and seizures.

Although GB cells are highly heterogeneous, they mostly originate from astrocytes, neural stem cells, or oligodendrocyte precursor cells (4). The cause of GB is currently unclear. However, we know that only a small percentage of GB is associated with hereditary factors (8). It has also been shown that GB is associated with increased exposure to ionizing radiation (9), high dietary intake of sugar (10), and exposure to human cytomegalovirus infection (7). Studies involving the genetic mutations of GB have shown that GB from different patient samples possess many common genetic mutations. Between 47 and 69% of GB showed a loss of heterozygosity in chromosome 10q (11, 12), and 34% of GB had EGFR amplification, $p16^{INK4a}$ deletion, or PTEN mutation (12). Chromosome 10q has many tumor suppressor genes, including PTEN, and allelic loss of 10q is often associated with tumorigenesis.

Current Treatments and Challenges

Current standard treatment for GB is a combination of surgical resection, radiation therapy, and chemotherapy. Due to the invasive nature of GB, surgical

resection is challenging, and it often does not remove all tumor tissue, which leads to recurrence. Currently, the only chemotherapeutic drug available for GB is temozolomide (TMZ). TMZ is a small lipophilic alkylating agent prodrug, which delivers a methyl group to O^6-guanine and generates O^6-methylguanine (13). O^6-methylguanine pairs with thymine during replication and results in a mismatch (14). This O^6-methylguanine:thymine mismatch then leads to cell death. Unlike most chemotherapeutic drugs, TMZ is not completely blocked by the blood-brain barrier (BBB) because of its small size (194 Da) and lipophilic properties. However, some GB cells express O^6-methylguanine-DNA methyltransferase (MGMT), which repairs DNA mismatch in GB, making them resistant to TMZ (15, 16). Further, GB expresses multidrug resistance transporters, such as the permeability glycoprotein (P-gp) and the multidrug resistance-associated protein 1 (MRP1) (17). These transporters can actively pump out chemotherapeutic drugs and make GB chemoresistant. Although GB is resistant to TMZ, studies have shown that epigenetic silencing of MGMT through methylation of the cysteine-phosphate-guanine (CpG) island on MGMT promoter is associated with increased TMZ efficacy (1, 18). This allows us to identify TMZ-susceptible GB patients and perform treatments accordingly.

Novel therapeutics, such as treatment with bevacizumab, an anti-vascular endothelial growth factor A (VEGF-A) antibody, was approved by the FDA in 2009 for GB. However, even though it was effective in other cancers, including lung cancer (19) and ovarian cancer (20, 21), bevacizumab only slightly prolonged progression-free survival and had no effect on the overall survival rate of GB patients (22).

CD73 and Extracellular Adenosine

Ecto-5'-nucleotidase (CD73)

Ecto-5'-nucleotidase, also known as CD73, is a glycosyl phosphatidylinositol (GPI)-anchored surface enzyme on eukaryotic cells. In naïve animals, CD73 is expressed in various tissues, including the colon, kidney, brain, lung, liver, heart, and muscle (23). The C-terminus of CD73 creates a noncovalent link between its two subunits to maintain a homodimer form (24). An α helix connects the N and C-terminal domains of CD73, allowing CD73 to alternate between an open and a closed conformation (24, 25) (**Figure 1.1**). This change in conformation allows CD73 to induce substrate binding and release during catalytic reactions (25–28). CD73 catalyzes the final step of adenosine triphosphate (ATP) hydrolysis and converts adenosine monophosphate (AMP) into adenosine and an inorganic phosphate. This catalytic activity of CD73 makes it the predominant regulator of extracellular adenosine production. Besides its enzymatic activity, CD73 also acts as a costimulatory molecule in T cell activation (29–32). Furthermore, extracellular adenosine generated by CD73 is a potent immune regulator through adenosine receptor signaling. Because of its immunoregulatory properties, CD73 is a highly desirable target for modulating immune responses in cancers, autoimmune diseases, and infectious diseases.

Extracellular Adenosine

Adenosine is a purine nucleoside that regulates a wide array of host functions (33). During tissue damage, ATP is released into the extracellular space, then broken down into ADP and AMP by the surface enzyme ectonucleoside triphosphate diphosphohydrolase-1 (CD39) (**Figure 1.2**). AMP is further converted to adenosine by CD73 (**Figure 1.2**). Purine nucleosides are signaling molecules that sense and signal

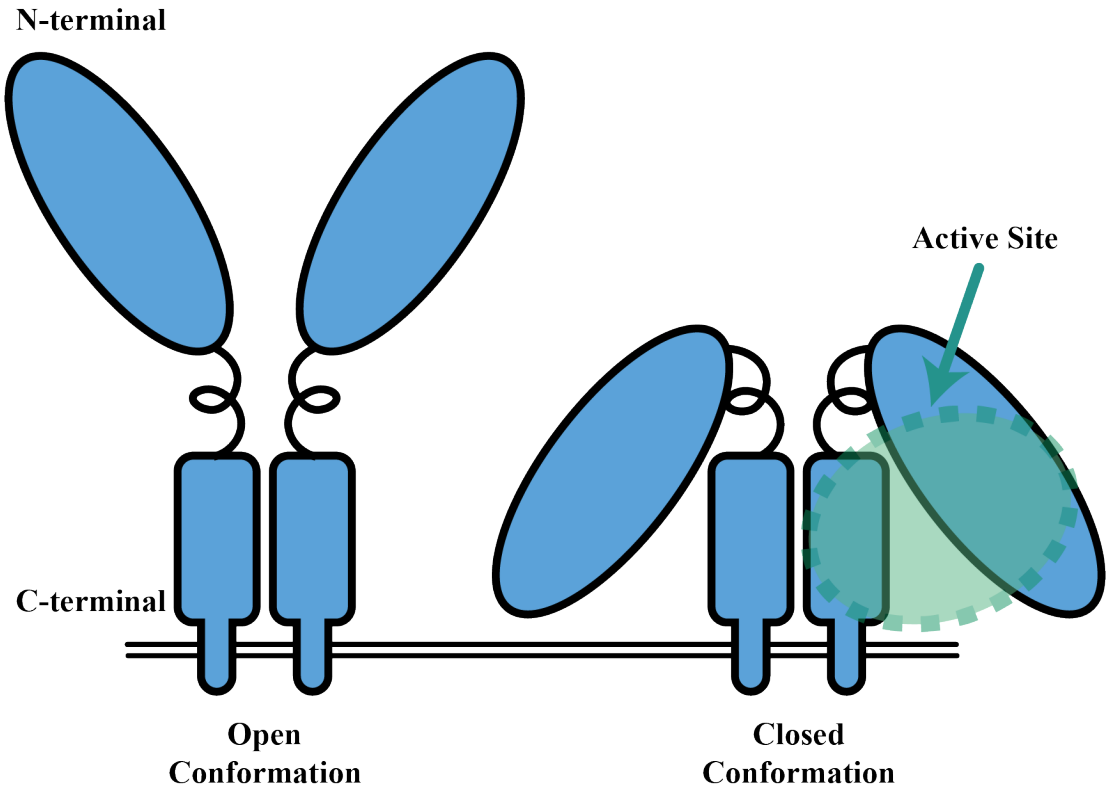

Figure 1.1 CD73 structure

An α helix connects the N and C-terminal domains of CD73, allowing CD73 to alternate between an open and a closed conformation. Transitioning between the open and the closed (active) conformation induce substrate binding and release during catalytic reactions.

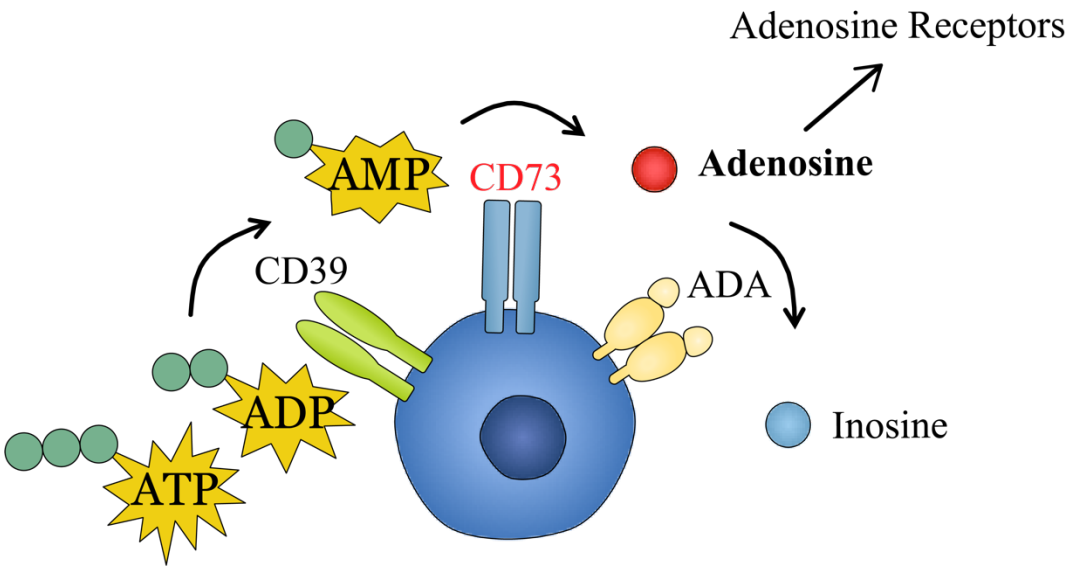

Figure 1.2 Schematic of ATP and adenosine metabolism.

Extracellular adenosine is produced from ATP released in the extracellular environment upon cell damage and is converted to ADP and AMP by CD39. AMP is further converted to adenosine by CD73. Extracellular adenosine binds to its receptors to mediate its function. Extracellular adenosine is rapidly degraded to inosine by adenosine deaminase (ADA).

danger, distress and/or tissue damage (34, 35). This is most evident in hypoxic and ischemic conditions in the heart, lungs, and central nervous system (CNS). Adenosine functions as a countermeasure, or safety signal, to counteract the ATP signal. It helps restrain harmful immune responses, recruits cells and molecules to the site of tissue damage, and induces various cellular factors that signal the termination and repair of injured tissue (35). Further, extracellular (CD73-generated) adenosine is a potent immune suppressor and has been shown to create an immunosuppressive tumor microenvironment (36). Adenosine mediates its effects via four G protein-coupled receptors, which are the A_1, A_{2A}, A_{2B} and A_3 adenosine receptors (ARs). ARs bind to adenosine with different affinities. The A_1 AR and A_{2A} AR have a high affinity for adenosine (70 nM and 150 nM respectively), while the A_{2B} and A_3 AR have a much lower affinity for adenosine (5100 nM and 6500 nM respectively) (37). Because of its wide-ranging effects, adenosine is used by many tumors to promote tumor malignancy through immune modulation, promotion of angiogenesis, and regulation of angiogenic and hypoxic genes, all of which are critical for tumor progression (38–41).

The Blood-Brain Barrier (BBB)

The BBB is a tightly regulated barrier separating the brain parenchyma from the blood circulation. It plays a critical role in protecting the brain parenchyma from neurotoxic factors. The BBB is composed of endothelial cells connected by tight junctions and adhesion molecules (42–47). The abluminal side of the endothelial cell layer is surrounded by the basement membrane, which is made up of extracellular matrix proteins secreted by endothelial cells and adjacent astrocytes (48) (**Figure 1.3**). Pericytes, also on the abluminal side, are closely associated with the endothelial layer. They help regulate endothelial junctions and BBB permeability (49–51). The outermost

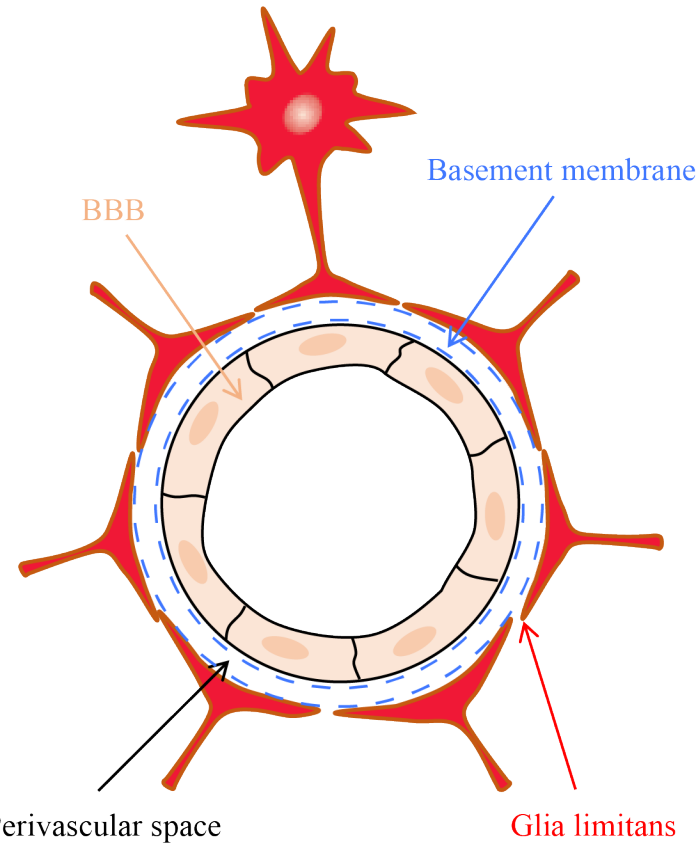

Figure 1.3 Schematic illustration of the BBB.

layer of the BBB is composed of astrocytic end-feet from neighboring astrocytes. The astrocytic end-feet form a second layer, abluminal to the endothelial layer, known as the glia limitans layer. This second layer creates the perivascular space between the endothelial layer and the glia limitans layer. Besides physically forming a barrier around the vessels, astrocytes also help maintain the BBB by regulating the electrical resistance and permeability of the BBB (52). They also secrete factors to regulate interactions between endothelial cells and pericytes (53).

Besides functioning as a physical barrier, the endothelial cells also express selective drug transporters that regulate brain parenchyma molecule influx and efflux. Many different drug transporters are expressed on the BBB, including the P-gp (MDR1/ABCB1), the breast-cancer-resistance protein (BCRP/ABCG2), and the MRP1 (ABCC1) (54, 55). Both P-gp and MRP1 are ATP-binding cassette transporters (ABC transporters), which use energy generated from ATP binding and hydrolysis to actively transport drugs out of the brain parenchyma (54, 55). Interestingly, P-gp and MRP1 are also highly expressed on GB, and they promote GB chemoresistance by actively pumping out chemotherapeutic drugs (56–58). However, because damage or inflammation in the CNS may have detrimental effects, it is critical for the BBB to restrict neurotoxic factors from entering the brain parenchyma. Unavoidably, this makes therapeutic drug delivery extremely difficult and hinders treatment for many CNS diseases. For example, diseases such as the Alzheimer's disease, Parkinson's disease, epilepsy, and brain tumors, can all benefit from having efficient drug delivery across the BBB to improve current treatments (54). In GB, the BBB in GB is not intact because its vessels are highly proliferative and often lack the proper CNS vessel integrity. Although studies have shown BBB disruption in GB (59, 60), clinically, therapeutic drugs cannot efficiently penetrate the tumor (61). For this reason, many studies are

exploring new ways of delivering drugs to GB (62).

Regulation of BBB Permeability by Adenosine Signaling

CD73 is naturally expressed in the central nervous system (CNS). Cells in the CNS, including astrocytes, microglia, pericytes and neurons, generate extracellular adenosine under normal physiological conditions to regulate sleep, arousal, neuroprotection, learning and memory, cerebral blood circulation, and neural transmission (43). Additionally, although endothelial cells forming the BBB in the CNS express low CD73 under physiological conditions, we demonstrated that adenosine signaling regulates BBB permeability (43). We previously showed that $CD73^{-/-}$ mice were resistant to experimental autoimmune encephalomyelitis (EAE) (63). Multiple sclerosis and EAE (its animal model) are debilitating, neuroinflammatory disorders of the CNS that are mediated by lymphocyte entry into the CNS. In addition to extracellular adenosine's role in down-modulating inflammation, it also has the potential to stimulate the migration of immune cells. We showed that extracellular adenosine promoted lymphocyte migration into the CNS through the induction of the chemokine/adhesion molecule CX3CL1 at the choroid plexus (64). Additionally, CD73 was required for efficient lymphocyte migration into the CNS during EAE (38). We showed that immune cells were unable to efficiently breach the BBB and cause EAE in the absence of CD73 (38). Moreover, broad spectrum AR antagonists, such as caffeine, or A_{2A} AR specific antagonists protected wild type (WT) mice from EAE development by preventing lymphocyte infiltration in the brain and spinal cord (63). Therefore, to define the role of the A_{2A} AR in EAE development, our lab induced EAE in the $A_{2A}AR^{-/-}$ mice and found that they developed a more severe form of EAE compared to WT mice (38). This increased severity in EAE was a result of the increased pro-inflammatory response mounted by $A_{2A}AR^{-/-}$ leukocytes, which overcame any

inhibition of leukocyte infiltration provided by the lack of A_{2A} AR signaling within the CNS (38).

Not only did we show that the CD73-AR axis regulates leukocyte migration into the CNS, we also demonstrated that the FDA-approved selective A_{2A} AR agonist Lexiscan (Regadenoson) increased the BBB permeability in murine models. We showed that A_{2A} AR signaling temporally and dose-dependently increased the BBB permeability (65) (**Figure 1.4**). We also showed that the broad-spectrum AR agonist NECA increased anti-β-amyloid antibody delivery into the CNS in a transgenic mouse model of Alzheimer's disease (65). These findings suggest that BBB permeability can be modulated in vivo through activation or inhibition of AR signaling to promote therapeutic compound delivery into the CNS. To better understand the mechanism behind A_{2A} AR signaling at the BBB, we investigated whether P-gp was regulated through A_{2A} AR signaling. We found that the multidrug resistance transporter P-gp expressed on brain endothelial cells blocked drug delivery to the brain parenchyma (66). Further, we found that activation of the A_{2A} AR with Lexiscan rapidly increased the BBB permeability and that this increased permeability was reversible (67). Together, these studies suggest that modulating the CD73-AR axis has the potential to block harmful immune cells entry into the brain and to deliver chemotherapeutic agents to treat diseases ranging from brain tumors to Alzheimer's disease.

CD73 and Its Implications in Cancer

Besides regulating the BBB, CD73 is also involved in immune modulation, promotion of angiogenesis, and regulation of angiogenic and hypoxic genes (38–41). Because of these properties, CD73 and adenosine have been implicated in many cancers, including breast cancer, bladder cancer, leukemia, glioma, melanoma, ovarian cancer,

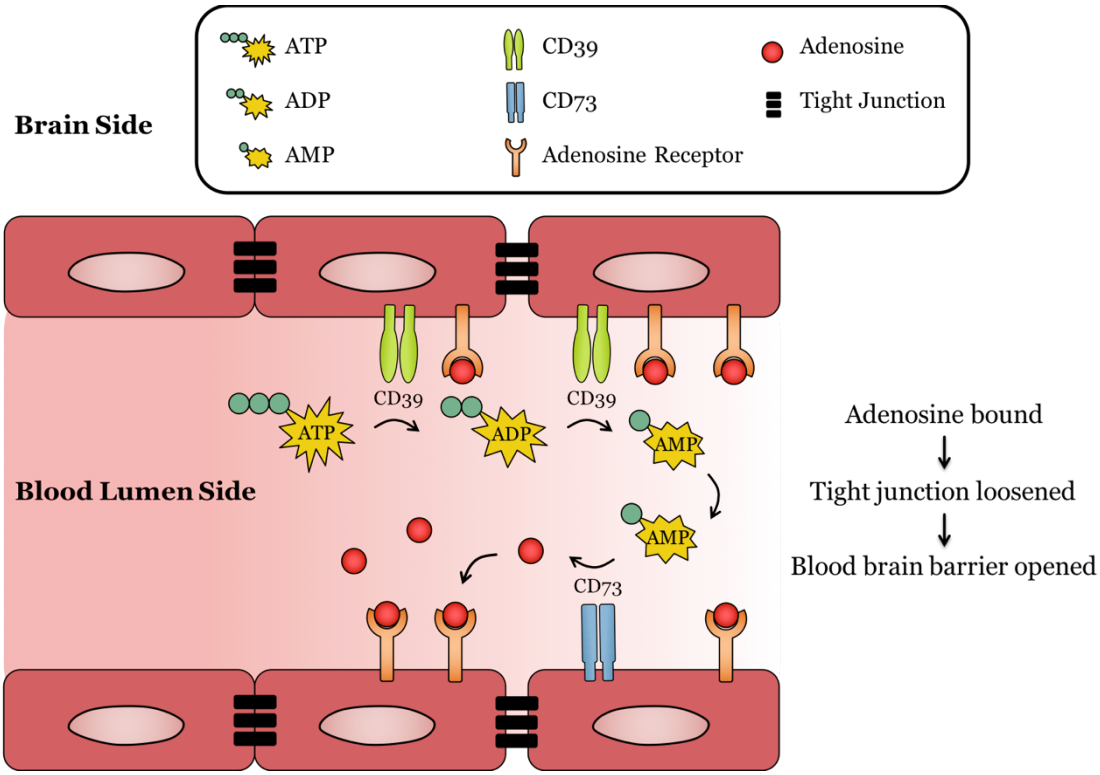

Figure 1.4 Adenosine modulation of BBB permeability.

Endothelial cells lining the brain vasculature express ARs, CD39, and CD73. In the presence of cell stress/inflammation or tissue damage, ATP is released and is rapidly converted to ADP and AMP by CD39; AMP is converted to adenosine by CD73. Adenosine binds to its receptor/s (A_1 or A_{2A}) on BBB endothelial cells, the activation of which induces reorganization of the actin cytoskeleton in BBB endothelial cells, resulting in tight and adherent junction disassembly and increasing paracellular permeability.

thyroid cancer, esophageal cancer, gastric cancer, colon cancer, and prostate cancer (68–77). CD73 expression is used as a diagnostic parameter in papillary thyroid cancer and is associated with increased metastasis in breast cancer and melanoma (78). CD73 promotes cancer cell proliferation and migration (78–80). In breast cancer, CD73 increases tumor metastasis and promotes angiogenesis (81–84). It has also been shown that melanoma in $CD73^{-/-}$ mice grew slower and was less malignant (85). Therefore, CD73 is a highly desirable target for cancer therapy, and inhibiting CD73 has the potential to improve treatment for multiple types of cancers.

CD73 and Adenosine Regulation of Cancer Immune Response

Adenosine Regulates Leukocyte Response Through Adenosine Receptor Signaling

Adenosine was first implicated in the regulation of anti-tumor immunity by the Blay group in 1994 (86–91). They showed that extracellular adenosine concentration is 10 to 20 times higher in tumor microenvironments compared to healthy tissues (90). This high extracellular adenosine concentration inhibited T cell and NK cell anti-tumor immune responses (86, 88, 89). It was later demonstrated by multiple groups that adenosine signaling through the A_{2A} AR is the main pathway that regulates the attenuation of inflammation (92–94). The A_{2A} AR is expressed on most leukocytes (95), including monocytes (96), macrophages (97), dendritic cells (98, 99), mast cells (100), neutrophils (100–102), lymphocytes (103–105), NK cells (106), and NKT cells (107). It is also found on endothelial and epithelial cells (95). Therefore, extracellular adenosine signaling through the A_{2A} AR regulates a wide range of leukocytes and elicits a broad anti-inflammatory effect.

ARs are G protein-coupled receptors and are composed of seven transmembrane

α-helices with an extracellular N-terminus and an intracellular C-terminus. The A_1 and A_3 ARs primarily couple with the G_i protein and the A_{2A} and A_{2B} AR primarily couple with the G_s protein. Adenosine binding to its receptor results in a conformational change in ARs. This change induces an interaction between the receptor and its G protein. The G_i protein-coupled A_1 and A_3 ARs inhibit downstream adenylate cyclase activity and reduce cyclic-AMP (cAMP) production. Conversely, the G_s protein-coupled A_{2A} and A_{2B} ARs excite downstream adenylate cyclase and increase cAMP production. cAMP acts as a secondary messenger that activates protein kinase A (PKA), which will then phosphorylates the cAMP response element binding protein (CREB) and regulates gene expression.

Depending on where the A_{2A} AR is expressed, A_{2A} AR signaling attenuates inflammation through different pathways. In macrophages, activation of the A_{2A} AR leads to increased cAMP, which activates PKA. Activated PKA phosphorylates CREB, which then leads to the transcription of the *CRBPβ* gene. Increased CRBPβ protein binds to the *IL10* gene promoter and increases macrophage IL-10 production (108). In regulatory T (Treg) cells, they express CD73 on their cell surface and generate extracellular adenosine, which acts through both the autocrine and the paracrine pathways. Activation of the A_{2A} AR on Treg cells upregulates their transcription factor Foxp3 and further enhances their ability to suppress inflammation (108). Without A_{2A} AR expression, the anti-inflammatory properties of Treg cells would be reduced (109). A_{2A} AR activation on effector T (Teff) cells is critical in regulating T cell activation. T cell receptor (TCR) signaling is required for Teff cell activation. When a TCR interacts with its antigen, a zeta chain of T cell receptor associated protein kinase 70 (ZAP70) is recruited and binds to the TCR. This TCR binding changes the conformation of ZAP70 and results in its phosphorylation (110). This then leads to activation of the downstream

transcription factor activator protein 1 (AP1) and activation of T effector cells. However, A_{2A} AR signaling in Teff cells inhibits ZAP70 phosphorylation; therefore, it inhibits TCR signaling and Teff cell activation. A_{2A} AR signaling leads to decreased Teff cell proliferation and decreased T helper 1 (T_H1), T_H2, and T_H17 lymphocyte development (108). Furthermore, A_{2A} AR signaling on Teff cells promotes cytotoxic T-lymphocyte-associated antigen 4 (CTLA4) and programmed cell death 1 (PD1) expression (108). All of these effects induced by A_{2A} AR signaling significantly dampen the inflammatory response.

While it is necessary to attenuate inflammation after clearing an infection to maintain immune homeostasis, this inhibitory effect is often used by cancer cells to evade the anti-tumor immune response. Understanding how CD73/adenosine signaling attenuates the anti-GB immune response will allow us to block or inhibit CD73/adenosine signaling in order to induce a stronger anti-GB immune response in GB patients.

Host Immune Response to GB and How GB Evades the Immune Response

Inflammation in the CNS

The CNS contains neuronal networks that are critical for survival and needs to be protected from excessive inflammation. Because the brain is enclosed by the skull, excessive leukocyte infiltration can cause swelling and an increase in intracranial pressure, damaging the CNS (111). Some pro-inflammatory molecules, including TNF-α and IL-1, induce neurotoxic activities in the CNS (112–114). Therefore, inflammation in the CNS can result in neuronal death. To protect the CNS from inflammation-derived neurodegeneration, CNS-infiltrating leukocytes are absent in normal physiological conditions.

Host Immune Response to GB

Chen and Mellan proposed the Cancer-Immunity Cycle, which is composed of seven sequential steps that lead to an effective immune response to cancer (115). First, cancer antigen must be released (step 1) and presented by antigen-presenting cells (APC) (step 2). Then, tumor-specific T cells need to be activated by APC (step 3) and travel to the tumor site (step 4). Finally, these T cells must infiltrate the tumor (step 5), recognize the tumor antigen-MHC complex (step 6), and elicit cytotoxic effector functions to remove the cancer cells (step 7). Killing the cancer cells will produces more cancer antigen for antigen presentation by APCs, which amplifies the subsequent 7-step cycle.

In GB, tumor antigen is often released through two main pathways. First, GB antigen is released from necrotic tumor cells. Necrosis almost always occurs in GB, and clinically, pseudopalisading necrosis is a GB diagnosis feature (116). Therefore, spontaneous necrotic cell death constantly releases tumor antigens into the tumor microenvironment. Second, GB therapeutic treatments, such as chemotherapy, radiotherapy, and surgical removal of the tumor, all lead to tumor-antigen release (117). These tumor antigens are then taken up by macrophages, microglia cells, or dendritic cells located in meninges, perivascular space, or the choroid plexus epithelium and stroma (118, 119). Cells in the brain perivascular space and meninges are able to sample antigens inside the cerebrospinal fluid (CSF) (117). Additionally, during CNS inflammation, APCs infiltrate the brain parenchyma (117), increasing tumor-antigen presentation to T cells.

Activated GB-specific T cells then travel to the CNS by two main routes. T cells travel to meningeal vessels and enter the brain parenchyma by crossing the subarachnoid

space (117). T cells also travel to the postcapillary venules, cross the BBB, enter the perivascular space formed by astrocytic end-feet, and then cross the glia limitans layer into the brain parenchyma (120).

In GB patients, 72.6% of newly diagnosed patient samples and 83.3% of recurrent patient samples showed tumor infiltrating lymphocytes (121). GB-infiltrating lymphocytes include $CD8^+$ T cells, $CD4^+$ T cells, and Treg cells. They make up about 17% of all GB-infiltrating leukocytes (122), while approximately 30% of all GB-infiltrating leukocytes are macrophages and microglia (123–125). Out of the GB-infiltrating lymphocytes, about 25% are $CD3^+$ T cells (122). Around 11% of GB-infiltrating T cells are $CD8^+$ T cells and 20% are $CD4^+$ T cells (125). Of the $CD4^+$ T cells, between 50 and 96% are positive for Foxp3, indicating that they are mostly Treg cells (122, 125).

GB-infiltrating T cells elicit different immune responses in GB. The main role of $CD8^+$ cytotoxic T cells in tumors is to recognize the tumor antigen-MHC I complex and induce cancer cell death through the release of granzyme B and perforin. $CD4^+$ T_H1 cells interact with the antigen-MHC II complex on local APCs and secrete immunomodulatory cytokines, such as IFN-γ and TNF-α, to activate macrophages and NK cells. On the other hand, $Foxp3^+$ Treg cells secrete IL-10 and TGF-β to suppress the inflammatory response to tumors. Whether the tumor escapes the host immune response is often determined by whether Teff cells successfully kill tumor cells. Because of the high $Foxp3^+$ Treg cell infiltration in GB, the cytotoxic T cell response to GB is often ineffective, and GB thrives under the highly attenuated immune microenvironment.

GB Immune Evasion Strategies

GB renders the anti-tumor immune response ineffective through multiple means.

One mechanism induces immune tolerance to GB through immune suppression by Treg cells. Most GB-infiltrating Treg cells are natural Treg cells (126), which are generated in the thymus and recruited to the GB site by the chemokine CCL2. Additionally, GB supports Treg cell expansion and survival through secretion of soluble factors that promote preferential Treg cell proliferation (127). Treg cells inhibit the immune response through production of anti-inflammatory cytokines, including IL-10 and TGFβ. Treg cells suppress $CD4^+$ and $CD8^+$ T cell activation and proliferation and reduce their inflammatory cytokine IL-2 and IFNγ production (128). Treg cells also express CD73 and generate extracellular adenosine to inhibit inflammation through A_{2A} AR signaling (108).

GB cells can also hijack the peripheral tolerance mechanism to eliminate GB-infiltrating T cells. This method of T cell elimination was first described in melanoma in 1993 (129, 130). The Fas receptor (Fas), also called Apo-1 or CD95, is a programmed cell death receptor that promotes apoptosis in self-reactive lymphocytes (131). Fas ligand (FasL) expression was found on melanoma cells and Fas^+ T cells were found in the microenvironment in $FasL^+$ melanoma (129). $FasL^+$ melanoma cells induced Fas^+ T cell apoptosis, and melanoma development was delayed in Fas-deficient mice (129). It was later found that, similar to melanoma, GB cells also express FasL, and apoptotic Fas^+ T cells were found in proximity to $FasL^+$ GB cells (132). Moreover, Fas^+ T cells in GB are 8 times more susceptible to apoptosis than Fas^- T cells (133), suggesting that the $FasL^+$ GB cells are inducing T cell apoptosis.

In addition to inducing T cell apoptosis through FasL, GB also induces apoptosis through indoleamine 2,3 dioxygenase 1 (IDO1). 90% of human GB expresses IDO1 (134), which is an enzyme that catabolizes the essential amino acid tryptophan into kynurenine. IDO1 expression in GB is negatively correlated with patient survival (135).

Tryptophan is critical for cell cycle progression in activated T cells (136). In the absence of tryptophan, the cell cycle of activated T cell halts at mid-G1 phase, and these cells become susceptible to apoptosis (136). Studies have also found that tryptophan metabolites suppress T cell proliferation and induces apoptosis independent of IDO1 (137, 138). Furthermore, GB-expressed IDO1 is required for Treg recruitment in GB (139). Overall, these studies showed that IDO1 expression on GB cells inhibited the anti-tumor immune response by inducing T cell apoptosis and promoting Treg cell recruitment.

Immune checkpoint molecules, such as CTLA-4 (CD152) and PD-1 (CD279)/PDL-1, are also used by GB to evade the immune response. CTLA-4 is expressed on T cells, and it competes with CD28 for the APC co-stimulatory molecules B7-1 (CD80) and B7-2 (CD86) (140). The ratio of CD28:B7 binding to CTLA-4:B7 binding on T cells determines whether they will become activated (140). CTLA-4 expression on T cells is negatively correlated with GB patient outcomes (141). Treatment with an anti-CTLA-4 antibody in a murine glioma model resulted in long-term survival in 80% of treated mice (142). Unlike CTLA-4, which competes for APC co-stimulatory molecules, PD-1 on activated lymphocytes binds to PDL-1 expressed on tumor cells or APCs (143). (144–146). This binding suppresses T cell activation and inhibits T cell cytotoxic functions (143–145). It also induces anti-inflammatory cytokine IL-10 production and inhibits the pro-inflammatory cytokine production of IFN-γ, IL-2, and TNFα (143–145). PDL-1 expression on glioma is strongly associated with World Health Organization (WHO) tumor grades, with a high PDL-1 expression in high grade GB and a low PDL-1 expression in low grade glioma (147). Whether GB directly induces lymphocyte CTLA-4 and PD-1 expression is currently unclear; however, CTLA-4 and PD-1/PDL-1 are key players in GB immune evasion.

Another major hurdle for the immune system to clear GB is myeloid-derived suppressor cells (MDSCs). Terminally differentiated myeloid cells, including macrophages, dendritic cells, and neutrophils, can become MDSCs in tumor environments (148). MDSCs suppress the anti-tumor immune response by producing anti-inflammatory cytokines, including TGFβ (149, 150), and inducing the activation and expansion of Treg cells (151, 152). They also secrete nitric oxide (NO) and reactive oxygen species (ROS) and suppress T cell functions through arginase activity (153). GB-associated microglia and macrophages are the most abundant cell types of all GB-infiltrating immune cells (154, 155), making them the dominant GB-infiltrating MDSCs. It has been shown that GB stem cells secrete periostin to recruit anti-inflammatory GB-associated macrophages (156). These GB-associated macrophages/microglia have reduced phagocytic activity (157) and increased production of IL-10 and TGFβ (157). They also downregulate the co-stimulatory molecules CD80 and CD86, limiting their ability to induce T cell activation (158). Overall, MDSCs help GB maintain an immune suppressive environment and further inactivate other GB-infiltrating leukocytes.

Current Immunotherapy and Challenges for GB Immunotherapy

Currently, immunotherapy against melanoma and non-small-cell lung cancer has shown remarkable results, successfully increasing patient survival (159–164). This was achieved mostly through the targeting of immune checkpoints using anti-CTLA-4 and anti-PD-1/PDL-1 antibodies (159–164). Unfortunately, the same result did not happen in GB patients. The PD-1 antibodies pembrolizumab and nivolumab did not show clinical efficacy in recurrent GB patients in two separate clinical studies (165, 166). Similarly, CheckMate-143 Phase I and III clinical trials using a nivolumab and ipilimumab (anti-CTLA-4 antibody) combination treatment in recurrent GB did not show improved overall patient survival compared with nivolumab treatment alone (167).

The Phase I clinical trial showed that nivolumab alone was well tolerated, while the toleration of the combination therapy with nivolumab and ipilimumab was dependent on the dose of ipilimumab (168). However, the Phase III clinical trial showed that nivolumab did not improve overall patient survival compared with approved bevacizumab (anti-VEGF-A antibody) treatment (169). Currently, clinical trials CheckMate-498 and CheckMate-548 using nivolumab in newly diagnosed GB patients are still ongoing.

One potential reason why PD-1 antibody therapy failed in recurrent GB patients is the BBB. Generally, only compounds smaller than 400-600 Da are able to cross the BBB, and cytokine-induced neutrophil chemoattractant-1 (7.8 kDa) was the largest compound found to cross the BBB through transmembrane diffusion (170). Because nivolumab has a calculated molecular mass of 146 kDa, it is plausible that it cannot cross the BBB to target GB-infiltrating PD-1^+ cells directly, and only targeting PD-1^+ cells in the periphery before they enter the CNS (171). This may dramatically decrease the efficacy of nivolumab in patients (172). Another possibility is that recurrent GBs are likely to contain a large pool of terminally differentiated T cells that were exhausted due to chronic exposure to GB antigens. Terminally differentiated exhausted T cells sometimes do not recover from PD-1:PDL-1 blockade (173); therefore, nivolumab treatment may not be ideal for recurrent GB.

Synthesis

The studies presented in this dissertation describe the role of host CD73 and the adenosine signaling pathway in GB pathogenesis and show the mechanism behind CD73 regulation of the host anti-tumor immune response. In **Chapter 2**, we demonstrate that host CD73 promotes GB pathogenesis using the GL261 syngeneic mouse model. In the absence of host CD73, GB size and invasiveness are reduced. We show that host CD73 promotes invasion by upregulating MMP9 along the tumor edge and inhibiting the MMP9 inhibitor TIMP1. Host CD73 also promotes GB angiogenesis. In the absence of host CD73, MMP2, VEGF, and α-dystroglycan are all upregulated, which results in increased glomeruloid vessels and reduced vessel density in GB-bearing $CD73^{-/-}$ mice. This suggests that host CD73 is required for promoting mother vessels division into smaller vessels. Furthermore, we demonstrate that blockade of A_{2B} AR signaling on mouse GL261 GB cells results in reduced chemoresistance to the chemotherapeutic drug temozolomide.

In **Chapter 3**, we demonstrate that host CD73 promotes GB immune evasion. We show that CD73 promotes anti-inflammatory microglia and macrophage GB-infiltration and cytokine CCL22 production. This leads to increased T regulatory cell recruitment to the CNS and further attenuates the anti-tumor immune response. Therefore, GB-bearing $CD73^{-/-}$ mice show an increase in $CD8^{+}$ T cell infiltration and a reduction in Treg cell recruitment. We also demonstrate that CD73 promotes leukocyte entry to the brain parenchyma by inducing them to cross the glia limitans layer formed by astrocyte end feet in GB-bearing mice.

In **Chapter 4**, we will summarize our findings, present our conclusions, and suggest future directions.

REFERENCES

1. Hegi ME, et al. (2005) *MGMT* Gene Silencing and Benefit from Temozolomide in Glioblastoma. *N Engl J Med* 352(10):997–1003.

2. Gao Z, Dong K, Zhang H (2014) The Roles of CD73 in Cancer. *Biomed Res Int* 2014:460654.

3. Antonioli L, Pacher P, Vizi E, Haskó G (2013) CD39 and CD73 in immunity and inflammation. *Trends Mol Med* 19(6):355–367.

4. Ostrom QT, et al. (2013) CBTRUS statistical report: Primary brain and central nervous system tumors diagnosed in the United States in 2006-2010. *Neuro Oncol* 15 Suppl 2:ii1--56.

5. Ohgaki H, Kleihues P (2007) Genetic pathways to primary and secondary glioblastoma. *Am J Pathol* 170(5):1445–1453.

6. Lakhan SE, Harle L (2009) Difficult diagnosis of brainstem glioblastoma multiforme in a woman: A case report and review of the literature. *J Med Case Rep* 3:1–3.

7. Lee J, et al. (2012) Morphological Characteristics of Brain Tumors Causing Seizures. *Arch Neurol* 67(3):336–342.

8. Schwartzbaum JA, Fisher JL, Aldape KD, Wrensch M (2006) Epidemiology and molecular pathology of glioma. *Nat Clin Pract Neurol* 2(9):494–503.

9. Prasad G, Haas-Kogan DA (2009) Radiation-induced gliomas. *Expert Rev Neurother* 9(10):1–13.

10. Burgess A, Shah K, Hough O, Hynynen K (2012) Potential risk factors for incident glioblastoma multiforme: the Honolulu Heart Program and Honolulu-Asia Aging Study. *J Neurooncol* 109(2):315–321.

11. Nakamura M, et al. (2000) Loss of Heterozygosity on Chromosome 10 Is More Extensive in Primary (De Novo) Than in Secondary Glioblastomas. *J Neuropathol Exp Neurol* 59(6):539–543.

12. Ohgak H, et al. (2003) Genetic Pathways to Glioblastoma: A Population-Based Study. *Cancer Res* 63(20):6962–70.

13. Wang T, Pickard AJ, Gallo JM (2016) Histone Methylation by Temozolomide; A Classic DNA Methylating Anticancer Drug. *Anticancer Res* 36(7):3289–3299.

14. Rye PT, et al. (2008) Mismatch repair proteins collaborate with methyltransferases in the repair of O6 -methylguanine. *DNA Repair* 7(2):170–

176.

15. Lee SY (2016) Temozolomide resistance in glioblastoma multiforme. *Genes Dis* 3(3):198–210.

16. Friedman HS, et al. (1998) DNA mismatch repair and O6-alkylguanine-DNA alkyltransferase analysis and response to Temodal in newly diagnosed malignant glioma. *J Clin Oncol* 16(12):3851–3857.

17. Calatozzolo C, et al. (2005) Expression of drug resistance proteins Pgp, MRP1, MRP3, MRP5 AND GST-π in human glioma. *J Neurooncol* 74(2):113–121.

18. Stupp R, et al. (2010) Commentary on effects of radiotherapy with concomitant and adjuvant temozolomide versus radiotherapy alone on survival in glioblastoma in a randomised phase III study: 5-Year analysis of the EORTC-NCIC trial (Lancet Oncol. 2009;10:459-466). *Cancer* 116(8):1844–1846.

19. Sandler A, et al. (2006) Paclitaxel–Carboplatin Alone or with Bevacizumab for Non–Small-Cell Lung Cancer. *N Engl J Med* 355(24):2542–2550.

20. Coleman RL, et al. (2017) Bevacizumab and paclitaxel–carboplatin chemotherapy and secondary cytoreduction in recurrent, platinum-sensitive ovarian cancer (NRG Oncology/Gynecologic Oncology Group study GOG-0213): a multicentre, open-label, randomised, phase 3 trial. *Lancet Oncol* 18(6):779–791.

21. Zhang L, Zhou Q (2018) Bevacizumab with dose-dense paclitaxel/carboplatin as first-line chemotherapy for advanced ovarian cancer. *Eur J Pharmacol* 837(28):64–71.

22. Chinot OL, et al. (2014) Bevacizumab plus Radiotherapy–Temozolomide for Newly Diagnosed Glioblastoma. *N Engl J Med* 370(8):709–722.

23. Colgan SP, Eltzschig HK, Eckle T, Thompson LF (2006) Physiological roles for ecto-5′-nucleotidase (CD73). *Purinergic Signal* 2(2):351–360.

24. Knapp K, et al. (2012) Crystal structure of the human ecto-5′-nucleotidase (CD73): Insights into the regulation of purinergic signaling. *Structure* 20(12):2161–2173.

25. Allard B, Turcotte M, Stagg J (2014) Targeting CD73 and downstream adenosine receptor signaling in triple-negative breast cancer. *Expert Opin Ther Targets* 18(8):863–881.

26. Knöfel T, Sträter N (2001) E. coli 5′-Nucleotidase undergoes a hinge-bending domain rotation resembling a ball-and-socket motion. *J Mol Biol* 309(1):255–266.

27. Schultz-Heienbrok R, Maier T, Sträter N (2004) Trapping a 96 degrees domain rotation in two distinct conformations by engineered disulfide bridges. *Protein Sci* 13(7):1811–22.

28. Schultz-Heienbrok R, Maier T, Sträter N (2005) A large hinge bending domain rotation is necessary for the catalytic function of Escherichia coli 5′-nucleotidase. *Biochemistry* 44(7):2244–2252.

29. Thompson LF, Ruedi JM, Glass A, Low MG, Lucas AH (1989) Antibodies to 5'-nucleotidase (CD73), a glycosyl-phosphatidylinositol-anchored protein, cause human peripheral blood T cells to proliferate. *J Immunol* 143(6):1815–1821.

30. Massaia M, et al. (1991) Amplification of T Cell Activation Induced by CD73 (Ecto-5′Nucleotidase) Engagement. *Purine and Pyrimidine Metabolism in Man VII: Part B: Structural Biochemistry, Pathogenesis and Metabolism*, eds Harkness RA, Elion GB, Zöllner N (Springer US, New York, NY), pp 155–158.

31. Resta R, et al. (1994) Glycosyl phosphatidylinositol membrane anchor is not required for T cell activation through CD73. *J Immunol* 153(3):1046–53.

32. Gutensohn W, Resta R, Misumi Y, Ikehara Y, Thompson LF (1995) Ecto-5'-nucleotidase activity is not required for T cell activation through CD73. *Cell Immunol* 161(2):213–217.

33. Eltzschig HK, Weissmüller T, Mager A, Eckle T (2006) Nucleotide Metabolism and Cell-Cell Interactions. *Cell-Cell Interactions: Methods and Protocols*, ed Colgan SP (Humana Press, Totowa, NJ), pp 73–87.

34. Junger WG (2011) Immune cell regulation by autocrine purinergic signalling. *Nat Rev Immunol* 11(3):201–212.

35. Deaglio S, Robson SC (2011) *Ectonucleotidases as Regulators of Purinergic Signaling in Thrombosis, Inflammation, and Immunity* (Elsevier Inc.). 1st Ed. doi:10.1016/B978-0-12-385526-8.00010-2.

36. Johansson B, Georgiev V, Lindstrom K, Fredholm BB (1997) A1 and A2A adenosine receptors and A1 mRNA in mouse brain: effect of long-term caffeine treatment. *Brain Res* 762(1–2):153–164.

37. Dunwiddie T V, Masino SA (2001) The role and regulation of adenosine in the central nervous system. *Annu Rev Neurosci* 24:31–55.

38. Mills JH, Kim D-G, Krenz A, Chen J-F, Bynoe MS (2012) A2A Adenosine Receptor Signaling in Lymphocytes and the Central Nervous System Regulates Inflammation during Experimental Autoimmune Encephalomyelitis. *J Immunol* 188(11):5713–5722.

39. Merighi S, et al. (2006) Adenosine modulates vascular endothelial growth factor

expression via hypoxia-inducible factor-1 in human glioblastoma cells. *Biochem Pharmacol* 72(1):19–31.

40. Allard B, et al. (2014) Anti-CD73 therapy impairs tumor angiogenesis. *Int J Cancer* 134(6):1466–1473.

41. Sitkovsky M, et al. (2014) Hostile, Hypoxia-A2-Adenosinergic Tumor Biology as the Next Barrier to Overcome for Tumor Immunologists. *Cancer Immunol Res* 2(7):598–605.

42. Abbott NJ, Rönnbäck L, Hansson E (2006) Astrocyte-endothelial interactions at the blood-brain barrier. *Nat Rev Neurosci* 7(1):41–53.

43. Bynoe MS, Viret C, Yan A, Kim DG (2015) Adenosine receptor signaling: a key to opening the blood-brain door. *Fluids Barriers CNS* 12:20.

44. Engelhardt B, Wolburg-Buchholz K, Wolburg H (2001) Involvement of the Choroid Plexus in Central Nervous System Inflammation. *Microsc Res Tech* 52(1):112–129.

45. Ousman SS, Kubes P (2012) Immune surveillance in the central nervous system. *Nat Neurosci* 15(8):1096–1101.

46. Rubin LL, Staddon JM (1999) The cell biology of the blood-brain barrier. *Annu Rev Neurosci* 22(1):11–28.

47. Aijaz S, Balda MS, Matter K (2006) Tight junctions: Molecular architecture and function. *Int Rev Cytol* 248(06):261–298.

48. Baeten KM, Katerina A (2011) Extracellular Matrix and Matrix Receptors in Blood-Brain Barrier Formation and Stroke. *Dev Neurobiol* 71(11):1018–1039.

49. Armulik A, et al. (2010) Pericytes regulate the blood-brain barrier. *Nature* 468(7323):557–561.

50. Dohgu S, et al. (2005) Brain pericytes contribute to the induction and up-regulation of blood-brain barrier functions through transforming growth factor-β production. *Brain Res* 1038(2):208–215.

51. Hori S, Ohtsuki S, Hosoya KI, Nakashima E, Terasaki T (2004) A pericyte-derived angiopoietin-1 multimeric complex induces occludin gene expression in brain capillary endothelial cells through Tie-2 activation in vitro. *J Neurochem* 89(2):503–513.

52. Alvarez JI, Katayama T, Prat A (2013) Glial influence on the blood brain barrier. *Glia* 61(12):1939–1958.

53. Cabezas R, et al. (2014) Astrocytic modulation of blood brain barrier: perspectives on Parkinson's disease. *Front Cell Neurosci* 8(August):1–11.

54. Urquhart BL, Kim RB (2009) Blood-brain barrier transporters and response to CNS-active drugs. *Eur J Clin Pharmacol* 65(11):1063–1070.

55. Lingineni K, Belekar V, Tangadpalliwar SR, Garg P (2017) The role of multidrug resistance protein (MRP-1) as an active efflux transporter on blood–brain barrier (BBB) permeability. *Mol Divers* 21(2):355–365.

56. Henson JW, Cordon-Cardo C, Posner JB (1992) P-glycoprotein expression in brain tumors. *J Neurooncol* 14(1):37–43.

57. Munoz JL, Walker ND, Scotto KW, Rameshwar P (2015) Temozolomide competes for P-glycoprotein and contributes to chemoresistance in glioblastoma cells. *Cancer Lett* 367(1):69–75.

58. Tivnan A, Zakaria Z, Leary CO, Kögel D, Pokorny JL (2015) Inhibition of multidrug resistance protein 1 (MRP1) improves chemotherapy drug response in primary and recurrent glioblastoma multiforme. *Front Neurosci* 9:218.

59. Schneider SW, et al. (2004) Glioblastoma cells release factors that disrupt blood-brain barrier features. *Acta Neuropathol* 107(3):272–276.

60. Dubois LG, et al. (2014) Gliomas and the vascular fragility of the blood brain barrier. *Front Cell Neurosci* 8(December):1–13.

61. Sarkaria JN, et al. (2018) Is the blood-brain barrier really disrupted in all glioblastomas? A critical assessment of existing clinical data. *Neuro Oncol* 20(2):184–191.

62. Kim SS, Harford JB, Pirollo KF, Chang EH (2015) Effective treatment of glioblastoma requires crossing the blood-brain barrier and targeting tumors including cancer stem cells: The promise of nanomedicine. *Biochem Biophys Res Commun* 468(3):485–489.

63. Mills JH, et al. (2008) CD73 is required for efficient entry of lymphocytes into the central nervous system during experimental autoimmune encephalomyelitis. *Proc Natl Acad Sci* 105(27):9325–9330.

64. Mills JH, Alabanza LM, Mahamed DA, Bynoe MS (2012) Extracellular adenosine signaling induces CX3CL1 expression in the brain to promote experimental autoimmune encephalomyelitis. *J Neuroinflammation* 9:193.

65. Carman AJ, Mills JH, Krenz A, Kim D, Bynoe MS (2011) Adenosine Receptor Signaling Modulates Permeability of the Blood – Brain Barrier. *J Neurosci* 31(37):13272–13280.

66. Kim D, Bynoe MS (2016) A2A adenosine receptor modulates drug efflux transporter P-glycoprotein at the blood-brain barrier. *J Clin Invest* 126(5):1717–1733.

67. Kim D, Bynoe MS (2015) A2A adenosine receptor regulates the human blood brain barrier permeability. *Mol Neurobiol* 52(1):664–678.

68. Beavis PA, Stagg J, Darcy PK, Smyth MJ (2012) CD73: A potent suppressor of antitumor immune responses. *Trends Immunol* 33(5):231–237.

69. Serra S, et al. (2011) CD73-generated extracellular adenosine in chronic lymphocytic leukemia creates local conditions counteracting drug-induced cell death. *Blood* 118(23):6141–6152.

70. Ludwig H, Rausch S, Schallock K, Markakis E (1998) Expression of CD 73 (ecto-5'-nucleotidase) in 165 glioblastomas by immunohistochemistry and electronmicroscopic histochemistry. *Anticancer Res* 19:1747–1752.

71. Häusler SFM, et al. (2011) Ectonucleotidases CD39 and CD73 on OvCA cells are potent adenosine-generating enzymes responsible for adenosine receptor 2A-dependent suppression of T cell function and NK cell cytotoxicity. *Cancer Immunol Immunother* 60(10):1405–1418.

72. Kondo T, Nakazawa T, Murata SI, Katoh R (2006) Expression of CD73 and its ecto-5'-nucleotidase activity are elevated in papillary thyroid carcinomas. *Histopathology* 48(5):612–614.

73. Durak I, et al. (1994) Adenosine deaminase, 5'-nucleotidase, guanase and cytidine deaminase activities in gastric tissues from patients with gastric cancer. *Cancer Lett* 84:199–202.

74. Eroğlu A, et al. (2000) Activities of adenosine deaminase and 5'-nucleotidase in cancerous and noncancerous human colorectal tissues. *Med Oncol* 17(4):319–324.

75. Leth-Larsen R, et al. (2009) Metastasis-related plasma membrane proteins of human breast cancer cells identified by comparative quantitative mass spectrometry. *Mol Cell Proteomics* 8(6):1436–1449.

76. Spychala J, et al. (2004) Role of Estrogen Receptor in the Regulation of Ecto-5′-Nucleotidase and Adenosine in Breast Cancer. *Clin Cancer Res* 10(2):708–717.

77. Mandapathil M, et al. (2009) Increased ectonucleotidase expression and activity in regulatory T cells of patients with head and neck cancer. *Clin Cancer Res* 15(20):6348–6357.

78. Zhang B (2012) CD73 promotes tumor growth and metastasis. *Oncoimmunology* 1(1):67–70.

79. Gao Z, et al. (2017) CD73 promotes proliferation and migration of human cervical cancer cells independent of its enzyme activity. *BMC Cancer* 17(1):135.

80. Yu J, et al. (2018) Extracellular 5'-nucleotidase (CD73) promotes human breast cancer cells growth through AKT/GSK-3β/β-catenin/cyclinD1 signaling pathway. *Int J Cancer* 142(5):959–967.

81. Stagg J, et al. (2010) Anti-CD73 antibody therapy inhibits breast tumor growth and metastasis. *PNAS* 107(4):1547–1552.

82. Terp MG, et al. (2013) Anti-Human CD73 Monoclonal Antibody Inhibits Metastasis Formation in Human Breast Cancer by Inducing Clustering and Internalization of CD73 Expressed on the Surface of Cancer Cells. *J Immunol* 191(8):4165–4173.

83. Ghalamfarsa G, et al. (2018) Anti-angiogenic effects of CD73-specific siRNA-loaded nanoparticles in breast cancer-bearing mice. *J Cell Physiol* 233(10):7165–7177.

84. Allard B, et al. (2014) Anti-CD73 therapy impairs tumor angiogenesis. *Int J Cancer* 134(6):1466–1473.

85. Koszałka P, Gołu M, Stanisławowski M, Urban A, Bigda J (2015) CD73 on B16F10 melanoma cells in CD73-deficient mice promotes tumor growth, angiogenesis, neovascularization, macrophage infiltration and metastasis. *Int J Biochem Cell Biol* 69:1–10.

86. Hoskin D, Reynolds T, Blay J (1994) 2-Chloroadenosine inhibits the MHC-unrestricted cytolytic activity of anti-CD3-activated killer cells: evidence for the involvement of a non-A1/A2 cell-surface adenosine receptor. *Cell Immunol* 159(1):85–84.

87. Hoskin DW, Reynolds T, Blay J (1994) Adenosine as a possible inhibitor of killer T-cell activation in the microenvironment of solid tumours. *Int J Cancer* 59(6):854–855.

88. Hoskin DW, Blay J (1994) Adenosine Inhibits the Adhesion of Anti-CD3-activated Killer Lymphocytes to Adenocarcinoma Cells through an A3 Receptor. *Cancer Res* 54(13):3521–3526.

89. Williams BA, Manzer A, Blay J, Hoskin DW (1997) Adenosine acts through a novel extracellular receptor to inhibit granule exocytosis by natural killer cells. *Biochem Biophys Res Commun* 231(2):264–269.

90. Blay J, White TD, Hoskin DW (1997) The extracellular fluid of solid carcinomas contains immunosuppressive concentrations of adenosine. *Cancer Res* 57(13):2602–2605.

91. Allard D, Allard B, Gaudreau PO, Chrobak P, Stagg J (2016) CD73-adenosine: A next-generation target in immuno-oncology. *Immunotherapy* 8(2):145–163.

92. Huang S, Apasov S, Koshiba M, Sitkovsky M (1997) Role of A2a extracellular adenosine receptor-mediated signaling in adenosine-mediated inhibition of T-cell activation and expansion. *Blood* 90(4):1600–10.

93. Ohta A, Sitkovsky M (2001) Role of G-protein-coupled adenosine receptors in downregulation of inflammation and protection from tissue damage. *Nature* 414(6866):916–920.

94. Ohta A, et al. (2006) A2A adenosine receptor protects tumors from antitumor T cells. *Proc Natl Acad Sci* 103(35):13132–13137.

95. Haskó G, Pacher P (2008) A2A receptors in inflammation and injury: lessons learned from transgenic animals. *J Leukoc Biol* 83(3):447–455.

96. Khoa ND, et al. (2001) Inflammatory Cytokines Regulate Function and Expression of Adenosine A2A Receptors in Human Monocytic THP-1 Cells. *J Immunol* 167(7):4026–32.

97. Haskó G, Pacher P, Deitch EA, Vizi ES (2007) Shaping of monocyte and macrophage function by adenosine receptors. *Pharmacol Ther* 113(3):264–275.

98. Panther E, Idzko M, Herouy Y, Rheinen H, Norgauer J (2001) Expression and function of adenosine receptors in human dendritic cells. *FASEB* 15(11):1963–1970.

99. Panther E, et al. (2003) Adenosine affects expression of membrane molecules, cytokine and chemokine release, and the T-cell stimulatory capacity of human dendritic cells. *Blood* 101(10):3985–3990.

100. Suzuki H, Takei M, Nakahata T, Fukamachi H (1998) Inhibitory Effect of Adenosine on Degranulation of Human Cultured Mast Cells upon Cross-linking of FcεRI. *Biochem Biophys Res Commun* 242(3):697–702.

101. Cronstein BN, Hutchison AJ, Williams M (1990) The adenosine/neutrophil paradox resolved: human neutrophils possess both A1 and A2 receptors that promote chemotaxis and inhibit O2 generation, respectively. *J Clin Invest* 85(4):1150–1157.

102. Fortin A, Harbour D, Fernandes M, Borgeat P, Bourgoin S (2005) Differential expression of adenosine receptors in human neutrophils: up-regulation by specific Th1 cytokines and lipopolysaccharide. *J Leukoc Biol* 79(3):574–585.

103. Koshiba M, Rosin DL, Hayashi N, Linden J, Sitkovsky M (1999) Patterns of A2A extracellular adenosine receptor expression in different functional subsets of human peripheral T cells. Flow cytometry studies with anti-A2A receptor monoclonal antibodies. *Mol Pharmacol* 55(3):614–624.

104. Apasov S, Chen J, Smith P, Sitkovsky M (2000) A2A receptor dependent and

A2A receptor independent effects ofextracellular adenosine on murine thymocytes in conditions of adenosine deaminase deficiency. *Blood* 95(12):3859–3867.

105. Armstrong JM, et al. (2001) Gene dose effect reveals no Gs-coupled A2A adenosine receptor reserve in murine T-lymphocytes: studies of cells from A2A-receptor-gene-deficient mice. *Biochem J* 354(Pt 1):123–130.

106. Raskovalova T, et al. (2005) Function of Activated NK Cells 1. *J Immunol* 175(7):4383–4391.

107. Lappas CM, Day Y, Marshall MA, Engelhard VH, Linden J (2006) Adenosine A 2A receptor activation reduces hepatic ischemia reperfusion injury by inhibiting CD1d-dependent NKT cell activation. *J Exp Med* 203(12):2639–2648.

108. Haskó G, Linden J, Cronstein B, Pacher P (2008) Adenosine receptors: Therapeutic aspects for inflammatory and immune diseases. *Nat Rev Drug Discov* 7(9):759–770.

109. Naganuma M, et al. (2006) Cutting Edge: Critical Role for A 2A Adenosine Receptors in the T Cell-Mediated Regulation of Colitis. *J Immunol* 177(5):2765–2769.

110. Wang H, et al. (2010) ZAP-70: An Essential Kinase in T-cell Signaling. *Cold Spring Harb Perspect Biol* 2(5):a002279.

111. Carson MJ, Doose JM, Melchior B, Schmid CD, Ploix CC (2009) CNS immune privilege: hiding in plain sight. *Immunol Rev* 213:48–65.

112. Chao C, Hu S, Ehrlich L, Peterso P (1995) Interleukin-1 and tumor necrosis factor-α synergistically mediate neurotoxicity: involvement of nitric oxide and of N-methyl-D-aspartate receptors. *Brain Behav Immun* 9(4):355–365.

113. Chao C, et al. (1996) Cytokine-Stimulated Astrocytes Damage Human Neurons via a Nitric Oxide Mechanism. *Glia* 16(3):276–284.

114. Ping B, Wen W, Strong MJ (2002) Activated microglia (BV-2) facilitation of TNF-α-mediated motor neuron death in vitro. *J Neuroimmunol* 128(1–2):31–38.

115. Chen DS, Mellman I (2013) Oncology Meets Immunology: The Cancer-Immunity Cycle. *Immunity* 39(1):1–10.

116. Rong Y, Durden DL, Meir EG Van, Brat DJ (2006) "Pseudopalisading" Necrosis in Glioblastoma: A Familiar Morphologic Feature That Links Vascular Pathology, Hypoxia, and Angiogenesis. *J Neuropathol Exp Neurol* 65(6):529–539.

117. Johanns TM, Dunn GP (2018) *The Immune Response to Glioblastoma: Overview*

and Focus on Checkpoint Blockade (Elsevier Inc.). 2nd Ed. doi:10.1016/B978-0-12-812100-9.00052-8.

118. Ransohoff RM, Engelhardt B (2012) The anatomical and cellular basis of immune surveillance in the central nervous system. *Nat Rev Immunol* 12(9):623–635.

119. Ransohoff RM, Cardona AE (2010) The myeloid cells of the central nervous system parenchyma. *Nature* 468(7321):253–262.

120. Goverman J (2009) Autoimmune T cell responses in the central nervous system. *Nat Rev Immunol* 9(6):393.

121. Berghoff AS, et al. (2015) Programmed death ligand 1 expression and tumor-infiltrating lymphocytes in glioblastoma. *Neuro Oncol* 17(8):1064–1075.

122. Andaloussi A El, Lesniak MS (2006) An increase in CD4+CD25+FOXP3+ regulatory T cells in tumor-infiltrating lymphocytes of human glioblastoma multiforme. *Neuro Oncol* 8(3):234–243.

123. Badie B, Schartner JM (2000) Flow cytometric characterization of tumor-associated macrophages in experimental gliomas. *Neurosurgery* 46(4):952–957.

124. Watters JJ, Schartner JM, Badie B, Tumors B (2005) Microglia Function in Brain Tumors. *J Neurosci Res* 81(3):447–455.

125. Hussain SF, et al. (2006) The role of human glioma-infiltrating microglia/macrophages in mediating antitumor immune responses. *Neuro Oncol* 8(3):261–279.

126. Wainwright DA, Sengupta S, Han Y, Lesniak MS (2011) Thymus-derived rather than tumor-induced regulatory T cells predominate in brain tumors. *Neuro Oncol* 13(12):1308–1323.

127. Crane CA, Ahn BJ, Han SJ, Parsa AT (2012) Soluble factors secreted by glioblastoma cell lines facilitate recruitment, survival, and expansion of regulatory T cells: implications for immunotherapy. *Neuro Oncol* 14(5):584–595.

128. Dieckmann BD, Plottner H, Berchtold S, Berger T, Schuler G (2001) Ex Vivo Isolation and Characterization of CD4+ CD25+ T Cells with Regulatory Properties from Human Blood. *J Exp Med* 193(11):1303–1310.

129. Hahne M, et al. (1996) Melanoma Cell Expression of Fas(Apo-1/CD95) Ligand: Implications for Tumor Immune Escape. *Science* 274(5291):1363–1366.

130. Woroniecka KI, Rhodin KE, Chongsathidkiet P, Keith KA, Fecci PE (2018) T-cell Dysfunction in Glioblastoma: Applying a New Framework. 24(16):3792–

3803.

131. Xing Y, Hogquist KA (2012) T-Cell Tolerance: Central and Peripheral. *Cold Spring Harb Perspect Biol* 4(4):a006957.

132. Didenko V, Ngo H, Minchew C, Baskin D (2002) Apoptosis of T lymphocytes invading glioblastomas multiforme: a possible tumor defense mechanism. *J Neurosurg* 96(3):580–584.

133. Walker DG, Chuah T, Rist MJ, Pender MP (2006) T-cell apoptosis in human glioblastoma multiforme: Implications for immunotherapy. *J Neuroimmunol* 175(1–2):59–68.

134. Uyttenhove C, et al. (2003) Evidence for a tumoral immune resistance mechanism based on tryptophan degradation by indoleamine 2,3-dioxygenase. *Nat Med* 9(10):1269–1274.

135. Wainwright DA, et al. (2012) IDO Expression in Brain Tumors Increases the Recruitment of Regulatory T Cells and Negatively Impacts Survival. *Hum Cancer Biol* 18(14):6110–6122.

136. Lee GK, et al. (2002) Tryptophan deprivation sensitizes activated T cells to apoptosis prior to cell division. *Immunity* 107(4):452–460.

137. Terness P, et al. (2002) Inhibition of Allogeneic T Cell Proliferation by Indoleamine 2, 3-Dioxygenase–expressing Dendritic Cells: Mediation of Suppression by Tryptophan Metabolites. *J Exp Med* 196(4):447–457.

138. Fallarino F, Grohmann U, Vacca C, Bianchi R (2002) T cell apoptosis by tryptophan catabolism. *Cell Death Differ* 9(10):1069–1077.

139. Zhai L, et al. (2015) The role of IDO in brain tumor immunotherapy. *J Neurooncol* 123(3):395–403.

140. Lee K, et al. (1998) Molecular Basis of T Cell Inactivation by CTLA-4. 282(December):2263–2267.

141. Fong B, et al. (2012) Monitoring of Regulatory T Cell Frequencies and Expression of CTLA-4 on T Cells, before and after DC Vaccination, Can Predict Survival in GBM Patients. *PLoS One* 7(4):1–9.

142. Fecci PE, et al. (2007) Systemic CTLA-4 Blockade Ameliorates Glioma-Induced Changes to the CD4 + T Cell Compartment without Affecting Regulatory T-Cell Function. 13(19):2158–2168.

143. Kim JE, Lim M (2015) The role of checkpoints in the treatment of GBM. *J Neurooncol* 123(3):413–423.

144. Cheng X, et al. (2013) Structure and Interactions of the Human Programmed Cell

Death 1 Receptor. *J Biol Chem* 288(17):11771–11785.

145. Francisco LM, et al. (2009) PD-L1 regulates the development, maintenance, and function of induced regulatory T cells. *J Exp Med* 206(13):3015–3029.

146. Romani M, Pistillo MP, Carosio R, Morabito A, Banelli B (2018) Immune Checkpoints and Innovative Therapies in Glioblastoma. *Front Oncol* 8:464.

147. Heiland DH, et al. (2017) Comprehensive analysis of PD-L1 expression in glioblastoma multiforme. *Oncotarget* 8(26):42214–42225.

148. Ji XY, Ma J, Dong J (2018) Myeloid-derived suppressor cells and nonresolving inflammatory cells in glioma microenvironment: molecular mechanisms and therapeutic strategies. *Glioma* 1(1):2–8.

149. Yang L, et al. (2008) Abrogation of TGFβ Signaling in Mammary Carcinomas Recruits Gr-1+CD11b+ Myeloid Cells that Promote Metastasis. *Cancer Cell* 13(1):23–35.

150. Li H, Han Y, Guo Q, Zhang M, Cao X (2009) Cancer-Expanded Myeloid-Derived Suppressor Cells Induce Anergy of NK Cells through Membrane-Bound TGF-β1. *J Immunol* 182(1):240–249.

151. Pan P, et al. (2010) Immune Stimulatory Receptor CD40 Is Required for T-Cell Suppression and T Regulatory Cell Activation Mediated by Myeloid-Derived Suppressor Cells in Cancer. *Cancer Res* 70(1):99–108.

152. Serafini P, Mgebroff S, Noonan K, Borrello I (2008) Myeloid-Derived Suppressor Cells Promote Cross-Tolerance in B-Cell Lymphoma by Expanding Regulatory T Cells. *Cancer Res* 68(13):5439–5449.

153. Gabrilovich DI, Nagaraj S (2009) Myeloid-derived suppressor cells as regulators of the immune system. *Nat Rev Immunol* 9(3):162–174.

154. Morantz RA, Wood GW, Foster M, Clark M, Gollahon K (1979) Macrophages in experimental and human brain tumors. Part 2: studies of the macrophage content of human brain tumors. *J Neurosurg* 50(3):305–311.

155. Poon CC, Sarkar S, Yong V, Kelly JJ (2017) Glioblastoma-associated microglia and macrophages: targets for therapies to improve prognosis. *Brain* 140(6):1548–1560.

156. Zhou W, et al. (2015) Periostin secreted by glioblastoma stem cells recruits M2 tumour-associated macrophages and promotes malignant growth. *Nat Cell Biol* 17(2):170–182.

157. Wu A, et al. (2010) Glioma cancer stem cells induce immunosuppressive macrophages/microglia. *Neuro Oncol* 12(11):1113–1125.

158. Hussain SF, et al. (2007) A Novel Small Molecule Inhibitor of Signal Transducers and Activators of Transcription 3 Reverses Immune Tolerance in Malignant Glioma Patients. *Cancer Res* 67(20):9630–9636.

159. Horn L, et al. (2017) Nivolumab Versus Docetaxel in Previously Treated Patients With Advanced Non–Small-Cell Lung Cancer: Two-Year Outcomes From Two Randomized, Open-Label, Phase III Trials (CheckMate 017 and CheckMate 057). *J Clin Oncol* 35(35):3924–3933.

160. Garon E, et al. (2015) Pembrolizumab for the Treatment of Non–Small-Cell Lung Cancer. *N Engl J Med* 372(21):2018–2028.

161. Herbst RS, et al. (2016) Pembrolizumab versus docetaxel for previously treated, PD-L1-positive, advanced non-small-cell lung cancer (KEYNOTE-010): a randomised controlled trial. *Lancet (London, England)* 387(10027):1540–1550.

162. Larkin J, et al. (2015) Combined Nivolumab and Ipilimumab or Monotherapy in Untreated Melanoma. *N Engl J Med* 373(1):23–24.

163. Larkin J, et al. (2017) Abstract CT075: Overall survival (OS) results from a phase III trial of nivolumab (NIVO) combined with ipilimumab (IPI) in treatment-naïve patients with advanced melanoma (CheckMate 067). *Cancer Res* 77(13 Supplement):CT075-CT075.

164. Robert C, et al. (2017) Long-term outcomes in patients (pts) with ipilimumab (ipi)-naive advanced melanoma in the phase 3 KEYNOTE-006 study who completed pembrolizumab (pembro) treatment. *J Clin Oncol* 35(15_suppl):9504.

165. Blumenthal DT, et al. (2016) Pembrolizumab: first experience with recurrent primary central nervous system (CNS) tumors. *J Neurooncol* 129(3):453–460.

166. Chamberlain MC, Kim BT (2017) Nivolumab for patients with recurrent glioblastoma progressing on bevacizumab: a retrospective case series. *J Neurooncol* 133(3):561–569.

167. Reardon DA, et al. (2016) Safety and activity of nivolumab (nivo) monotherapy and nivo in combination with ipilimumab (ipi) in recurrent glioblastoma (GBM): Updated results from checkmate-143. *J Clin Oncol* 34(15_suppl):2014.

168. Omuro A, et al. (2017) Nivolumab with or without ipilimumab in patients with recurrent glioblastoma: results from exploratory phase I cohorts of CheckMate 143. *Neuro Oncol* 20(5):674–686.

169. Reardon DA, et al. (2017) OS10.3 Randomized Phase 3 Study Evaluating the Efficacy and Safety of Nivolumab vs Bevacizumab in Patients With Recurrent Glioblastoma: CheckMate 143. *Neuro Oncol* 19(suppl_3):iii21-iii21.

170. Banks WA (2009) Characteristics of compounds that cross the blood-brain

barrier. *BMC Neurol* 9(Suppl I):S3.

171. Filley AC, Henriquez M, Dey M (2017) Recurrent glioma clinical trial, CheckMate-143: the game is not over yet. *Oncotarget* 8(53):91779–91794.

172. Lamberti G, Franceschi E, Brandes AA (2018) The burden of oncology promises not kept in glioblastoma. *Futur Neurol* 13(1):1–4.

173. Blackburn SD, Shin H, Freeman GJ, Wherry EJ (2008) Selective expansion of a subset of exhausted CD8 T cells by αPD-L1 blockade. *PNAS* 105(39):15016–15021.

CHAPTER 2

CD73 PROMOTES GLIOBLASTOMA PATHOGENESIS AND ENHANCES ITS CHEMORESISTANCE VIA A_{2B} ADENOSINE RECEPTOR SIGNALING

Abstract

Glioblastoma (GB) is one of the deadliest brain cancers to afflict humans, and it has a very poor survival rate even with treatment. The extracellular adenosine-generating enzyme CD73 is involved in many cellular functions that can be usurped by tumors, including cell adhesion, proliferation, invasion, and angiogenesis. We set out to determine the role of CD73 in GB pathogenesis. To do this, we established a unique GB mouse model (CD73-FLK) in which we spatially expressed CD73 on endothelial cells in $CD73^{-/-}$ mice. This allowed us to elucidate the mechanism of host CD73 versus GB-expressed CD73 by comparing GB pathogenesis in WT, $CD73^{-/-}$, and CD73-FLK mice. GB in $CD73^{-/-}$ mice had decreased tumor size, decreased tumor vessel density, and reduced tumor invasiveness compared with GB in WT mice. Interestingly, GBs in CD73-FLK mice were much more invasive and caused complete distortion of the brain morphology. We showed a 20-fold upregulation of the A_{2B} AR on GB compared with sham, and its activation induced matrix metalloproteinase-2, which enhanced GB pathogenesis. Inhibition of A_{2B} AR signaling decreased multidrug resistance transporter protein expression, including the permeability glycoprotein (P-gp) and the multidrug resistance-associated protein 1 (MRP1). Further, we showed that blockade of A_{2B} AR signaling potently increased GB cell death induced by the chemotherapeutic drug temozolomide. Together, these findings suggest that CD73 and the A_{2B} AR play a multifaceted role in GB pathogenesis and progression and that targeting the CD73–A_{2B} AR axis can benefit GB patients and inform new approaches for therapy to treat GB patients.

Significance Statement

Glioblastoma (GB) is the most devastating primary brain tumor. GB patients' median survival is 16 months even with treatment. It is critical that we develop prophylaxes to advance GB treatment and improve patient survival. CD73-generated adenosine has been implicated in cancer pathogenesis, but its role in GB was not ascertained. Here, we demonstrated that host CD73 plays a prominent role in multiple areas of glioblastoma pathogenesis, including promotion of GB growth, angiogenesis, and invasiveness. We found a 20-fold increase in A_{2B} adenosine receptor (AR) expression on GB compared with sham, and its inhibition increased GB chemosensitivity to temozolomide. These findings strongly indicate that blockade or inhibition of CD73 and the A_{2B} AR are prime targets for future GB therapy.

Introduction

Glioblastoma (GB) is the most common and most fatal primary malignant brain tumor (1) due to its high capacity to proliferate and its extreme chemoresistance (2). Further, the impermeability of the blood-brain barrier (BBB) makes chemotherapeutic drug delivery challenging for GB treatment (3). Currently, the median survival for GB patients is 16 months even with treatment (4).

In this report, we investigated the role of the surface enzyme CD73 (ecto-5'-nucleotidase) in GB pathogenesis as CD73 and its product, extracellular adenosine, have been implicated in the progression of other types of tumors (5–8). CD73 is a key enzyme in the adenosine triphosphate (ATP) metabolic pathway. In damaged tissues, ATP is released into the extracellular space (9, 10) and converted to adenosine diphosphate (ADP) and adenosine monophosphate (AMP) by the surface enzyme CD39 (ectonucleoside triphosphate diphosphohydrolase-1); AMP is further converted to adenosine by CD73.

Adenosine is a purine nucleoside that promotes tumor proliferation and angiogenesis (6, 11). To elicit its function, adenosine signals through four G-protein coupled receptors, A_1, A_{2A}, A_{2B}, and A_3. The A_{2B} adenosine receptor (AR) has a very low affinity for adenosine and is activated under high, usually pathological, extracellular adenosine concentrations (in the μM range) (12–15), whereas the A_1 AR has the highest affinity and is activated under basal adenosine concentrations (16, 17). Adenosine signaling through the A_{2B} AR modulates tumor apoptosis and proliferation and the tumor immune microenvironment (13, 18–20).

CD73 and adenosine are involved in tumor adhesion, invasion, proliferation, angiogenesis, and chemoresistance (6, 7, 11, 21–27). For example, under hypoxic

conditions, upregulation of the hypoxia-inducible factor 1 (HIF-1) transcription factor increases CD73 generation of extracellular adenosine (11). Adenosine signaling through the A_{2A} and A_{2B} ARs induces the release of vascular endothelial growth factor (VEGF), which induces proliferation of endothelial cells and angiogenesis to promote tumor growth (11). CD73 and AR signaling also regulate matrix metalloproteinases (MMPs) (6, 25), which play crucial roles in angiogenesis and tumor invasion by degrading the extracellular matrix (ECM) (6). MMP2 and MMP9 have been shown to promote GB angiogenesis and invasion and to regulate vascular patterning (26, 27). However, how CD73 regulates GB pathogenesis and whether host CD73 contributes to tumor pathogenesis have not been elucidated. We hypothesized that GB usurped the host and its own CD73 (GB-CD73) to promote its growth and survival. To test this, we used unique mouse models lacking CD73 or expressing CD73 on endothelial cells to study GB pathogenesis. Our data revealed that both the host and GB-CD73 were key contributors to GB pathogenesis. These studies provide a potential target for GB therapeutic intervention through modulation of CD73 and/or CD73-AR axis.

Materials and Methods

Cell culture

GL261 and U251 cell lines were obtained from the National Cancer Institute and cultured in DMEM (10-013-CV, Cellgro; Corning) or RPMI 1640 (10-040-CM, Cellgro; Corning) respectively, with 10% fetal bovine serum, 100 units/ml penicillin and streptomycin at 37ºC/5% CO_2 in a humidified incubator. Medium was changed every 2-3 days and cells were used when grown to confluency.

Mice

C57BL/6 mice were purchased from Jackson Laboratories. $CD73^{-/-}$ mice have been described previously (28) and were backcrossed to C57BL/6 mice for more than 14 generations. Mice expressing CD73 primarily on endothelial cells (CD73-FLK mice) were produced by generating mice expressing murine CD73 under the control of the *Flk-1* promoter (see details below) and crossing them to $CD73^{-/-}$ mice. All mice used in this study were males and age-matched. Mice were housed in specific-pathogen-free rooms until they were 8 weeks of age and moved to a broken barrier/biosafety level 2 room for experiments in the mouse facility at Cornell University. Animal studies were approved by the institutional animal care and use committee of Cornell University (protocol no. 2008–0092).

Generation of CD73-FLK mice

Full-length CD73 was amplified by PCR from a murine CD73 plasmid (29) to add a consensus Kozak sequence and flanking restriction sites and then cloned into a plasmid containing promoter and intronic enhancer sequences from the murine *Flk-1* gene (30) (a gift from Dr. Lijun Xia, Oklahoma Medical Research Foundation) using NheI and

EcoR I restriction sites. All plasmids were verified by sequencing. The full-length 5.4 kb transgene was released by digesting this plasmid with SalI and XmaI and, after purification, was injected into C57BL/6 blastocysts at the University of North Carolina Animal Models Core Facility. The presence of the transgene was verified by PCR using the following primers: CD73Tg forward: 5'-GGGCGGATCAAGTTCTCTGCAGC-3'; CD73Tg reverse: 5'-TTAACTGGGACTGGGGC-AAAGTC-3'. Transgene-positive mice were bred to *cd73*$^{-/-}$ mice to generate offspring that expressed CD73 only under the control of the *Flk-1* promoter.

GB implantation

GL261 and GL261^{CD73low} cells were suspended in saline (15,000 cells/μl) and kept on ice. Mice were anesthetized with ketamine-xylazine (100 mg/kg) and ketoprofen (2 mg/kg) was administered as an analgesic. Eye ointment was applied before hair removal. The scalps were sterilized by wiping three times with chlorhexidine solution followed by 70% ethanol. A midsagittal incision was made through the scalp and the bregma was located. A small hole was drilled 0.1 mm posterior and 2.3 mm lateral of the bregma. Then, 30,000 GL261 cells or saline (2 μl, sham) were injected 3 mm from the brain surface using a 27-gauge needle with a Hamilton syringe. The wound was closed using sutures and ketoprofen (2 mg/kg) was administered the day after surgery.

Tissue harvest

Mice were anesthetized with ketamine-xylazine and transcardial perfusion with ice-cold PBS was performed. Brains were cut coronally in half, flash frozen in Tissue-Tek optimal cutting temperature medium (Sakura Finetek), and stored at -80ºC. Brains were sectioned to 8 or 10 μm thick with a microtome, collected on Supefrost/Plus slides (Fisher Scientific), fixed in acetone, and stored at -80ºC.

Hematoxylin and eosin staining

Frozen sections were fixed with acetone, stained with 0.1% hematoxylin and 0.5% eosin and mounted with Eukitt quick hardening mounting reagent.

Invasion score

GB invasion scores were measured using 20X scanned whole-brain images of H&E-stained brain sections taken by Aperio CS2. GB invasion scores were the sum of the meninges invasion score, the invasion area score, and the invasion distance score. The meninges invasion score equaled the ceiling of the percentage of meninges invaded divided by 5 (to transform the percentage into a score ranging from 0 to 10). The invasion area score equaled the area of tumor-infiltrating non-neoplastic area divided by the total area of the tissue section (31). The invasion distance score equaled the ceiling of the displacement (in μm) between the farthest point of the tumor infiltrating non-neoplastic area and the tumor edge (32) divided by 500 (to transform the displacement into a score ranging from 0 to 10).

Flow cytometry

GL261 and GL261^{CD73low} cells were stained with PE-conjugated antibody against mouse CD73 (1:200, 12-0731-83; eBioscience) and/or FITC-conjugated antibody against mouse CD44 (1:200, 553133; BD Biosciences), and U251 cells were stained with FITC-conjugated antibody against human CD73 (1:200, 344015; BioLegend). Cells were then washed twice with 0.5% BSA/PBS. Brain tissues were collected from GB-bearing WT mice 3 weeks after implantation. Tumors were removed with a blade and homogenized with a Dounce homogenizer in RPMI 1640 (10-040-CM, Cellgro; Corning) with 10% fetal bovine serum. Tumor homogenates were centrifuged at 450 g for 10 minutes and

pellets were resuspended in 30% Percoll underlaid with 70% Percoll. Cells were centrifuged at 600 g for 20 min at room temperature and the layer at the 70% and 30% Percoll junction was collected and washed with 0.5% BSA/PBS. Red blood cells were lysed with ACK lysing buffer (A1049201; Thermo Fisher Scientific) according to the manufacturer's protocol. Cells were blocked with anti-CD16/CD32 antibody (1:200, 14-0161-85; eBioscience) and stained with PE-conjugated antibody against mouse CD73 (1:200, 12-0731-83; eBioscience). For intracellular staining, cells were fixed with 4% paraformaldehyde (15710; Electron Microscopy Sciences) for 20 minutes, permeabilized with 0.1% saponin (A18820; Alfa Aesar) for 15 minutes, and then stained with PE-conjugated antibody against mouse CD73 (1:200, 12-0731-83; eBioscience) in 0.1% saponin (A18820; Alfa Aesar). Cells were analyzed with BD Biosciences FACSCanto II. Laser configurations were as follows: GL261 – FSC 176 V, SSC 313 V, PE 493 V, FITC 533 V; U251 – FSC 176 V, SSC 313 V, FITC 533 V; Tumor homogenate – FSC 335 V, SSC 410 V, PE 400 V. Data were analyzed using FlowJo software version 10.

Immunostaining

For immunohistochemistry staining, slides were immersed in 0.3% H_2O_2 for 10 min to inactivate peroxidases. After two PBS washes, slides were blocked at room temperature with casein (Vector Laboratories) and 10% goat serum. Slides were then incubated overnight with primary antibody against CD31 (1:30, 550274; BD Pharmingen), MMP9 (1:200, AB19016; Millipore), MMP2 (1:500, MAB3308; Millipore), or CD73 (1:100, BD Pharmingen, 550738) followed by two PBS washes. Slides were then incubated with HRP-conjugated secondary antibody, washed, and developed with an AEC substrate kit (Zymed) and stained with hematoxylin. Slides were mounted with Fluoromount-G. For immunofluorescence staining, slides or cells grown on coverslips

were blocked the same way as immunohistochemistry staining. For Ki-67 staining, slides were permeabilized using Foxp3 staining buffer set (00-5523-00; eBioscience) following the manufacturer's protocol. Slides or coverslips were incubated overnight with primary antibody against CD73 (1:100, 550738; BD Pharmingen), CD133 (1:200, ab19898; Abcam), Ki-67 (1:50, 550609; BD Pharmingen), GFAP (1:500, 556330; BD Pharmingen), NeuN (1:200, 12943S; Cell Signaling), A_1 AR (1:100, AAR-006; Alomone Labs), A_{2A} AR (1:100, AAR-002; Alomone Labs), A_{2B} AR (1:100, SC-7507; Santa Cruz), A_3 AR (1:100, AAR-004; Alomone Labs), VEGFA (1:200, ab46154; Abcam), CD31 (1:30, 550274; BD Pharmingen), alpha-dystroglycan (1:100, 05-298; Millipore), MMP9 (1:200, AB19016; Millipore; 1:100, ab38898; Abcam), TIMP1 (1:500, ab86482; Abcam), MMP2 (1:500, MAB3308; Millipore), P-gp (1:100, GTX23364; GeneTex), or MRP1 (1:100, ab32574; Abcam) followed by two PBS washes. Slides were then incubated with fluorophore-conjugated secondary antibody, washed, and mounted with ProLong Gold with DAPI. Slides were imaged with Zeiss Axio Imager.M1 with Zeiss Plan-Neofluar 20X objective (44 03 40).

Sorting GL261^{CD73low} cells

GL261 cells were stained with PE-conjugated antibody against mouse CD73 (1:200, 12-0731-83; eBioscience) and washed twice with 1% fetal bovine serum/PBS. Cells were sorted by BD Biosciences FACSAria II with the following laser configurations: FSC 250 V, SSC 160 V, PE 550 V. Data were analyzed using FlowJo software version 10. Sorted cells were collected in 50% fetal bovine serum in DMEM (10-013-CV, Cellgro; Corning) and cultured as normal until confluent. CD73 expression of sorted GL261^{CD73low} cells was analyzed by flow cytometry one day before implantation in mice.

Survival study

GB-bearing mice were monitored by their weight loss. They were euthanized once they lost 20% of their pre-GB implantation weight.

Isolation of primary mouse astrocytes

Primary mouse cerebellar astrocytes were isolated following Current Protocols in Neuroscience – Isolation and Purification of Primary Rodent Astrocytes (33). Briefly, cerebella of p4 neonatal C57BL/6 mice were ground with a Dounce homogenizer, centrifuged through 30% and 60% Percoll gradients, and astrocytes were enriched at the medium and 30% Percoll interphase. Differential adhesion was performed to enrich the astrocyte population. Primary astrocytes were cultured in DMEM (10-013-CV, Cellgro; Corning) with 10% fetal bovine serum and 100 units/ml penicillin/streptomycin at 37ºC/5% CO_2 in 6-well plates or on coverslips in 96-well plates in a humidified incubator until confluent. Primary astrocytes were stained with the astrocyte marker GFAP and the neuronal marker NeuN following the immunofluorescent staining protocol to verify that they were GFAP-positive and NeuN-negative.

Western blotting

Protein concentrations of GL261 and U251 whole-cell lysates and brain tissue homogenates from sham or GB-implanted mice were measured with the Dc Protein Assay (Bio-Rad); 5 μg of samples were loaded onto an 8% or 10% SDS acrylamide gel and separated for 1 hour. Samples were transferred to a nitrocellulose membrane and then blocked with 1% BSA/tris-buffered saline with Tween 20 (TBST). Membrane was incubated with antibodies against A_1 AR, A_{2A} AR, A_{2B} AR, A_3 AR, P-gp, CD73, and VEGFA (1:2000, AAR-006, AAR-002, AAR-003, AAR-004; Alomone Labs; 1:1000,

GTX108354; GeneTex; 1:2000, AP2014b; Abgent; 1:1000, ab46154; Abcam, respectively) overnight at 4°C. Membrane was then washed three times with TBST and incubated with HRP-conjugated secondary antibody for 1 hour at room temperature. Following three TBST washes, the membrane was developed using Super Signal West Pico ECL solution (Thermo Scientific) and imaged with a Konica SRX-101A Medical Film Processor. Densitometry analysis was performed using ImageJ software. CD73 protein expression inside the GB was measured by subtracting the CD73 protein level of sham-implanted WT or $CD73^{-/-}$ coronal brain sections from the CD73 protein level of GB-implanted WT or $CD73^{-/-}$ coronal brain sections.

Vessel density and glomeruloid vessel quantification

Brain sections were stained for CD31-positive vessels following the immunohistochemistry staining protocol described above. Vessel density was quantified by manually counting the number of CD31-positive vessel per area (1.5 mm^2). Glomeruloid vessels were identified by their multiple lumens in the thickened vessel wall and quantified by manually counting the number of glomeruloid vessels per area (1.5 mm^2).

Quantitative real-time PCR

Brain mRNA was extracted with TRIzol reagent (Invitrogen) and cDNA was synthesized with High-Capacity cDNA Reverse Transcription Kits (Applied Biosystems) according to the manufacturers' protocols. qRT-PCR was performed with specific primers (sequences included below) and KAPA SYBR FAST qPCR Kit (KAPA Biosystems) according to manufacturer's protocol. qRT-PCR was done on Bio-Rad CFX96 Real-Time System C1000 Thermal Cycler. Gene expression levels were analyzed using GAPDH as a reference gene and normalized to controls using the $2^{-\Delta\Delta CT}$

method (34). The following qRT-PCR primers were used: mouse MMP9 forward 5'-GCCCTGGAACTCACAC-GACA-3' and reverse 5'-TTGGAAACTCACACGCCAG-AAG-3'; mouse MMP2 forward 5'-AAGGATGGACTCCTGGCACATGCCTTT-3' and reverse 5'-ACCTGTGGGCTTG-TCACGTGGTGT-3'; mouse TIMP1 forward 5'-CCAGAGCCGTCACTTTGCTT-3' and reverse 5'-AGGAAAAGTAGACAGTGTT-CAGGCTT-3'; mouse TIMP2 forward 5'-ACGCTTAGCATCACCCAGAAG-3' and reverse 5'-TGGGACAGCGAGTGAT-CTTG-3'; human Pgp forward 5'-GCTCCTG-ACTATGCCAAAGC-3' and reverse 5'-TCTTCACCTCCAGGCTCAGT-3'; mouse GAPDH forward 5'-CATGGCCTTCCG-TGTTCCTA-3' and reverse 5'-GCGGCAC-GTCAGAT-CCA-3'; and human GAPDH forward 5'-GGTGGTCTCCTCTGACTTC-AACA-3' and reverse 5'-GTTGCTGTAG-CCAAATTCGTTGT-3'.

MMP activity measurement

MMP activity was measured according to the manufacturer's protocol using the SensoLyte 520 Generic MMP Assay Kit (AS-71158; AnaSpec). Briefly, the A_{2B} AR antagonist-treated GL261 cells were collected in assay buffer and brain tissues from sham or GB-implanted mice were homogenized in assay buffer and centrifuged to remove debris. Protein concentrations were measured with the Dc Protein Assay (Bio-Rad); 400 μg of protein from each brain sample and 55.7 μg of protein from each A_{2B} AR antagonist-treated GL261 sample were incubated with MMP substrate (fluorescence resonance energy transfer peptide) for 1 hr at room temperature in darkness. Fluorescence intensity was measured at Ex/Em = 490 nm/520 nm with BioTek Synergy 4. Concentrations of cleaved MMP substrate were calculated by a standard curve and normalized to sham-implanted CTs.

A_{2B} AR agonist and antagonist treatment on GB cell lines

GL261 and U251 cells were grown in 6- or 12-well plates until confluent. Culture medium was replaced with an A_{2B} AR agonist (BAY 60-6583, Torcis Bioscience) or antagonist (PSB 603; Torcis Bioscience) diluted in culture medium at concentrations tested to have an optimal inhibition effect for the GL261 and U251 cells (0.1, 10, or 100 μM), or DMSO for 24 hours. Cells were washed twice with PBS, then lysed with 1% Igepal CA-630 lysis buffer or with TRIzol (Invitrogen) to collect protein or mRNA for Western blotting or qRT-PCR analysis.

Rhodamine 123 (rho-123) uptake assay

GL261 cells were grown in 96-well plates or coverslips until confluent and were treated with rho-123 (2.5 μM) and DMSO or PSB 603 (10 to 400 μM) for 4 to 24 hours. Cells were then washed with ice-cold PBS to remove extracellular rho-123. Cells in 96-well plates were lysed with 1% Igepal CA-630 lysis buffer to measure rho-123 and protein concentration with BioTek Synergy 4. Cells on coverslips were fixed and stained with anti-P-gp antibody following the immunofluorescence staining protocol.

GL261 temozolomide (TMZ) survival assay

GL261 cells grown in 12-well plates were treated with DMSO (0.54%), TMZ (30 μM), PSB 603 (100 μM), and TMZ (30 μM) + PSB 603 (100 μM) for 72 hours. TMZ stock was prepared by dissolving TMZ in DMSO (20 g/ml). Both adherent cells and cells in suspension were collected and stained with 4% Trypan blue, and viable/dead cell numbers were counted with a hemocytometer.

Experimental design and statistical analysis

All mice used in this study were age-matched male mice assigned randomly into sham or GB-implanted groups. All statistical analyses were performed on GraphPad Prism 6.0 software. *P* values were calculated using either one-way ANOVA followed by Bonferroni's post hoc test, two-way ANOVA followed by Tukey's post hoc test, or an unpaired 2-tailed Student's t test. A *p*-value of less than 0.05 was considered significant. Immunofluorescent intensity quantifications were performed using Zen software. Positive pixel count analyses were performed using ImageScope analysis program. Densitometry analysis for Western blot results were performed using ImageJ software.

Results

GB cells express CD73 and upregulates their own CD73 in CD73$^{-/-}$ mice.

To investigate whether GB expressed CD73, we first quantified CD73 expression in vitro on glioma cell lines. Both mouse GL261 and human U251 glioma cell lines expressed CD73 at 30.4% and 93.4%, respectively (**Figure 2.1A** and **B**; SD = 13.45 and 13.46 respectively). Because CD44 is commonly expressed on GL261 cells, it was used as an additional marker for GL261 identification. We observed that 9.2% of GL261 cells coexpressed CD44 and CD73 (**Figure 2.1C**; SD = 1.43). We then intracranially implanted mouse GL261 glioma cells or saline (sham) into wild-type (WT) or CD73$^{-/-}$ mice to determine whether host CD73 contributed to GB pathogenesis or if CD73 expression on GB (GB-CD73) alone was sufficient to promote GB pathogenesis.

Sham-implanted and naïve WT mice expressed abundant CD73 in specific brain regions, especially the caudoputamen (**Figure 2.1D**, **E**; $p < 0.0001$, $t = 20.04$, $df = 16$, t test, **G**, and **H**; $p < 0.0001$, $t = 38.42$, $df = 15$, t test) but not in other areas such as the cortex (**Figure 2.1D** and **F**; $p = 0.2544$, $t = 1.185$, $df = 16$, t test). This was compared with the absence of CD73 in sham-implanted and naïve CD73$^{-/-}$ mice (**Figure 2.1D**, **E**; $p < 0.0001$, $t = 20.04$, $df = 16$, t test, **G**, and **H**; $p < 0.0001$, $t = 38.42$, $df = 15$, t test). More importantly, GB-CD73 was significantly upregulated in GB-bearing CD73$^{-/-}$ mice (**Figure 2.1I** and **J**; $p = 0.0399$, $t = 2.236$, $df = 16$, t test). We also calculated the GB-CD73 protein level by subtracting the GAPDH normalized CD73 level in brain tissue in sham WT or CD73$^{-/-}$ mice from the GAPDH normalized CD73 level in respective GB-bearing mice and compared the fold change over sham WT mice (**Figure 2.1K**; $p = 0.004$, $t = 6.399$, $df = 7$, t test). We found a significant increase in GB-CD73 in CD73^{-}

$^{/-}$ mice compared with WT mice (**Figure 2.1K**; p = 0.004, t = 6.399, df = 7, t test). To investigate whether GB-CD73 was expressed on the cell surface, we performed flow cytometry analysis on tumor cells isolated 3 weeks after GB implantation and found a similar percentage of $CD73^{+}$ GB cells from both the permeabilized and non-permeabilized cell populations (**Figure 2.1L**; p = 0.096, t = 2.168, df = 4, t test). However, the median fluorescent intensity (MFI) was significantly increased in permeabilized GB cells (**Figure 2.1M** and **N**; p = 0.003, t = 6.415, df = 4, t test). This indicated that CD73 was expressed both on the cell surface and in the cytoplasm of $CD73^{+}$ GB cells. The increased GB-CD73 expression in GB-bearing $CD73^{-/-}$ mice suggests that GB either upregulates GB-CD73 expression to compensate for the absence of host CD73, or that CD73-expressing GB cells are positively selected in the absence of host CD73. This is critical because it suggests that CD73 plays a substantial role in GB pathogenesis and that host CD73 contributes to GB pathogenesis.

Figure 2.1

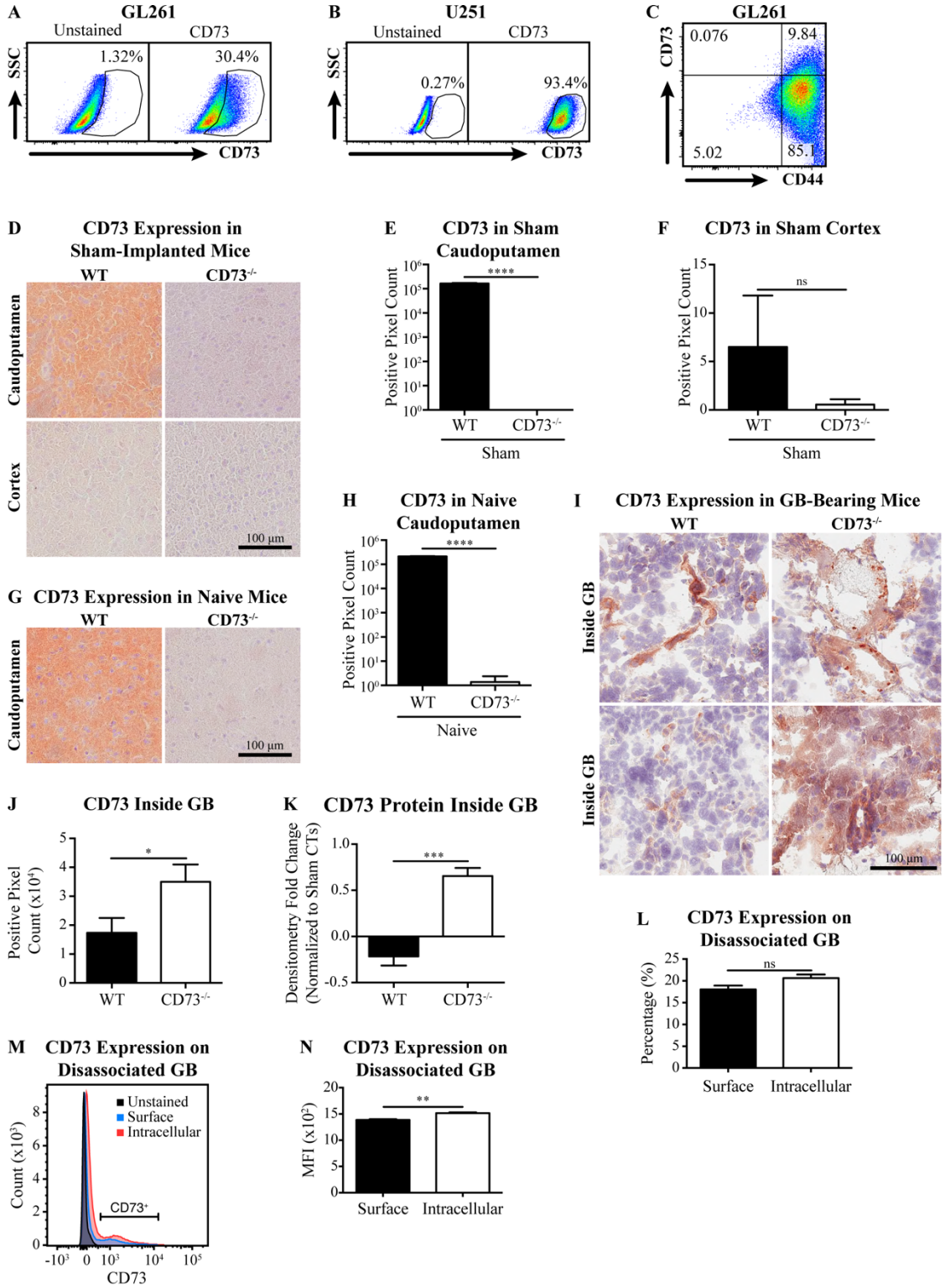
A
GL261
Unstained
CD73
1.32%
30.4%
SSC
CD73
B
U251
Unstained
CD73
0.27%
93.4%
SSC
CD73
C
GL261
CD73
0.076
9.84
5.02
85.1
CD44
D
CD73 Expression in Sham-Implanted Mice
WT
CD73-/-
Caudoputamen
Cortex
100 µm
E
CD73 in Sham Caudoputamen
Positive Pixel Count
****
WT
CD73-/-
Sham
F
CD73 in Sham Cortex
Positive Pixel Count
ns
WT
CD73-/-
Sham
G
CD73 Expression in Naive Mice
WT
CD73-/-
Caudoputamen
100 µm
H
CD73 in Naive Caudoputamen
Positive Pixel Count
****
WT
CD73-/-
Naive
I
CD73 Expression in GB-Bearing Mice
WT
CD73-/-
Inside GB
Inside GB
100 µm
J
CD73 Inside GB
Positive Pixel Count (x10⁴)
*
WT
CD73-/-
K
CD73 Protein Inside GB
Densitometry Fold Change (Normalized to Sham CTs)
***
WT
CD73-/-
L
CD73 Expression on Disassociated GB
Percentage (%)
ns
Surface
Intracellular
M
CD73 Expression on Disassociated GB
Count (x10³)
Unstained
Surface
Intracellular
CD73+
CD73
N
CD73 Expression on Disassociated GB
MFI (x10²)
**
Surface
Intracellular

Figure 2.1. GB expresses CD73 in vitro and upregulates CD73 in CD73$^{-/-}$ mice in vivo. A, **B**, Representative flow cytometry analysis of CD73 expression on GL261 (**A**) and U251 (**B**) GB cell lines. Data are representative of three experiments. **C**, Representative flow cytometry analysis of CD44 and CD73 expression on GL261. Data are representative of three experiments. **D**, **G**, Representative images of sham-implanted (**D**) and naive (**G**) mice brain sections stained with anti-CD73 antibody (brown) (n = 3). **E**, **F**, **H**, Quantification of CD73 expression in caudoputamen or cortex of sham-implanted or naive mice was performed by measuring positive pixel count using ImageScope analysis program (n = 3, three images analyzed/sample, Student's two-tailed t test). **I**, Representative images of brain sections from GL261-implanted mice stained with anti-CD73 antibody (brown) (n = 3– 4). **J**, Quantification of CD73 expression inside tumors was performed by measuring positive pixel count using ImageScope analysis program (n = 3– 4, 3 images analyzed/sample, Student's two-tailed t test). **K**, Densitometry quantification of CD73 protein expression inside tumors using ImageJ, normalizing to GAPDH and sham CTs (n = 4 –5, Student's two-tailed t test). **L**, **M**, **N**, Flow cytometry analysis of CD73 expression percentage (**L**) (n = 3, Student's two-tailed t test), histogram (**M**), and median fluorescent intensity quantification (**N**) (n = 3, Student's two-tailed t test) on disassociated tumors from GB-bearing WT mice 3 weeks after implantation (n = 3, Student's two-tailed t test). Data are shown as mean ± SEM. *$p < 0.05$, **$p \leq 0.01$, ***$p \leq 0.001$, ****$p < 0.0001$.

Host CD73 promotes GB growth and invasiveness.

To test the hypothesis that host CD73 promotes GB pathogenesis, we harvested brains from GB-bearing WT and CD73$^{-/-}$ mice and quantified GB size 17 days or 3 weeks after GB implantation. GB cells were identified by nuclear atypia, such as nuclear enlargement, pleomorphism, and hyperchromasia. The tumor border was defined as a distinct area that distinguishes between the non-neoplastic tissue and the GB tissue. GB tissue also showed distinctive tissue discoloration under H&E staining, making the tumor edge easy to identify. We found that WT mice consistently harbored significantly larger tumors compared with CD73$^{-/-}$ mice 3 weeks after implantation (**Figure 2.2A** and **B**; $p = 0.0130$, $t = 2.960$, $df = 11$, t test); this was despite the increase in GB-CD73 in CD73$^{-/-}$ mice, indicating that GB-CD73 cannot fully compensate for the lack of host CD73. GB size at day 17 after implantation also showed a similar, though not significantly different, trend of reduced GB size in CD73$^{-/-}$ mice at this time point (**Figure 2.2C** and **D**; $p = 0.58$, $t = 0.59$, $df = 4$, t test). In addition to the size difference, the tumors in WT mice were more invasive 3 weeks after implantation; they penetrated the meninges and invaded other non-neoplastic areas, whereas GBs in CD73$^{-/-}$ mice remained mainly at the site of GB implantation (**Figure 2.2A**). Because GBs generally do not metastasize but tend to invade surrounding tissues (characterized by tumor cells infiltrating non-neoplastic areas (35)), we scored GB invasion based on meningeal invasion percentage, invasion area percentage, and distance from the invaded cells to the edge of the tumor (31, 32). GBs in CD73$^{-/-}$ mice were significantly less invasive 3 weeks after implantation (**Figure 2.2A** and **E**; $p = 0.0003$, $F(2, 28) = 10.77$, ANOVA), suggesting that despite increased GB-CD73, the lack of host CD73 critically hindered GB invasiveness in CD73$^{-/-}$ mice.

Vascular expression of CD73 increases GB invasiveness.

To investigate how host CD73 promoted GB invasiveness in WT mice, we generated a CD73-FLK mouse model in which we enforced CD73 expression under the flk promoter (**Figure 2.2F**) that was specific for endothelial cells in $CD73^{-/-}$ mice. Alexiades et al. (36) have shown that flk is expressed on neuronal stem cells; therefore, we double stained naïve CD73-FLK brain tissue with the stem cell marker CD133 and CD73. However, we did not observe CD73 expression on neuronal stem cells in CD73-FLK mice (**Figure 2.2G**). We confirmed CD73 expression on the vasculature in CD73-FLK mice by immunohistochemical staining (**Figure 2.2H**). CD73 was observed on vascular structures in areas such as the dentate gyrus in CD73-FLK mice, but not in WT mice (**Figure 2.2H**), because WT endothelial cells do not express detectable levels of CD73 in vivo (37, 38). Because GB naturally tends to invade along vascular beds (39, 40) and host CD73 promotes GB invasiveness, we hypothesized that increased host CD73 along the vascular beds would further enhance GB invasiveness. Indeed, we found that GBs in CD73-FLK mice were significantly more invasive than GBs in WT mice at both 17 days and 3 weeks after implantation (**Figure 2.2A**, **C**, **E**; $p = 0.0003$, $F(2, 28) = 10.77$, ANOVA, and **I**; $p = 0.0288$, $F(2, 6) = 6.783$, ANOVA). This indicates that host CD73 expression on the vasculature significantly increases GB invasion when it is the only source of host CD73.

Host CD73 contributes more significantly to GB growth and invasiveness than GB-CD73.

To investigate whether GB-CD73 contributes to GB growth and invasiveness in addition to host CD73, we sorted GL261 mouse glioma cells and selected only CD73-negative cells (referred to as $GL261^{CD73low}$) for implantation (**Figure 2.2J**).

GL261^{CD73low} cells were cultured until confluent and were implanted into WT or CD73$^{-/-}$ mice (cells were 98.4% CD73-negative at the time of implantation (**Figure 2.2K**). Three weeks after implantation, brain tissues from GB-bearing mice were analyzed by H&E staining. We found that tumors from GL261^{CD73low}-implanted CD73$^{-/-}$ mice were significantly smaller than those from GL261^{CD73low}-implanted WT mice (**Figure 2.2L** and **M**; $p = 0.0379$, $t = 3.052$, $df = 4$, t test). Despite the difference in tumor size between WT and CD73$^{-/-}$ mice, the tumors were similar in size compared with their unsorted GL261-implanted counterparts (**Figure 2.2B**; $p = 0.0130$, $t = 2.960$, $df = 11$, t test). This suggests that host CD73 plays a greater role in promoting GB growth than GB-CD73. Interestingly, tumors from GL261^{CD73low}-implanted WT and CD73$^{-/-}$ mice and unsorted GL261-implanted WT mice all had similar invasion scores (**Figure 2.2E**; $p = 0.0003$, $F(2, 28) = 10.77$, ANOVA, and **N**; $p = 0.4167$, $t = 0.9050$, $df = 4$, t test). This suggests that GB-CD73 does not contribute significantly to GB invasiveness in WT mice and that, in the absence of both GB-CD73 and host CD73, other pathways regulating GB invasiveness may be induced to promote GB pathogenesis.

Absence of host CD73 prolongs the survival of GB-bearing mice.

To determine whether the reduction in GB size and invasiveness in GB-bearing CD73$^{-/-}$ mice is enough to increase survival in GB-bearing mice, we implanted GL261 in WT, CD73$^{-/-}$, and CD73-FLK mice; these mice were euthanized after they lost 20% of their initial weight. We found that GB-bearing CD73$^{-/-}$ mice had a significant increase in survival compared with GB-bearing CD73-FLK mice (**Figure 2.2O**; $p = 0.0362$, $df = 2$, log-rank test). This indicates that in the absence of host CD73, GB is less pathogenic and thus prolongs survival in GB-bearing mice.

Figure 2.2

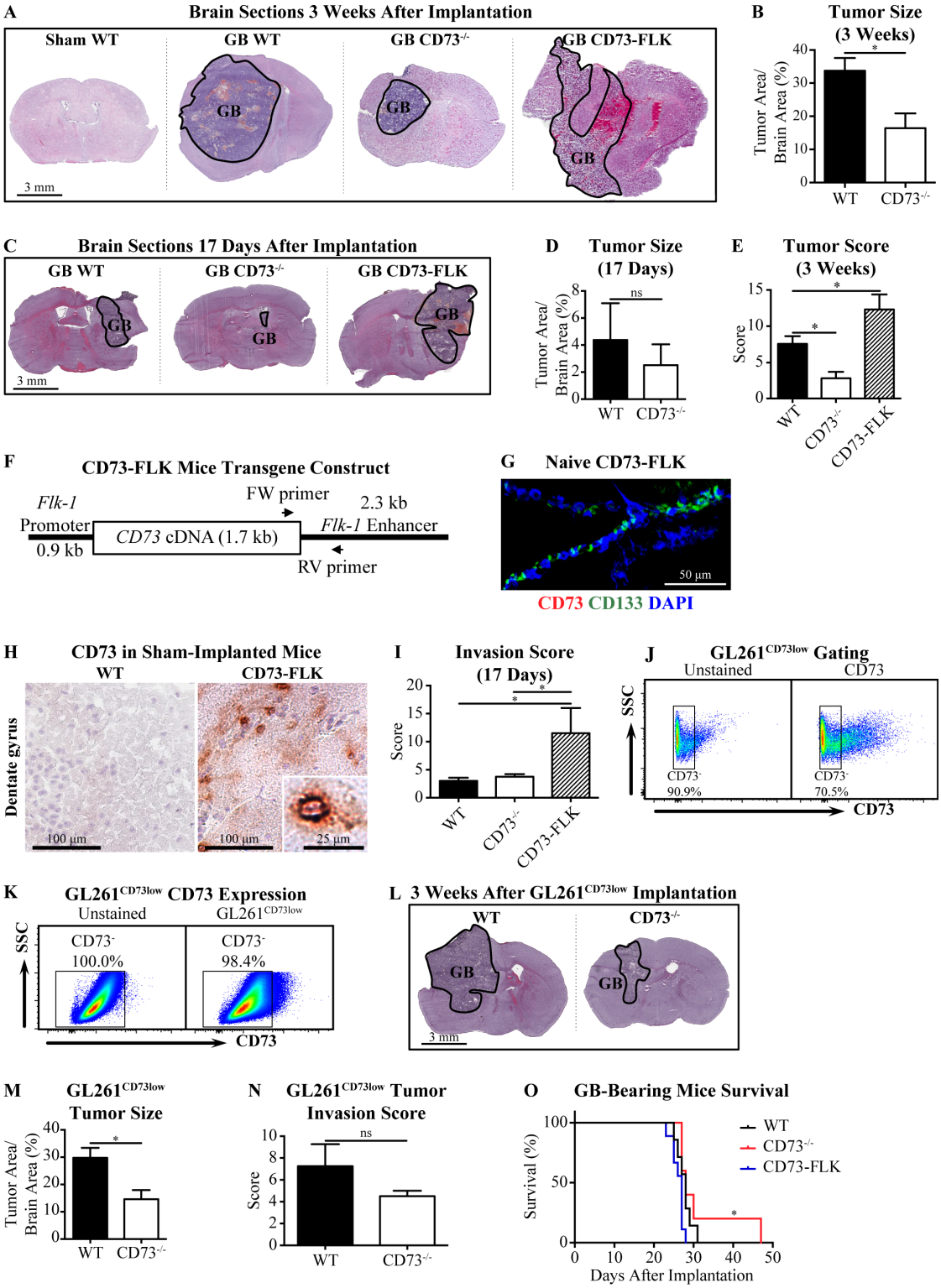
A
Brain Sections 3 Weeks After Implantation
Sham WT
GB WT
GB CD73-/-
GB CD73-FLK
GB
3 mm
B
Tumor Size (3 Weeks)
Tumor Area/ Brain Area (%)
WT
CD73-/-
C
Brain Sections 17 Days After Implantation
GB WT
GB CD73-/-
GB CD73-FLK
D
Tumor Size (17 Days)
ns
E
Tumor Score (3 Weeks)
Score
CD73-FLK
F
CD73-FLK Mice Transgene Construct
Flk-1 Promoter
0.9 kb
CD73 cDNA (1.7 kb)
FW primer
2.3 kb
Flk-1 Enhancer
RV primer
G
Naive CD73-FLK
50 µm
CD73 CD133 DAPI
H
CD73 in Sham-Implanted Mice
WT
CD73-FLK
Dentate gyrus
100 µm
25 µm
I
Invasion Score (17 Days)
J
GL261CD73low Gating
Unstained
CD73
SSC
CD73-
90.9%
70.5%
K
GL261CD73low CD73 Expression
Unstained
GL261CD73low
100.0%
98.4%
L
3 Weeks After GL261CD73low Implantation
M
GL261CD73low Tumor Size
N
GL261CD73low Tumor Invasion Score
O
GB-Bearing Mice Survival
Survival (%)
Days After Implantation

Figure 2.2. Host CD73 promotes GB growth and invasion. A, **C**, Representative H&E-stained brain sections from GL261- or sham-implanted mice 3 weeks after implantation (**A**) (n = 6–7 per group) or 17 d after implantation (C) (n = 3 per group). Solid black lines are tumor borders. **B**, **E**, Quantification of H&E-stained brain sections (n = 6–7 per group, Student's two-tailed t test and one-way ANOVA, respectively). **B**, **D**, **M**, Tumor size is quantified by percentage of tumor area as follows: (tumor area/brain section area) X100. **E**, **I**, **N**, Tumor invasiveness was scored based on invasion area, invasion distance, and meningeal invasion. (**D**, **I**, **M**, **N**) (n = 3 per group, Student's two-tailed t test for **D**, **M**, and **N** and one-way ANOVA for **I**). **F**, Schematic of CD73-FLK mice transgene construct. FW, Forward; RV, reverse. **G**, Representative images of naïve CD73-FLK mice brain sections stained with anti-CD73 antibody (red), CD133 (green), and DAPI (blue) (n = 3). **H**, Representative images of sham-implanted WT and CD73-FLK mice brain sections stained with anti-CD73 antibody (brown) (n = 3). **J**, CD73-negative gating used for sorting GL261 cells. **K**, Flow cytometry analysis of CD73 expression on GL261^{CD73low} cells. **L**, H&E-stained brain sections from GL261^{CD73low}-implanted mice 3 weeks after implantation (n = 3). Solid black lines are tumor borders. **O**, GL261-implanted mice survival (n = 5–9 per group, log-rank test). Data are shown as mean ± SEM. *$p < 0.05$.

Absence of host CD73 inhibits GB angiogenesis and promotes glomeruloid vessel formation.

Because GB size was significantly reduced in CD73$^{-/-}$ mice and angiogenesis is a key factor in regulating tumor growth, we next investigated whether host CD73 regulated GB angiogenesis. We found a significant decrease in vessel density within the tumors of CD73$^{-/-}$ and CD73-FLK mice (**Figure 2.3A** and **B**; $p < 0.0001$, $F(5, 37) = 16.37$, ANOVA). Interestingly, compared with WT mice, the vessel diameter and the number of glomeruloid vessels within the tumors were increased in CD73$^{-/-}$ and CD73-FLK mice (**Figure 2.2A**, **C**; $p = 0.0140$, $F(2, 12) = 6.228$, ANOVA, and **D**; $p = 0.0036$, $F(2, 32) = 6.740$ respectively, ANOVA). Because glomeruloid vessels are formed by highly proliferative endothelial cells (41), we investigated whether these GBs showed increased expression of the proliferation marker Ki-67. Indeed, Ki-67 expression was upregulated in glomeruloid vessels compared with non-glomeruloid vessels in GB (**Figure 2.3E** and **F**; $p = 0.0001$, $t = 4.007$, $df = 91$, t test). In addition to nuclear Ki-67 staining, we also observed a high Ki-67 expression outside of the nucleus in glomeruloid vessels. Even though Ki-67 is mainly found in the nucleus, membrane and cytoplasmic Ki-67 expression have been found in other cancers, including breast cancer and laryngeal squamous cell carcinoma (42, 43). Therefore, the cytoplasmic Ki-67 expression observed in glomeruloid vessels was likely real. This increase in Ki-67 expression indicates that increased GB-CD73 in CD73$^{-/-}$ mice and increased host CD73 on the vasculature in CD73-FLK mice promote intravascular endothelial cell proliferation. However, in the absence of the full complement of host CD73 (such as in WT mice), proliferating endothelial cells cannot adequately form new vessels, suggesting that both GB-CD73 and host CD73 regulate GB angiogenesis.

Figure 3

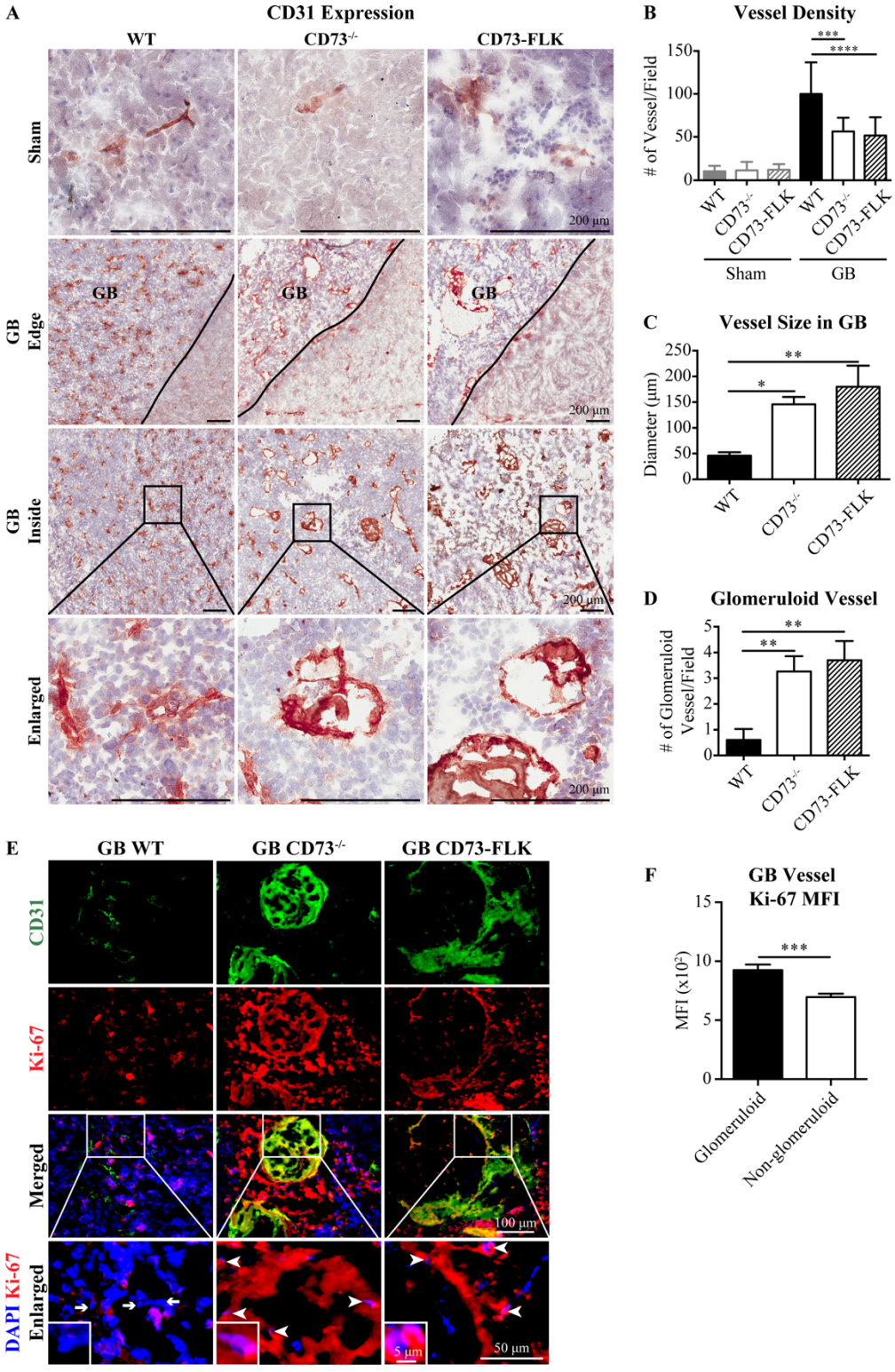
A
CD31 Expression
WT
CD73-/-
CD73-FLK
Sham
GB Edge
GB Inside
Enlarged
GB
200 μm
B
Vessel Density
# of Vessel/Field
***
****
WT
CD73-/-
CD73-FLK
Sham
GB
C
Vessel Size in GB
Diameter (μm)
**
*
D
Glomeruloid Vessel
# of Glomeruloid Vessel/Field
E
GB WT
GB CD73-/-
GB CD73-FLK
CD31
Ki-67
Merged
DAPI Ki-67
Enlarged
100 μm
5 μm
50 μm
F
GB Vessel Ki-67 MFI
MFI (x10²)
Glomeruloid
Non-glomeruloid

Figure 2.3. Absence of host CD73 inhibits GB angiogenesis and promotes glomeruloid vessel formation. **A**, Representative images of brain sections from GL261- or sham-implanted mice stained with anti-CD31 antibody (brown) (n = 4–6 per GB-implanted group and n = 2 for sham-implanted group). **B**, Quantification of vessel number per area (1.5 mm^2) (n = 3– 6 per GB-implanted group and n = 2 per sham-implanted group, three images analyzed/sample, one-way ANOVA). **C**, Vessel diameter measured by ImageScope software (n = 4–6 per group, three images analyzed/sample, one-way ANOVA). **D**, Quantification of glomeruloid vessel number per area (1.5 mm^2) (n = 3–5 per group, 10 vessels analyzed/sample, one-way ANOVA). **E**, Representative images of brain sections from GL261-implanted mice 3 weeks after implantation stained with anti-CD31 (green), anti-Ki-67 antibody (red), and DAPI (blue). Arrowheads indicate Ki-67 endothelial nuclear expression and arrows indicate the absence of Ki-67 expression in endothelial nuclei (n = 3– 4 per group). **F**, Ki-67 mean fluorescent intensity (MFI) quantified using Zen image analysis program (n = 10, 3 images analyzed/sample, 3 areas analyzed/image, Student's two-tailed t test). Data are shown as mean ± SEM. *$p < 0.05$, **$p \leq 0.01$, ***$p \leq 0.001$, ****$p < 0.0001$.

Host CD73 promotes GB angiogenesis via regulation of VEGF and α-dystroglycan.

We next investigated whether CD73 regulated angiogenesis-related factors that contributed to the dramatic differences observed in GB vessel phenotype between GB-bearing WT and $CD73^{-/-}$ mice. We found that VEGF closely lined GB-associated blood vessels in CD73-FLK mouse (**Figure 2.4A**), supporting its role in GB angiogenesis. Further, we observed increased VEGF protein expression on GBs in $CD73^{-/-}$ mice (**Figure 2.4B**, **C**; $p < 0.0001$, $F(3, 276) = 33.32$, ANOVA, and **D**; $p = 0.0084$, $F(3, 18) = 5.316$, ANOVA), which could lead to intravascular proliferation and increased glomeruloid vessels. This also suggests that increased GB-CD73 in GB-bearing $CD73^{-/-}$ mice promotes VEGF expression. However, the decreased vessel number indicates that host CD73 is critical for GBs to form vascular beds required for their growth and expansion.

The decrease in vessel density despite increased VEGF in GB-bearing $CD73^{-/-}$ mice was likely a result of reduced endothelial cell migration. Therefore, we next investigated the expression of α-dystroglycan. α-dystroglycan is a membrane receptor that tethers the basement membranes on vessels to endothelial cells and is involved in angiogenesis regulation, endothelial cell migration, and tube formation (44, 45). We observed a significant increase in α-dystroglycan expression around $CD31^{+}$ endothelial cells inside GBs in $CD73^{-/-}$ mice compared with GBs in WT mice (**Figure 2.4E** and **F**; $p < 0.0001$, $F(3, 61) = 32.05$, ANOVA). This suggests that host CD73 inhibits α-dystroglycan expression in GB and that increased α-dystroglycan and VEGF promotes glomeruloid vessel formation in GB. Further, reduction in α-dystroglycan expression is also associated with poor prognosis for human GB (46), suggesting that the absence of host CD73 leads to a an improved prognosis for GB patients.

Figure 2.4

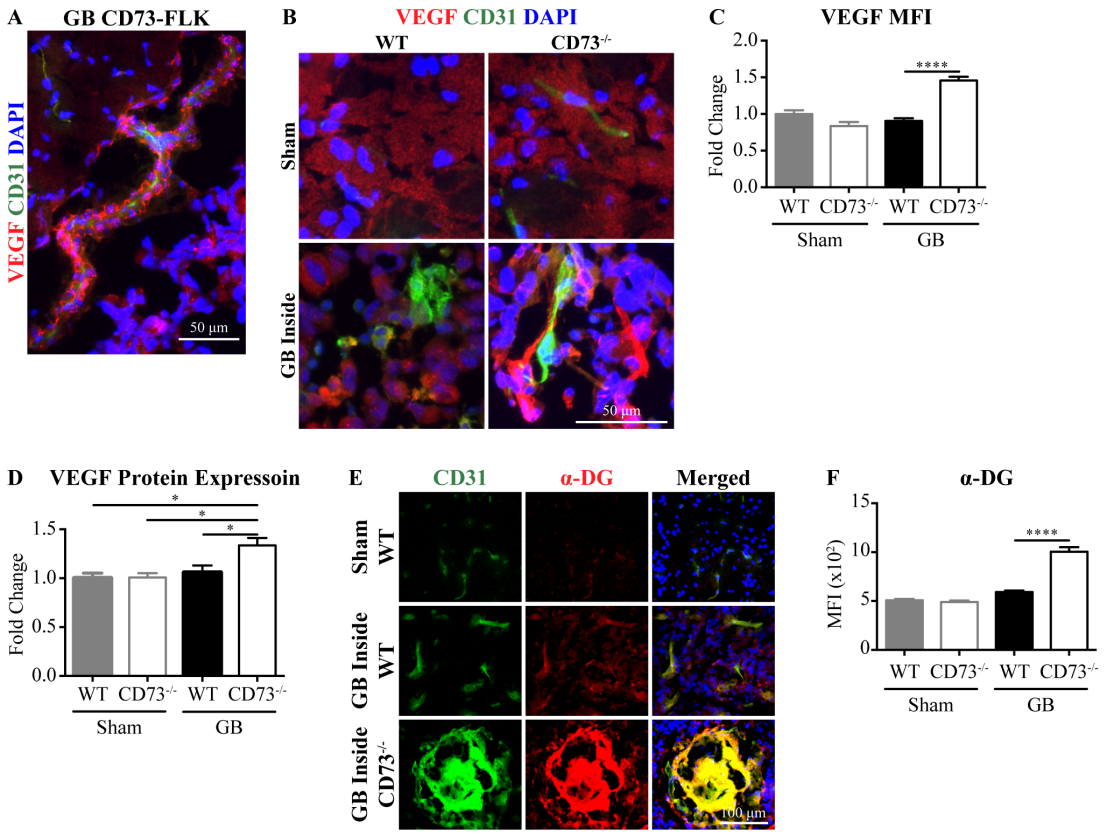
A
GB CD73-FLK
VEGF CD31 DAPI
50 µm
B
VEGF CD31 DAPI
WT
CD73-/-
Sham
GB Inside
50 µm
C
VEGF MFI
Fold Change
2.0
1.5
1.0
0.5
0.0
****
WT CD73-/- WT CD73-/-
Sham
GB
D
VEGF Protein Expressoin
Fold Change
1.5
1.0
0.5
0.0
*
*
*
WT CD73-/- WT CD73-/-
Sham
GB
E
CD31
α-DG
Merged
Sham WT
GB Inside WT
GB Inside CD73-/-
100 µm
F
α-DG
MFI (x10²)
15
10
5
0
****
WT CD73-/- WT CD73-/-
Sham
GB

Figure 2.4. Host CD73 promotes GB angiogenesis via regulating VEGF and α-dystroglycan. A, **B**, Representative images of brain sections from GL261- or sham-implanted mice stained with anti-CD31 (green), anti-VEGF antibody (red), and DAPI (blue) (n = 4–5 per GB-implanted group and n = 2 per sham-implanted group). **C**, VEGF mean fluorescent intensity (MFI) quantified using Zen image analysis program (n = 4–5 per GB-implanted group and n = 2 per sham-implanted group, 2– 6 images analyzed/sample, one-way ANOVA). **D**, Western blot densitometry analysis of VEGF (n = 5–7 per group, one-way ANOVA). **E**, Representative images of brain sections from GL261- or sham-implanted mice (3 weeks after implantation) stained with anti-CD31 (green), anti-α-dystroglycan antibody (red), and DAPI (blue); images taken from inside the tumor (n = 3– 4 per GB-implanted group and n = 2 per sham-implanted group). **F**, α-dystroglycan MFI inside the tumor quantified using Zen image analysis program (n = 3–4 per GB-implanted group and n = 2 per sham-implanted group, five areas analyzed/sample, one-way ANOVA). Data are shown as mean ± SEM. *$p < 0.05$, ****$p < 0.0001$.

Host CD73 promotes GB angiogenesis and invasiveness through regulation of matrix metalloproteinases (MMPs).

Because both angiogenesis and invasion require remodeling of the extracellular matrix, which is often performed by MMP activity, we next investigated whether CD73 regulated MMPs and/or their inhibitors, tissue inhibitor of matrix metalloproteinases (TIMPs). We found MMP2 expression surrounding the vessels of GB, labeled by CD31 (**Figure 2.5A** and **B**), and it was significantly higher in GB-implanted $CD73^{-/-}$ and CD73-FLK mice (**Figure 2.5C**; $p < 0.0001$, $F(2, 27) = 16.87$, ANOVA). Conversely, the MMP2 inhibitor TIMP2 mRNA expression was similar between $CD73^{-/-}$, CD73-FLK, and WT GB-implanted mice (**Figure 2.5D**; $p = 0.3036$, $F(3, 22) = 1.287$, ANOVA). This suggests that CD73 regulates MMP2 expression but not TIMP2 expression in GB and that increased GB-CD73 expression in a host with little or no CD73 promotes MMP2 upregulation.

We next examined MMP9 in WT and $CD73^{-/-}$ mice and found strong MMP9 expression lining the tumor's edge (**Figure 2.5E**, **F**, and **G**), which was consistent with its role in GB invasion. Interestingly, MMP9 expression at the edge of the tumor was highest in CD73-FLK mice (**Figure 2.5H**; $p < 0.0001$, $F(2, 27) = 13.22$, ANOVA), suggesting that the increased MMP9 contributed to the increased invasiveness observed in these mice (**Figure 2.2A**, **C**, **E**; $p = 0.0003$, $F(2, 28) = 10.77$, ANOVA, and **H**; $p = 0.0288$, $F(2, 6) = 6.783$, ANOVA) and that host CD73 expression on endothelial cells increased MMP9 expression on the edge of GBs. Even more interestingly, the expression of the MMP9 inhibitor TIMP1 was significantly higher in GB-implanted $CD73^{-/-}$ mice (**Figure 2.5G** and **I**; $p < 0.0001$, $F(2, 187) = 78.35$, ANOVA). This indicates that host CD73 inhibits TIMP1 expression and that MMP9 activity was

inhibited in GB-bearing CD73$^{-/-}$ mice, leading to decreased GB invasiveness (**Figure 2.2A** and **C**, **E**; $p = 0.0003$, $F (2, 28) = 10.77$, ANOVA, and **H**; $p = 0.0288$, $F (2, 6) = 6.783$, ANOVA). Moreover, TIMP1 expression was significantly lower in GB-bearing CD73-FLK mice compared with WT mice (**Figure 2.5G** and **I**; $p < 0.0001$, $F (2, 187) = 78.35$, ANOVA). This suggests that host CD73 expression on endothelial cells contributes greatly to TIMP1 inhibition and results in increased GB invasiveness in CD73-FLK mice (**Figure 2.2A** and **C**, **E**; $p = 0.0003$, $F (2, 28) = 10.77$, ANOVA, and **H**; $p = 0.0288$, $F (2, 6) = 6.783$, ANOVA). Furthermore, to determine whether MMP activity was altered in our GB models, we incubated tissue homogenates collected from sham and GB-implanted brain tissues with fluorescence resonance energy transfer (FRET) MMP substrate peptide as a MMP activity indicator. We found that MMP activity was significantly lower in homogenates from GB-bearing CD73$^{-/-}$ mice (**Figure 2.5J**; $p = 0.0465$, $df = 11$, $t = 2.242$, t test). This indicates that, despite the increase in MMP2 expression, the overall MMP activity in GB-bearing CD73$^{-/-}$ mice is decreased compared with GB-bearing WT mice. This suggests that host CD73 regulates MMP activity in GB, increasing MMP9 expression and inhibiting TIMP1 to promote GB invasiveness. Therefore, increased GB-CD73 alone cannot compensate for the lack of host CD73 in regulating MMP activity.

Figure 2.5

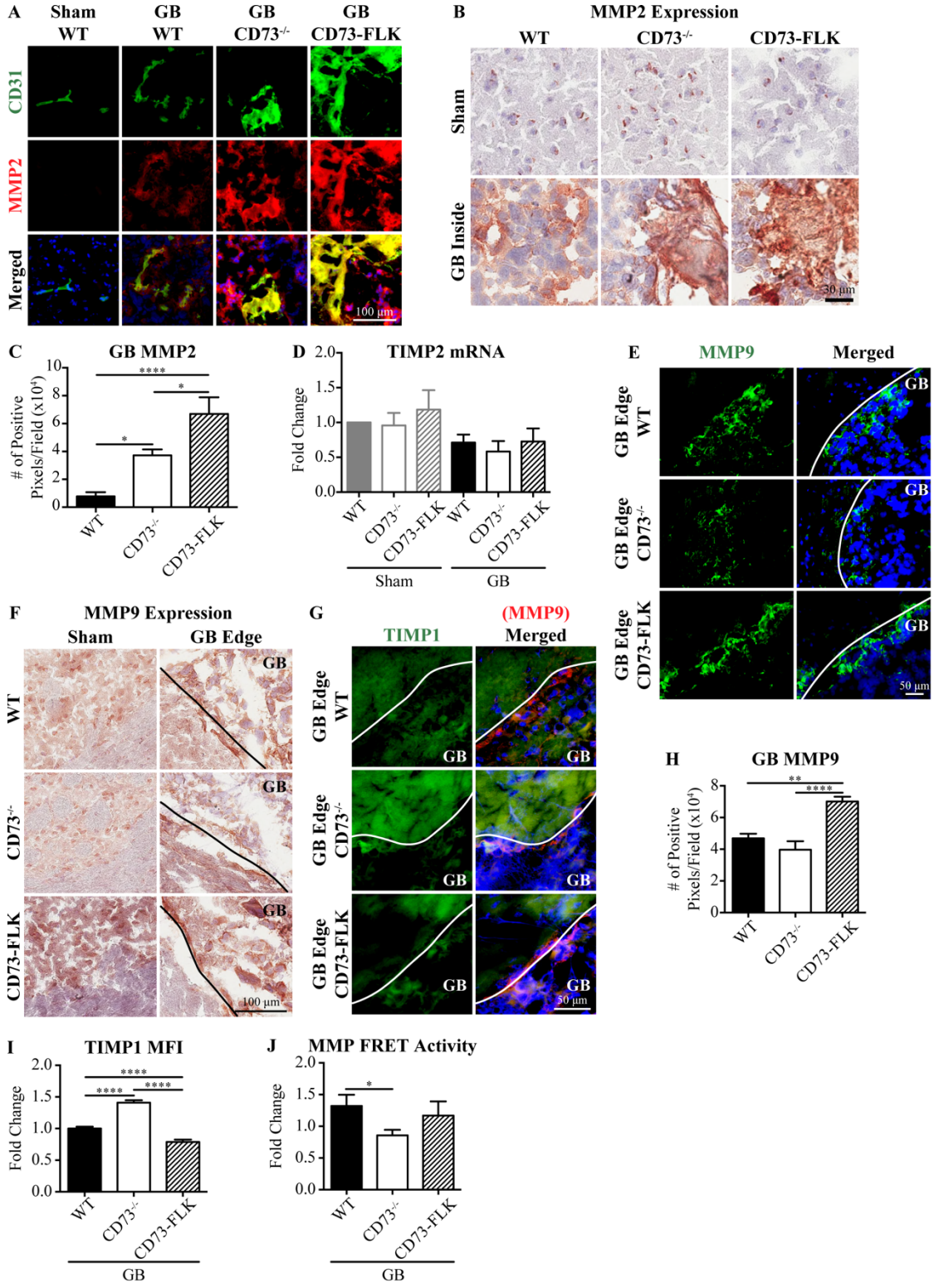
A
Sham WT
GB WT
GB CD73-/-
GB CD73-FLK
CD31
MMP2
Merged
100 μm
B
MMP2 Expression
WT
CD73-/-
CD73-FLK
Sham
GB Inside
30 μm
C
GB MMP2
# of Positive Pixels/Field (x10⁴)
WT
CD73-/-
CD73-FLK
D
TIMP2 mRNA
Fold Change
Sham
GB
E
MMP9
Merged
GB Edge WT
GB Edge CD73-/-
GB Edge CD73-FLK
GB
50 μm
F
MMP9 Expression
Sham
GB Edge
WT
CD73-/-
CD73-FLK
100 μm
G
TIMP1
(MMP9)
Merged
H
GB MMP9
I
TIMP1 MFI
J
MMP FRET Activity

Figure 2.5. CD73 regulates MMP2, MMP9, and TIMP1 to promote GB invasiveness and angiogenesis. **A**, Representative images of brain sections from GL261- or sham-implanted mice (3 weeks after implantation) stained with anti-CD31 (green), anti-MMP2 antibody (red), and DAPI (blue) (n = 3– 4 per GB-implanted group and n = 2 per sham-implanted group). **B**, Representative images of brain sections from GL261- or sham-implanted mice (3 weeks after implantation) stained with anti-MMP2 antibody (brown) (n = 3– 4 per GB-implanted group and n = 2 per sham-implanted group). **C**, MMP2 immunohistochemistry staining positive pixel count was quantified using ImageScope analysis program (n = 3– 4 per group, three images analyzed/sample, one-way ANOVA). **D**, qRT-PCR analysis of TIMP2 mRNA collected from GL261- or sham-implanted mice (3 weeks after implantation) (n = 8 –11 per GB-implanted group and n = 2–3 per sham-implanted group, one-way ANOVA). **E**, Representative images of brain sections from GL261- or sham-implanted mice (3 weeks after implantation) stained with anti-MMP9 antibody (green) and DAPI (blue); images taken from the edge of the tumor (n = 3– 4 per GB-implanted group and n = 2 per sham-implanted group). **F**, Representative images of brain sections from GL261- or sham-implanted mice (3 weeks after implantation) stained with anti-MMP9 antibody (brown) (n = 3–4 per GB-implanted group and n = 2 per sham-implanted group). **G**, Representative images of brain sections from GL261- or sham-implanted mice (3 weeks after implantation) stained with anti-TIMP1 (green), anti-MMP9 antibody (red), and DAPI (blue); images taken from the edge of the tumor (n = 4–5 per GB-implanted group and n = 2 per sham-implanted group). **H**, MMP9 immunohistochemistry staining positive pixel count on the tumor edge quantified using ImageScope analysis program (n = 3– 4 per group, three images analyzed/sample, one-way ANOVA). **I**, TIMP1 MFI in brain sections quantified using Zen image analysis program (n = 4 –5, three images analyzed/sample, one-way

ANOVA). **J**, MMP activity of brain tissue homogenates from GB-bearing mice (3 weeks after implantation) normalized to sham-implanted CTs (n = 4 –7, Student's two-tailed t test). Data are shown as mean ± SEM. *$p < 0.05$, **$p \leq 0.01$, ****$p < 0.0001$.

GB upregulates the A_{2B} AR in vivo.

To elucidate whether CD73 regulated GB pathogenesis through AR signaling, we first compared AR expression on GB with AR expression on mouse primary astrocytes from which the GB cells originated. The primary astrocytes we isolated expressed the astrocyte marker glial fibrillary acidic protein (GFAP), but not the neuronal marker (NeuN) (**Figure 2.6A**). GL261 cells in vitro expressed A_1, A_{2A}, and A_{2B} AR proteins at levels similar to that of primary astrocytes, whereas the A_3 AR was expressed at a much lower level (**Figure 2.6B**; $p = 0.0002$, $t = 12.73$, $df = 4$, t test). Similarly, the human U251 GB cells expressed all four adenosine receptors (**Figure 2.6C**). When we examined AR expression on sham or GB-implanted mice brain sections, A_1 and A_3 AR expression were similar between sham mice and inside GB in both WT and $CD73^{-/-}$ mice (**Figure 2.6D**, **E** and **G**; $p = 0.0043$, $F(3, 153) = 4.557$, ANOVA). A_{2A} AR expression was lower in GB-bearing $CD73^{-/-}$ mice, but it was not significantly different between GB and sham-implanted WT mice (**Figure 2.6F** and **G**; $p = 0.0043$, $F(3, 153) = 4.557$, ANOVA). However, we found that the A_{2B} AR expression was significantly upregulated by almost 20-fold in GB compared with sham in vivo, whereas very little expression was found on astrocytes in sham-implanted mice stained with the astrocyte marker GFAP (**Figure 2.6F**; $p = 0.0043$, $F(3, 153) = 4.557$, ANOVA, and **H**). This indicates that astrocytes express very low levels of the A_{2B} AR in vivo, whereas transformed GB cells highly upregulate the A_{2B} AR in vivo. This is consistent with previous reports of low or diminished A_{2B} AR expression under basal conditions (12). Because the A_{2B} AR is often activated under pathological conditions with high extracellular adenosine concentrations (in the μM range) and it was highly upregulated in GBs in vivo, we further investigated the role the A_{2B} AR plays in GB pathogenesis.

GB A_{2B} AR signaling increases MMP2 mRNA expression and MMP activity.

To investigate whether CD73 promoted GB MMP activity through A_{2B} AR signaling, we treated mouse GL261 glioma cells with the A_{2B} AR agonist BAY 60-6583 and found that activation of the A_{2B} AR upregulated MMP2 mRNA expression (**Figure 2.6I**; p = 0.0040, F (2, 14) = 8.412, ANOVA). This suggests that the upregulation of GB-CD73 in $CD73^{-/-}$ mice (**Figure 2.1J**; p = 0.0399, t = 2.236, df = 16, t test) increases A_{2B} AR signaling on GBs, which leads to increased MMP2 expression in GBs in $CD73^{-/-}$ mice. We found no difference in MMP9, TIMP1, and TIMP2 mRNA levels in GL261 cells upon A_{2B} AR agonist treatment (**Figure 2.6J**; p = 0.8896, F (2,15) = 0.1178, ANOVA, **K**; p = 0.8343, F (2, 15) = 0.1834, ANOVA, and **L**; p = 0.2283, F (2, 15) = 1.633, ANOVA). This suggests that the increased MMP9 in GB-bearing CD73-FLK mice and the increased TIMP1 in GB-bearing $CD73^{-/-}$ mice are not regulated by A_{2B} AR signaling on GB cells. Because TIMP2 expression was not altered in vivo in GB-bearing $CD73^{-/-}$ mice or in vitro through A_{2B} AR signaling on GBs, it is plausible that TIMP2 is not regulated by CD73. To determine whether changes in MMP2 mRNA expression induced by the A_{2B} AR led to changes in MMP activity, we treated the mouse glioma cell line GL261 with the A_{2B} AR antagonist PSB 603 and the FRET MMP substrate peptide as a MMP activity indicator. We found that the A_{2B} AR antagonist significantly decreased GL261 MMP activity (**Figure 2.6M**; p = 0.0216, F (2, 15) = 5.010, ANOVA), suggesting that A_{2B} AR signaling on GB cells contributed to the regulation of GB-MMP activity.

Figure 2.6

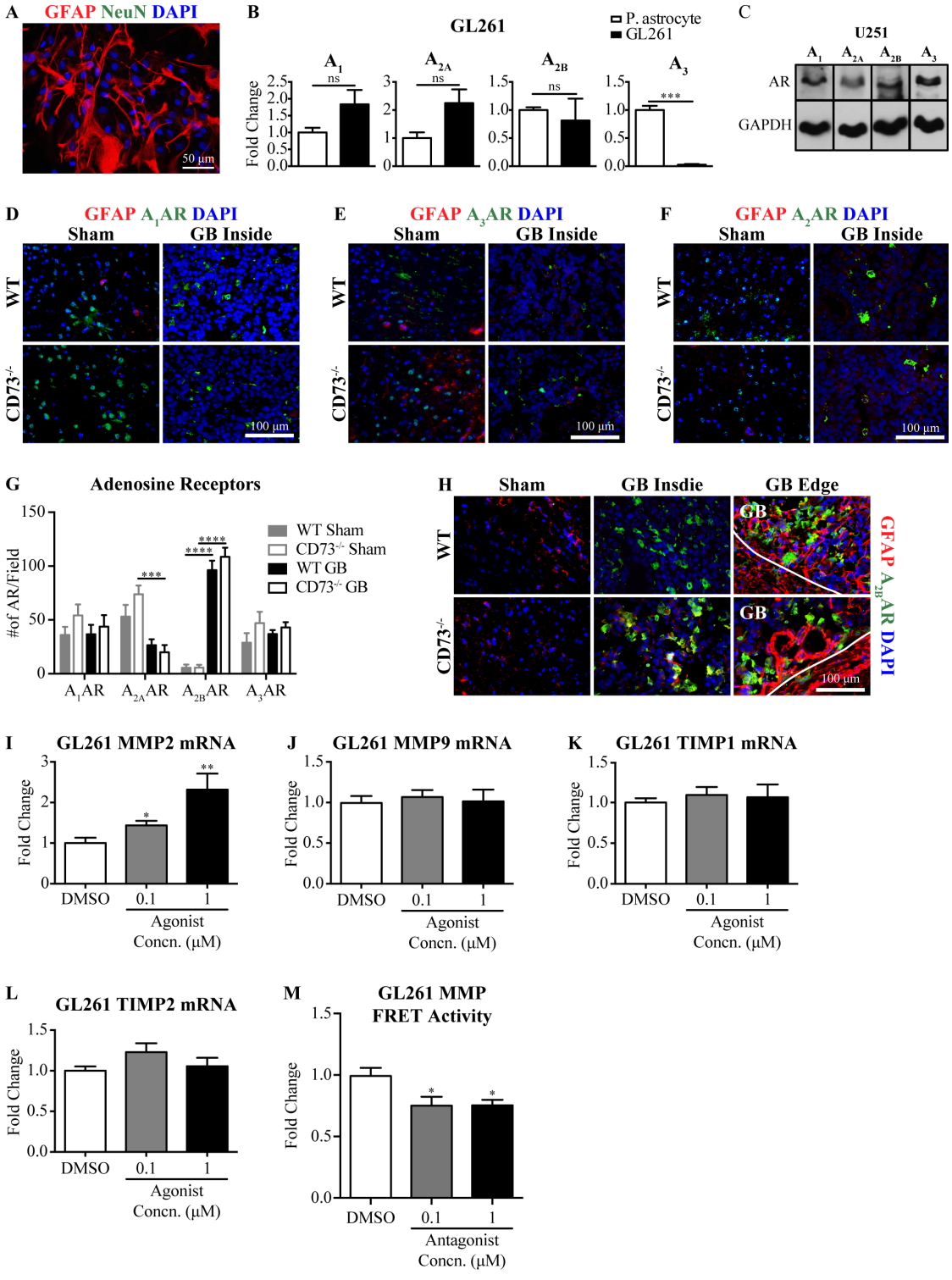
A
GFAP NeuN DAPI
50 µm
B
GL261
P. astrocyte
GL261
A1
A2A
A2B
A3
ns
ns
ns
***
Fold Change
C
U251
A1
A2A
A2B
A3
AR
GAPDH
D
GFAP A1AR DAPI
Sham
GB Inside
WT
CD73-/-
100 µm
E
GFAP A3AR DAPI
Sham
GB Inside
WT
CD73-/-
100 µm
F
GFAP A2AR DAPI
Sham
GB Inside
WT
CD73-/-
100 µm
G
Adenosine Receptors
#of AR/Field
WT Sham
CD73-/- Sham
WT GB
CD73-/- GB
***
****
****
A1AR
A2AAR
A2BAR
A3AR
H
Sham
GB Insdie
GB Edge
WT
CD73-/-
GB
GB
100 µm
GFAP A2BAR DAPI
I
GL261 MMP2 mRNA
Fold Change
DMSO
0.1
1
Agonist
Concn. (µM)
J
GL261 MMP9 mRNA
Fold Change
DMSO
0.1
1
Agonist
Concn. (µM)
K
GL261 TIMP1 mRNA
Fold Change
DMSO
0.1
1
Agonist
Concn. (µM)
L
GL261 TIMP2 mRNA
Fold Change
DMSO
0.1
1
Agonist
Concn. (µM)
M
GL261 MMP
FRET Activity
Fold Change
DMSO
0.1
1
Antagonist
Concn. (µM)

Figure 2.6. GB upregulates A_{2B} AR, and signaling through A_{2B} AR promotes MMP2 expression on GB. A, Representative image of primary astrocyte stained with anti-GFAP antibody (red), anti-NeuN (green), and DAPI (blue). **B**, Densitometry quantification of ARs protein expression in GL261 cells and in primary mouse astrocytes using ImageJ and normalizing to GAPDH (n = 3, Student's two-tailed t test). **C**, Western blot analysis of ARs on human U251 cells (n = 4). **D**–**F**, Representative images of brain sections from GL261- or sham-implanted mice (3 weeks after implantation) stained with anti-GFAP antibody (red), DAPI (blue), and anti-A_1 AR (green) (**D**), anti-A_3 AR (**E**), or anti-A_{2A} AR (**F**) (n = 3–4 per group). **G**, Number of ARs per microscopic field (n = 3–8 per group, two-way ANOVA). **H**, Representative images of brain sections from GL261- or sham-implanted mice (3 weeks after implantation) stained with anti-A2B AR (green), anti-GFAP antibody (red), and DAPI (blue) (n = 5– 6 per GB-implanted group and n = 2 per sham-treated group). **I**–**L**, qRT-PCR analysis of MMP2 (**I**), MMP9 (**J**), TIMP1 (**K**), and TIMP2 (**L**) mRNA from GL261 treated with BAY 60–6583 (n = 6, one-way ANOVA for **I**–**L**). **M**, MMP FRET activity of GL261 cells treated with BAY 60–6583 (n = 6, one-way ANOVA). Data are shown as mean ± SEM. *$p < 0.05$, **$p \leq 0.01$, ***$p \leq 0.001$, ****$p < 0.0001$.

A_{2B} AR signaling blockade downregulates GB multidrug resistance (MDR) transporter function and increases GB chemosensitivity.

GB is resistant to most chemotherapy partly because it highly expresses MDR transporters such as the P-glycoprotein (P-gp) and the multidrug resistance-associated protein (MRP1) (47) (**Figure 2.7A** and **B**), which expel chemotherapeutic drugs from tumor cells. Our lab has shown that activation of the A_{2A} AR increases BBB permeability by modulating P-gp function in brain endothelial cells (48–50). Because P-gp, MRP1, and the A_{2B} AR were all highly upregulated in GB in vivo (**Figure 2.7C**; $p < 0.0001$, $F (3, 71) = 17.15$, ANOVA, **D**; $p < 0.0001$, $F (3, 77) = 28.34$, ANOVA**,** 6F; $p = 0.0043$, $F (3, 153) = 4.557$, ANOVA, and **G**) and MRP1 and P-gp expression were significantly higher in GB in $CD73^{-/-}$ mice (**Figure 2.7C**; $p < 0.0001$, $F (3, 71) = 17.15$, ANOVA and **D**; $p < 0.0001$, $F (3, 77) = 28.34$, ANOVA), we hypothesized that signaling through the A_{2B} AR induced the upregulation of P-gp and/or MRP1 in GB. Indeed, treatment of GL261 cells with an A_{2B} AR-specific antagonist (PSB 603) dose-dependently decreased both P-gp and MRP1 protein expression (**Figure 2.7E**; $p = 0.0002$, $F (2, 19) = 14.15$, ANOVA and **F**; $p = 0.0123$, $F (2, 6) = 9.980$, ANOVA). Moreover, A_{2B} AR antagonist treatment of U251 cells also resulted in a significant decrease in P-gp mRNA expression levels (**Figure 2.7G**; $p = 0.0188$, $F (2, 5) = 9.748$, ANOVA), indicating that A_{2B} AR signaling regulated MDR transporters both in human and mouse GB. This suggests that the increased GB-CD73 in $CD73^{-/-}$ mice (**Figure 2.1J**; $p = 0.0399$, $t = 2.236$, $df = 16$, t test) results in increased activation of the A_{2B} AR, and thus increases P-gp and MRP1 in GB in $CD73^{-/-}$ mice (**Figure 2.7C**; $p < 0.001$, $F (3, 71) = 17.15$, ANOVA and **D**; $p < 0.001$, $F (3, 77) = 28.34$, ANOVA).

To investigate whether inhibition of A_{2B} AR signaling led to increased P-gp

substrate uptake, we concomitantly treated GL261 cells with the P-gp substrate rhodamine 123 (rho-123) and the A_{2B} AR antagonist PSB 603 and measured intracellular rho-123 uptake (**Figure 2.7H**). We found that inhibition of the A_{2B} AR led to increased intracellular rho-123 concentrations in the tumor cells (**Figure 2.7I** and **J**; $p = 0.0277$, $t = 2.889$, $df = 6$, t test), suggesting that inhibiting A_{2B} AR signaling led to increased intracellular accumulation of P-gp substrate by downregulating P-gp expression. Because $CD31^+$ endothelial cells in GBs strongly upregulated P-gp and MRP1 (**Figure 2.7A** and **B**), we hypothesized that GBs regulated MDR transporters on host endothelial cells by signaling through the A_{2B} AR to promote GB chemoresistance. We found that inhibition of the A_{2B} AR on primary mouse brain endothelial cells also downregulated P-gp expression (**Figure 2.7K**; $p = 0.0414$, $F (2, 4) = 7.829$, ANOVA), suggesting that increased extracellular adenosine level during pathological conditions (12), such as in the GB microenvironment, could potentially alter host endothelial cells of the BBB through the A_{2B} AR and alter BBB permeability to promote chemoresistance.

We next investigated whether A_{2B} AR antagonist treatment increased GB sensitivity to chemotherapeutic drugs by treating GL261 cells with temozolomide (TMZ, 30 μM), a known P-gp substrate (51), in the presence or absence of A_{2B} AR antagonist treatment for 3 days and then quantified the number of live/dead cells (**Figure 2.7L**). TMZ treatment alone did not increase the percentage of dead cells but decreased the total number of cells compared with controls (**Figure 2.7M**; $p < 0.0001$, $F (3, 8) = 279.9$, ANOVA, and **N**; $p < 0.0001$, $F (3, 8) = 65.41$, ANOVA). This indicated that GL261 cells were indeed resistant to TMZ-induced cell death, and that the reduction in cell numbers could be a result of decreased cell proliferation. However, cotreatment with TMZ and the A_{2B} AR antagonist significantly increased GL261 cell death up to

95% (**Figure 2.7M**; $p < 0.0001$, $F(3, 8) = 279.9$, ANOVA), indicating that GB cells were more sensitive to chemotherapeutic drugs when A_{2B} AR signaling was inhibited. These findings suggest that GB uses A_{2B} AR signaling to upregulate P-gp and MRP1 expression and to increase its chemoresistance. Together, these findings suggest that CD73 and the A_{2B} AR are potential targets for GB treatment.

Figure 2.7

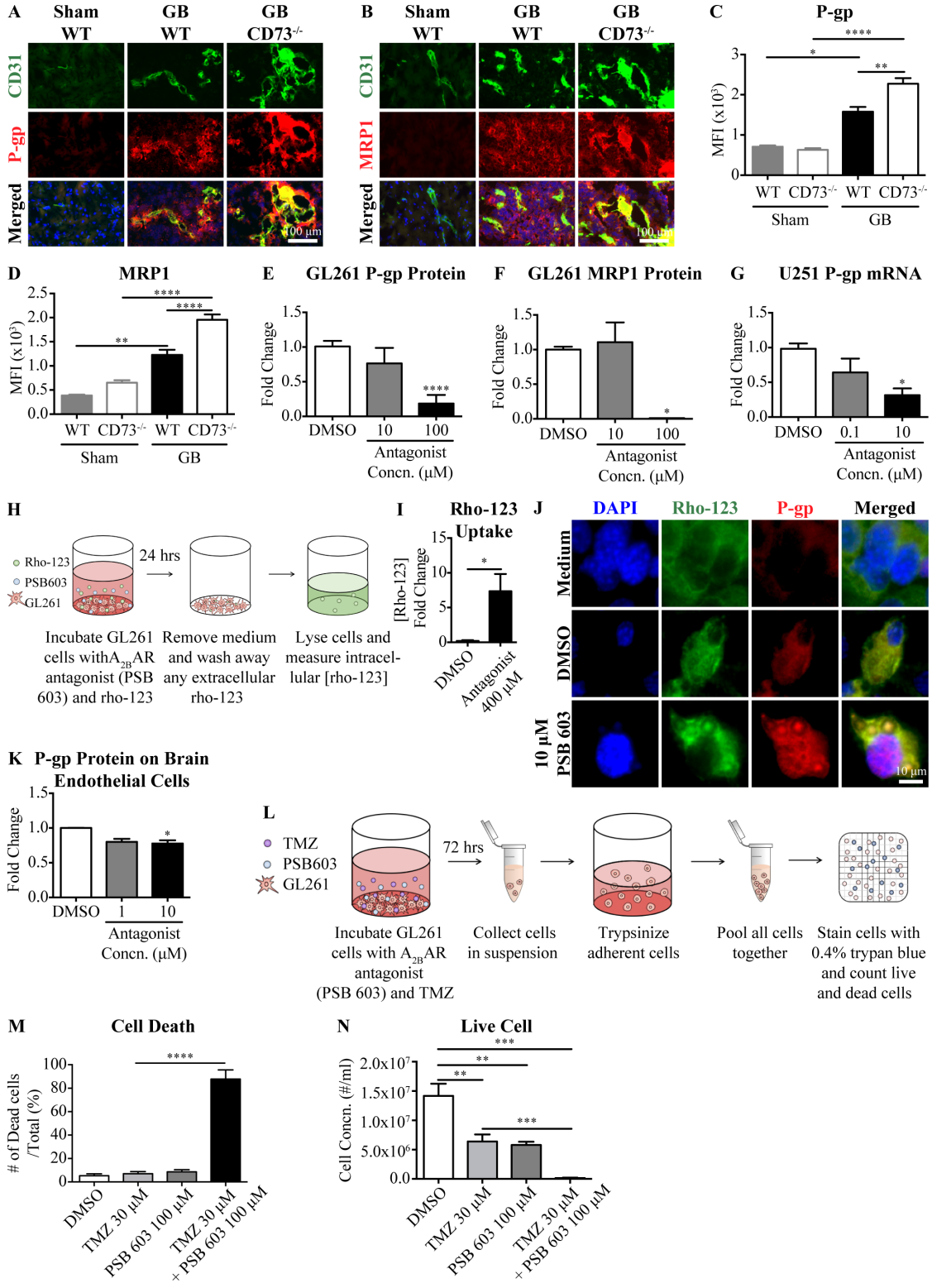
A
Sham WT
GB WT
GB CD73-/-
CD31
P-gp
Merged
100 µm
B
Sham WT
GB WT
GB CD73-/-
CD31
MRP1
Merged
100 µm
C
P-gp
MFI (x10³)
WT CD73-/- WT CD73-/-
Sham
GB
D
MRP1
MFI (x10³)
WT CD73-/- WT CD73-/-
Sham
GB
E
GL261 P-gp Protein
Fold Change
DMSO 10 100
Antagonist Concn. (µM)
F
GL261 MRP1 Protein
Fold Change
DMSO 10 100
Antagonist Concn. (µM)
G
U251 P-gp mRNA
Fold Change
DMSO 0.1 10
Antagonist Concn. (µM)
H
Rho-123
PSB603
GL261
24 hrs
Incubate GL261 cells withA2BAR antagonist (PSB 603) and rho-123
Remove medium and wash away any extracellular rho-123
Lyse cells and measure intracel-lular [rho-123]
I
Rho-123 Uptake
[Rho-123] Fold Change
DMSO
Antagonist 400 µM
J
DAPI
Rho-123
P-gp
Merged
Medium
DMSO
10 µM PSB 603
10 µm
K
P-gp Protein on Brain Endothelial Cells
Fold Change
DMSO 1 10
Antagonist Concn. (µM)
L
TMZ
PSB603
GL261
72 hrs
Incubate GL261 cells with A2BAR antagonist (PSB 603) and TMZ
Collect cells in suspension
Trypsinize adherent cells
Pool all cells together
Stain cells with 0.4% trypan blue and count live and dead cells
M
Cell Death
# of Dead cells /Total (%)
DMSO
TMZ 30 µM
PSB 603 100 µM
TMZ 30 µM + PSB 603 100 µM
N
Live Cell
Cell Concn. (#/ml)
DMSO
TMZ 30 µM
PSB 603 100 µM
TMZ 30 µM + PSB 603 100 µM

Figure 2.7. A_{2B} AR signaling promotes GB MDR transporter expression and enhances its chemoresistance. **A**, **B**, Representative images of brain sections from GL261- or sham-implanted mice (3 weeks after implantation) stained with anti-CD31 (green) and anti-P-gp antibody (red) (**A**) or anti-CD31 (green) and anti-MRP1 antibody (red) (**B**) (n = 3– 4 per GB-implanted group and n = 2 per sham-implanted group). **C**, **D**, P-gp (**C**) and MRP1(**D**) MFI in brain sections quantified using the Zen image analysis program (n = 3– 4 per GB-implanted group and n = 2 per sham-implanted group, three images analyzed/sample, one-way ANOVA for **C** and **D**). **E**, **F**, Western blot densitometry analysis of P-gp (**E**) (n = 4 –10 per group) or MRP1 (**F**) (n = 2– 4 per group, one-way ANOVA for **E** and **F**) on GL261 treated with PSB 603. **G**, qRT-PCR analysis of P-gp mRNA from U251 cells treated with PSB 603 (n = 3, one-way ANOVA). **H**, Rho-123 uptake assay procedure. **I**, Quantification of rho-123 concentration from GL261 cell lysate treated with PSB 603 (400 μM) relative to DMSO control (n = 4, Student's two-tailed t test). **J**, GL261 treated with cell culture medium (no-treatment control), DMSO, or PSB 603 and rho-123 (green) for 4 h and stained with anti-Pgp antibody (red) and DAPI (blue) (n = 3). **K**, Western blot densitometry analysis of P-gp on primary mouse brain endothelial cells treated with PSB 603 or DMSO control normalized to GAPDH using ImageJ software (n = 2–3 per group, one-way ANOVA). **L**, GL261 chemotherapy sensitivity assay procedure. **M**, **N**, Cell death percentage (**M**) and live cell concentration (**N**) of GL261 cultured with DMSO control, TMZ (30 μM), PSB 603 (100 μM), or the latter two together for 72 h (n = 3, one-way ANOVA for **M** and **N**). Data are shown as mean ± SEM. *$p < 0.05$, **$p \leq 0.01$, ***$p \leq 0.001$, ****$p < 0.0001$.

Discussion

Purinergic molecules such as adenosine are conserved across species and play critical roles in regulating cell survival and proliferation and mediating cell communication between glial cells and neurons in the CNS (52). Studies have suggested that adenosine plays a significant role in cancer development and progression by attenuating the immune response (5). However, these studies were not able to show how host and GB-CD73 affect GB pathogenesis and progression. In this report, we hypothesized that GBs used the purinergic enzyme CD73 to promote their growth and development. We further hypothesized that $CD73^{-/-}$ mice would produce smaller GBs compared with WT mice, with their full complement of host CD73. Indeed, GBs in $CD73^{-/-}$ mice were significantly smaller and less invasive. Further, we showed that GBs in CD73-FLK mice were much more invasive than GBs in WT mice. This observation aligns with our hypothesis that host CD73 promotes GB pathogenesis, including increasing its invasiveness.

We observed that WT mice exhibited a high density of blood vessels within GBs, whereas GB-bearing $CD73^{-/-}$ mice had significantly fewer vessels. In addition, vessels in GB-bearing $CD73^{-/-}$ mice had enlarged lumens and increased glomeruloid vessel morphology. Glomeruloid vessels are surrounded by multiple layers of basement membrane and are poorly perfused (53). The decreased vessel density causes a reduction in vessel surface area to volume ratio and is likely to result in insufficient nutrient supply. In sporadic vestibular schwannoma, vessel density is positively correlated with tumor size and growth (54). We propose that the decreased vessel density and increased (layered) basement membrane, combined with insufficient nutrient supply, in GB-bearing $CD73^{-/-}$ mice contributed to the decreased tumor size.

We observed increased VEGF expression in GB-bearing CD73$^{-/-}$ mice. Sundberg et al. have shown that VEGF delivered by adenovirus in the ears of a-thymic mice is sufficient to induce and maintain glomeruloid bodies similar to GB glomeruloid vessels (41). This suggests that the elevated VEGF expression seen in GB-bearing CD73$^{-/-}$ mice promotes endothelial cell proliferation and glomeruloid vessel formation. However, increased α-dystroglycan in GB-bearing CD73$^{-/-}$ mice, but not in WT mice, suggests that GB endothelial cells in CD73$^{-/-}$ mice are more tightly associated with the basement membrane. Therefore, their ability to migrate and form new vessels is limited. We propose that increased VEGF, which promotes endothelial cell proliferation, along with increased α-dystroglycan expression, which reduces endothelial cell migration, lead to glomeruloid vessel formation in GBs.

In addition to VEGF and α-dystroglycan, MMP2 has been shown to regulate GB angiogenesis by promoting vascular branching (26). Although we observed increased MMP2 expression in GB-bearing CD73$^{-/-}$ mice, the overall MMP activity was decreased compared with GB-bearing WT mice. This suggests that, in the absence of host CD73, MMP activity decreased, resulting in reduced vascular branching and increased glomeruloid vessel formation. This also indicates that increased GB-CD73 is insufficient to promote angiogenesis in the absence of host CD73.

The increased GB-CD73 in GB-bearing CD73$^{-/-}$ mice suggests that GB-CD73 and host CD73 have overlapping roles in GB pathogenesis. When implanted in an environment lacking CD73, CD73-positive GB cells will be selected and/or GB cells will upregulate GB-CD73 to promote their survival. To investigate whether GB-CD73 contributes to GB pathogenesis, we implanted GL261^{CD73low} cells in WT and CD73$^{-/-}$ mice. Interestingly, GL261^{CD73low}-implanted WT and CD73$^{-/-}$ mice did not show significant alterations in GB growth. This indicates that, although host CD73 and GB-

CD73 may have overlapping roles in regulating GB pathogenesis, host CD73 contributes more significantly to GB growth.

The tumor microenvironment contributes significantly to tumor development, and host glial cells (astrocytes and microglia) are major producers of TIMPs, MMPs, and VEGF in the CNS (55–58). We investigated whether CD73 on host glial cells regulate extracellular matrix remodeling through MMPs and/or TIMPs to promote GB angiogenesis and invasion. We observed increased expression of the MMP9 inhibitor TIMP1 in GB-bearing $CD73^{-/-}$ mice. TIMP1 was observed mostly on the edge and outside the borders of GB. This suggests that TIMP1 is regulated by CD73 expressed on host cells. In addition, MMP9 expression was the highest in GB-bearing CD73-FLK mice and TIMP1 expression was the highest in GB-bearing $CD73^{-/-}$ mice, suggesting that they are both regulated by CD73. It has been shown that GB-associated microglial cells are the main contributors of MMP9 and not tumor cells (59). Therefore, because we could not find any alteration in MMP9 and TIMP1 expression by antagonizing the A_{2B} AR on GB cells, it is more likely that host cells such as astrocytes and microglia are the main producers of MMP9 and TIMP1 in GB-bearing mice. Because MMP9 expression is mostly observed at the tumor edge, it is likely that it is the host cells responding to the tumor and/or the interaction between GB cells and host cells that lead to increased MMP9 at the tumor edge. This further emphasizes the importance of host CD73 in GB pathogenesis.

Additionally, because CD73 is a prominent immune regulator, the host immune response to GB may be significantly altered in $CD73^{-/-}$ mice. For instance, $CD73^{-/-}$ microglial cells do not become ramified when exposed to ATP (60), and this can significantly alter GB pathogenesis. Therefore, the upregulation of GB-CD73 in $CD73^{-/-}$ mice could not fully compensate for the lack of host CD73 in the host environment.

We found increased GB P-gp and MRP1 expression in CD73$^{-/-}$ mice. GB cells were also more sensitive to chemotherapeutic drugs when GB A_{2B} AR signaling was inhibited. We showed that A_{2B} AR signaling in GB promotes GB chemoresistance by upregulating P-gp and MRP1. These data suggest that GB-CD73 is the main driver of GB MDR transporter expression and show that both host CD73 and GB-CD73 contribute to GB pathogenesis independently. As a result, when using anti-CD73 antibody or CD73 inhibitor as a treatment, it is important to know that the host and GB may respond to the treatment differently, and that targeting specific cells may help predict the treatment outcome.

We showed that the A_{2B} AR played a critical role in GB pathogenesis. The A_{2B} AR has a low affinity for adenosine compared with other adenosine receptors, which further supports the hypothesis that the A_{2B} AR is activated during high/pathological adenosine concentrations (12–15), such as during hypoxia and inflammation. This coincides with our findings of increased A_{2B} AR in pathological GB conditions compared with sham mice, along with its involvement in regulating MMP activity and MDR transporters in GB.

Based on these findings, we propose that GB uses host CD73 to increase MMP9 expression and inhibit TIMP1 to promote GB invasion (**Figure 2.8A**). Host CD73 also promotes GB angiogenesis by increasing GB vessel number (**Figure 2.8B**). The absence of host CD73 leads to increased GB-CD73, VEGF, MMP2, and α-dystroglycan and results in the formation of glomeruloid vessels (**Figure 2.8B**). Finally, A_{2B} AR signaling on GB cells promotes P-gp/MRP1 expression and increases GB chemoresistance (**Figure 2.8C**).

GB is the deadliest of all brain tumors, with a median patient survival time of up

to 16 months, even with treatment (4). Here, we demonstrated multiple pathways of host and GB-CD73 contribution to GB pathogenesis, such as GB angiogenesis, invasion, and its chemoresistance. These studies indicate that modulating host CD73 and GB-CD73/AR_{2B} AR signaling may significantly improve treatment and increase the lifespan of GB patients.

Figure 2.8

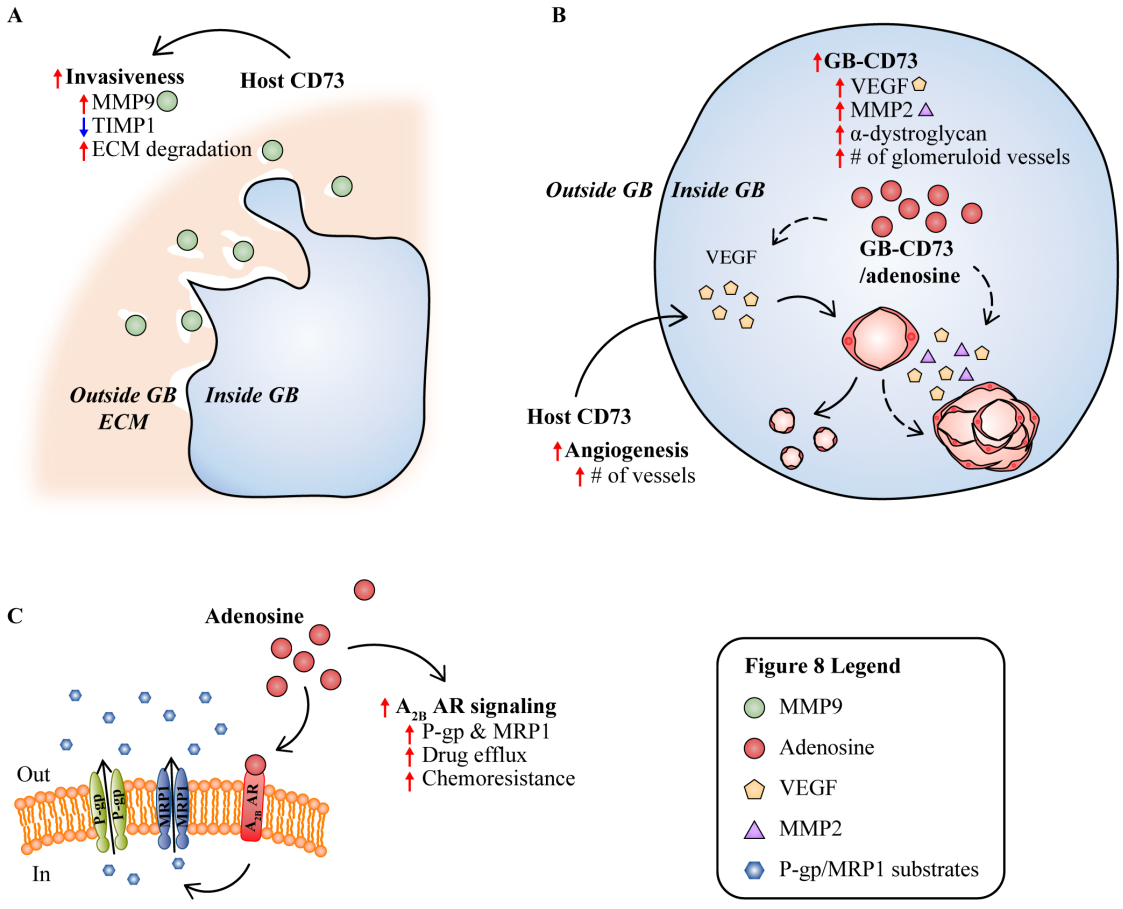
A
Invasiveness
MMP9
TIMP1
ECM degradation
Host CD73
Outside GB
ECM
Inside GB
B
GB-CD73
VEGF
MMP2
α-dystroglycan
# of glomeruloid vessels
Outside GB
Inside GB
VEGF
GB-CD73
/adenosine
Host CD73
Angiogenesis
# of vessels
C
Adenosine
A2B AR signaling
P-gp & MRP1
Drug efflux
Chemoresistance
Out
In
P-gp
P-gp
MRP1
MRP1
A2B AR
Figure 8 Legend
MMP9
Adenosine
VEGF
MMP2
P-gp/MRP1 substrates

Figure 2.8. Working model describing how CD73 promotes GB pathogenesis. A, Host CD73 promotes GB invasiveness by upregulating MMP9 and inhibiting its inhibitor, TIMP1. **B**, Host CD73 upregulates angiogenesis by promoting mother vessels to divide into smaller vessels, thereby increasing the vessel density in GB (solid arrows). In the absence of host CD73, GB upregulates GB-CD73 and increases MMP2 expression through A_{2B} AR signaling. GB-CD73 promotes VEGF and α-dystroglycan expression, which leads to intravascular endothelial cell proliferation and glomeruloid vessel formation in GB (dotted arrows). **C**, CD73-generated adenosine acts via the A_{2B} AR to promote P-gp and MRP1 upregulation, which results in increased drug efflux, thereby increasing GB chemoresistance

REFERENCES

1. Wen PY, Kesari S (2008) Malignant gliomas in Adults. *N Engl J Med* 359(5):492–507.

2. Sarkaria JN, et al. (2008) Mechanisms of chemoresistance to alkylating agents in malignant glioma. *Clin Cancer Res* 14(10):2900–2908.

3. Neuwelt EA, Barnett P a, Bigner DD, Frenkel EP (1982) Effects of adrenal cortical steroids and osmotic blood-brain barrier opening on methotrexate delivery to gliomas in the rodent: the factor of the blood-brain barrier. *Proc Natl Acad Sci* 79(14):4420–4423.

4. Topkan E, et al. (2018) Prognostic value of the Glasgow Prognostic Score for glioblastoma multiforme patients treated with radiotherapy and temozolomide. *J Neurooncol* 139(2):411–419.

5. Antonioli L, Blandizzi C, Pacher P, Haskó G (2013) Immunity, inflammation and cancer: a leading role for adenosine. *Nat Rev Cancer* 13(12):842–57.

6. Zhi X, et al. (2007) RNA interference of ecto-5'-nucleotidase (CD73) inhibits human breast cancer cell growth and invasion. *Clin Exp Metastasis* 24:439–448.

7. Yegutkin GG, et al. (2011) Altered purinergic signaling in CD73-deficient mice inhibits tumor progression. *Eur J Immunol* 41(5):1231–1241.

8. Zhang B (2012) CD73 promotes tumor growth and metastasis. *Oncoimmunology* 1(1):67–70.

9. Yin J, Xu K, Zhang J, Kumar A, Yu F-SX (2007) Wound-induced ATP release and EGF receptor activation in epithelial cells. *J Cell Sci* 120(Pt 5):815–25.

10. Cauwels A, Rogge E, Vandendriessche B, Shiva S, Brouckaert P (2014) Extracellular ATP drives systemic inflammation, tissue damage and mortality. *Cell Death Dis* 5(3):e1102.

11. Adair TH (2005) Growth regulation of the vascular system: an emerging role for adenosine. *Am J Physiol Regul Integr Comp Physiol* 289(53):R283–R296.

12. Haskó G, Csóka B, Németh ZH, Vizi ES, Pacher P (2009) A2B adenosine receptors in immunity and inflammation. *Trends Immunol* 30(6):263–270.

13. Daniele S, Zappelli E, Natali L, Martini C, Trincavelli ML (2014) Modulation of A1 and A2B adenosine receptor activity: a new strategy to sensitise glioblastoma stem cells to chemotherapy. *Cell Death Dis* 5(11):e1539.

14. Mundd SJ, Kelly E (1998) Evidence for Co-Expression and Desensitization of

A2a and A2b Adenosine Receptors in NGl08-15 Cells. *Science* 55:595–603.

15. Aherne CM, Kewley EM, Eltzschig HK (2011) The resurgence of A2B adenosine receptor signaling. *Biochim Biophys Acta* 1808(5):1329–1339.

16. Fredholm BB (2007) Adenosine, an endogenous distress signal, modulates tissue damage and repair. *Cell Death Differ* 14(7):1315–1323.

17. Müller CE, Jacobson KA (2011) Recent developments in adenosine receptor ligands and their potential as novel drugs. *Biochim Biophys Acta* 1808(5):1290–1308.

18. Liu TZ, et al. (2014) The HIF-2alpha dependent induction of PAP and adenosine synthesis regulates glioblastoma stem cell function through the A2B adenosine receptor. *Int J Biochem Cell Biol* 49(1):8–16.

19. Fiebich BL, et al. (2005) IL-6 expression induced by adenosine A2b receptor stimulation in U373 MG cells depends on p38 mitogen activated kinase and protein kinase C. *Neurochem Int* 46(6):501–512.

20. Trincavelli ML, et al. (2004) Regulation of A2B adenosine receptor functioning by tumour necrosis factor a in human astroglial cells. *J Neurochem* 91(5):1180–1190.

21. Burnstock G, Di Virgilio F (2013) Purinergic signalling and cancer. *Purinergic Signal* 9(4):491–540.

22. Cappellari AR, Vasques GJ, Bavaresco L, Braganhol E, Battastini AMO (2012) Involvement of ecto-5'-nucleotidase/CD73 in U138MG glioma cell adhesion. *Mol Cell Biochem* 359(1–2):315–322.

23. Koszalka P, et al. (2014) Inhibition of CD73 stimulates the migration and invasion of B16F10 melanoma cells in vitro, but results in impaired angiogenesis and reduced melanoma growth in vivo. *Oncol Rep* 31(2):819–827.

24. Bavaresco L, et al. (2008) The role of ecto-5′nucleotidase/CD73 in glioma cell line proliferation. *Mol Cell Biochem* 319(1–2):61–68.

25. Chan ESL, et al. (2006) Adenosine A(2A) receptors play a role in the pathogenesis of hepatic cirrhosis. *Br J Pharmacol* 148(8):1144–1155.

26. Du R, et al. (2008) Matrix metalloproteinase-2 regulates vascular patterning and growth affecting tumor cell survival and invasion in GBM. *Neuro Oncol* 10(3):254–264.

27. Wang M, Wang T, Liu S, Yoshida D, Teramoto A (2003) The expression of matrix metalloproteinase-2 and-9 in human gliomas of different pathological grades. *Brain Tumor Pathol* 20(2):65–72.

28. Thompson LF, et al. (2004) Crucial role for ecto-5'-nucleotidase (CD73) in vascular leakage during hypoxia. *J Exp Med* 200(11):1395–1405.

29. Resta R, et al. (1993) Murine ecto-5'-nucleotidase (CD73): cDNA cloning and tissue distribution. *Gene* 133(2):171–177.

30. Kappel A, et al. (1999) Identification of vascular endothelial growth factor (VEGF) receptor-2 (Flk-1) promoter/enhancer sequences sufficient for angioblast and endothelial cell-specific transcription in transgenic mice. *Blood* 93(12):4284–92.

31. Guillamo JS, et al. (2009) Molecular mechanisms underlying effects of epidermal growth factor receptor inhibition on invasion, proliferation, and angiogenesis in experimental glioma. *Clin Cancer Res* 15(11):3697–3704.

32. Williams SP, et al. (2011) Indirubins decrease glioma invasion by blocking migratory phenotypes in both the tumor and stromal endothelial cell compartments. *Cancer Res* 71(16):5374–5380.

33. Weinstein DE (2001) Isolation and purification of primary rodent astrocytes. *Curr Protoc Neurosci* Chapter 3:Unit 3.5.

34. Livak KJ, Schmittgen TD (2001) Analysis of Relative Gene Expression Data Using Real-Time Quantitative PCR and the 2(-Delta Delta C(T)) Method. *Methods* 25(4):402–408.

35. Ahluwalia MS, de Groot J, Liu WM, Gladson CL (2010) Targeting SRC in glioblastoma tumors and brain metastases: Rationale and preclinical studies. *Cancer Lett* 298(2):139–149.

36. Alexiades NG, et al. (2015) MMP14 as a novel downstream target of VEGFR2 in migratory glioma-tropic neural stem cells. *Stem Cell Res* 15(3):598–607.

37. Mills JH, et al. (2008) CD73 is required for efficient entry of lymphocytes into the central nervous system during experimental autoimmune encephalomyelitis. *Proc Natl Acad Sci* 105(27):9325–9330.

38. Bynoe MS, Viret C, Yan A, Kim DG (2015) Adenosine receptor signaling: a key to opening the blood-brain door. *Fluids Barriers CNS* 12:20.

39. Watkins S, et al. (2014) Disruption of astrocyte-vascular coupling and the blood-brain barrier by invading glioma cells. *Nat Commun* 5(May):4196.

40. Fazel FS, et al. (2018) Predictive value of braden risk factors in pressure ulcers of outpatients with spinal cord injury. *Acta Med Iran* 56(1):56–61.

41. Sundberg C, et al. (2001) Glomeruloid Microvascular Proliferation Follows Adenoviral Vascular Permeability Factor/Vascular Endothelial Growth Factor-

164 Gene Delivery. *Am J Pathol* 158(3):1145–1160.

42. Faratian D, Munro A, Twelves C, Bartlett J (2009) Membranous and cytoplasmic staining of Ki67 is associated with HER2 and ER status in invasive breast carcinoma. *Histopathology* 54(2):254–257.

43. Grzanka A, Sujkowska R, Janiak A, Adamska M (2000) Immunogold labelling of PCNA and Ki-67 antigen at the ultrastructural level in laryngeal squamous cell carcinoma and its correlation with lymph node metastasis and histological grade. *Acta Histochem* 102(2):139–149.

44. Hosokawa H, Ninomiya H, Kitamura Y, Fujiwara K, Masaki T (2002) Vascular endothelial cells that express dystroglycan are involved in angiogenesis. *J Cell Sci* 115:1487–1496.

45. Gee SH, et al. (1993) Laminin-binding protein 120 from brain is closely related to the dystrophin-associated glycoprotein, dystroglycan, and binds with high affinity to the major heparin binding domain of laminin. *J Biol Chem* 268(20):14972–14980.

46. Zhang X, et al. (2014) Reduction of a-dystroglycan expression is correlated with poor prognosis in glioma. *Tumor Biol* 35(11):11621–11629.

47. Calatozzolo C, et al. (2005) Expression of drug resistance proteins Pgp, MRP1, MRP3, MRP5 AND GST-π in human glioma. *J Neurooncol* 74(2):113–121.

48. Kim DG, Bynoe MS (2016) A2A adenosine receptor modulates drug efflux transporter P-glycoprotein at the blood-brain barrier. *J Clin Invest* 126(5):1–17.

49. Kim DG, Bynoe MS (2015) A2A Adenosine Receptor Regulates the Human Blood-Brain Barrier Permeability. *Mol Neurobiol* 52(1):664–78.

50. Carman AJ, Mills JH, Krenz A, Kim D, Bynoe MS (2011) Adenosine Receptor Signaling Modulates Permeability of the Blood – Brain Barrier. *J Neurosci* 31(37):13272–13280.

51. Veringa SJ, et al. (2013) In vitro drug response and efflux transporters associated with drug resistance in pediatric high grade glioma and diffuse intrinsic pontine glioma. *PLoS One* 8(4):e61512.

52. Fields RD, Burnstock G (2006) Purinergic signalling in neuron-glia interactions. *Nat Rev Neurosci* 7(6):423–436.

53. Nagy J, Chang S, Dvorak A, Dvorak H (2009) Why are tumour blood vessels abnormal and why is it important to know? *Br J Cancer* 100(6):865–869.

54. De Vries M, Hogendoorn PCW, De Bruyn IB, Malessy MJA, Van Der Mey AGL (2012) Intratumoral hemorrhage, vessel density, and the inflammatory reaction

contribute to volume increase of sporadic vestibular schwannomas. *Virchows Arch* 460(6):629–636.

55. Könnecke H, Bechmann I (2013) The role of microglia and matrix metalloproteinases involvement in neuroinflammation and gliomas. *Clin Dev Immunol* 2013. doi:10.1155/2013/914104.

56. Wang L, et al. (2013) Astrocytes directly influence tumor cell invasion and metastasis in vivo. *PLoS One* 8(12):e80933.

57. Stone J, et al. (1995) Development of retinal vasculature is mediated by hypoxia-induced vascular endothelial growth factor (VEGF) expression by neuroglia. *J Neurosci* 15(7 Pt 1):4738–4747.

58. Pagenstecher A, Stalder AK, Kincaid CL, Shapiro SD, Campbell IL (1998) Differential expression of matrix metalloproteinase and tissue inhibitor of matrix metalloproteinase genes in the mouse central nervous system in normal and inflammatory states. *Am J Pathol* 152(3):729–741.

59. Hu F, Ku M, Markovic D, Dildar O, Lehnardt S (2015) Glioma associated microglial MMP9 expression is up regulated by TLR2 signalling and sensitive to minocycline. *Int J cancer* 135(11):2569–2578.

60. Matyash M, Zabiegalov O, Wendt S, Matyash V, Kettenmann H (2017) The adenosine generating enzymes CD39/CD73 control microglial processes ramification in the mouse brain. *PLoS One* 12(4):1–27.

CHAPTER 3

HOST CD73 PROMOTES GLIOBLASTOMA EVASION OF HOST IMMUNE RESPONSE

Abstract

The adenosine-generating enzyme CD73 is a key immune regulator that attenuates inflammation and restores immune homeostasis. We set out to determine the role of CD73 in regulating the immune response to glioblastoma (GB), which is the most aggressive primary brain tumor. We intracranially implanted mouse GB cells in wild-type (WT) and $CD73^{-/-}$ mice to determine the anti-GB immune response in the presence or absence of host CD73. We found that compared with GB-bearing WT mice, GB-bearing $CD73^{-/-}$ mice mounted an overall stronger immune response. GB-bearing $CD73^{-/-}$ mice had increased pro-inflammatory cytokine TNF-α, reduced T regulatory cell-infiltration, increased cytotoxic T cell infiltration, and increased M1 microglia and/or macrophages. This reduction in T regulatory cell-recruitment was associated with reduction in the CCL22 chemokine and its receptor, CCR4, in GB-bearing $CD73^{-/-}$ mice. In addition, $CD73^{-/-}$ macrophages were intrinsically more pro-inflammatory compared with WT macrophages. CD73 also promoted leukocyte entry into the brain parenchyma by allowing them to cross the glia limitans layer and exit the perivascular space. These findings show that host CD73 attenuates anti-tumor immune responses and promots GB immune evasion. Taken together, inhibiting host CD73 may benefit patients by allowing them to elicit a stronger inflammatory response to GB, thereby increasing the potency of immunotherapy for GB patients.

Introduction

The purinergic nucleoside adenosine is a primal immune-attenuating signaling molecule that exists in all life forms (1). It is the metabolic product of adenosine triphosphate (ATP). Extracellular ATP is metabolized into adenosine diphosphate (ADP) and adenosine monophosphate (AMP) via the surface enzyme ectonucleoside triphosphate diphosphohydrolase-1 (CD39); AMP is converted to adenosine via another surface enzyme ecto-5'-nucleotidase (CD73). Therefore, CD39 and CD73 regulate the ratio of extracellular ATP concentration to extracellular adenosine concentration. This balance of extracellular ATP and adenosine concentration is crucial to maintaining the immune homeostasis (2).

The physiological extracellular ATP concentration is around 1 μM under basal conditions (3). However, upon infection (4) or tissue damage/stress (5), or under hypoxic/necrotic conditions (6, 7), cells release ATP into the extracellular space, increasing the extracellular ATP concentration to threefold or more (8). ATP can be passively released by necrotic cells or actively transported out by apoptotic or activated cells (8). This increase in extracellular ATP concentration often serves as a danger signal and promotes inflammatory responses to clear pathogens or damaged/apoptotic cells. Extracellular ATP signals through purinergic P2 receptors to induce inflammatory responses. For example, ATP induces the chemotaxis of inflammatory cells (9) and promotes the release of inflammatory cytokines (10) and oxygen free radicals (11). On the other hand, extracellular adenosine signaling provides a countermeasure to the often-damaging inflammatory response and restores immune homeostasis. Adenosine reduces the release of pro-inflammatory cytokines (12) and promotes the production of the anti-inflammatory cytokine IL-10 (13). It also inhibits immune cell recruitment by reducing chemokine secretion (14) and inhibiting endothelial cell adhesion molecule expression

(15). Besides attenuating inflammation, adenosine also promotes tissue repair and regeneration, including inducing fibrosis, wound healing, and angiogenesis to increase oxygen supply (16). Due to the potent immune-attenuating effects of adenosine, it has a short half-life and only lasts for less than 10 seconds in the extracellular environment (17, 18) before it is quickly converted to inosine by adenosine deaminase (ADA). Thus, the extracellular adenosine-generating enzyme CD73 is an important immune regulator that promotes anti-inflammatory immune responses and restores immune homeostasis.

Interestingly, CD73 is expressed on many types of cancers including glioblastoma (GB) (19), bladder cancer (20), breast cancer (21), colon cancer (22), esophageal cancer (23), melanoma (24), ovarian cancer (25), prostate cancer (26), and thyroid cancer (27). We have previously shown that host CD73 promotes GB pathogenesis by increasing GB invasiveness, angiogenesis, and chemoresistance (28). Besides promoting GB pathogenesis, extracellular adenosine also has strong immune-attenuating effects. Thus, we wanted to further investigate how CD73 contributed to the host anti-GB immune response. We hypothesized that in the absence of the host extracellular adenosine-generating enzyme CD73, the immune system would be able to mount a stronger inflammatory response against GB. This study allows us to elucidate the role host CD73 plays in the anti-GB immune response, and to determine whether targeting the CD73/adenosine signaling pathway has the potential to improve immunotherapy for GB patients.

Materials and Methods

Cell Culture

Mouse glioma cell line GL261 was obtained from the National Cancer Institute. Cell were cultured in DMEM with 10% fetal bovine serum (FBS) and 100 units/ml penicillin and streptomycin at 37ºC in a humidified incubator with 5% CO_2. Media was changed every 2-3 days and cells were split or used for experiments when grown to confluency.

Mice

C57BL/6 mice were purchased from Jackson Laboratories. $CD73^{-/-}$ mice have been described previously (29) and were backcrossed to C57BL/6 mice for more than 14 generations. Mice were housed in specific-pathogen-free rooms until 8 weeks of age and moved to a broken barrier/biosafety level 2 room for experiments in the mouse facility at Cornell University. Animal studies were approved by the Institutional Animal Care and Use Committee (IACUC) of Cornell University (protocol no. 2008–0092).

GB implantation

Mice were anesthetized with ketamine-xylazine (100mg/kg), and 2mg/kg of ketroprofen were administered as analgesic. Eye ointment was applied before the mice's heads were shaved. The scalps were sterilized by wiping 3 times with chlorhexidine solution followed by 70% ethanol. A midsagittal incision was made through the scalp and the bregma was located. A small hole was drilled 0.1mm posterior and 2.3 mm lateral of the bregma. 30,000 GL261 mouse glioma cells in 2 μl of saline were injected 3mm from the surface of the brain using a 27-gauge needle with Hamilton syringe. The wound was closed using suture and ketoprofen (2mg/kg) administered the day after surgery.

Tissue harvest

Mice were anesthetized with ketamine-xylazine and transcardial perfusion with ice-cold PBS was performed. Brains were cut coronally in half, flash frozen in Tissue-Tek O.C.T. (Sakura Finetek), and stored at -80ºC. Brains were sectioned to 8 or 10 μm thick with a microtome, collected on Supefrost/Plus slides (Fisher Scientific), fixed in acetone, and stored at -80ºC.

Immunostaining

For immunohistochemistry staining, slides were air dried and immersed in 0.3% H_2O_2 for 10 minutes to inactivate peroxidases. After two PBS washes, slides were blocked at room temperature with casein (Vector Laboratories) and 10% goat serum. Slides were then incubated overnight with primary antibody followed by two PBS washes. Slides were then incubated with HRP conjugated secondary antibody, washed, developed with an AEC substrate kit (Zymed), and stained with hematoxylin. Slides were mounted with Fluoromount-G and sealed with nail polish. For immunofluorescence staining, slides were blocked at room temperature with casein (Vector Laboratories) and 10% goat serum and incubated overnight with primary antibody followed by two PBS washes. Slides were then incubated with fluorophore conjugated secondary antibody, washed, and mounted with ProLong Gold with DAPI.

Quantitative real-time PCR

Brain mRNA was extracted with TRIzol (Invitrogen) and cDNA was synthesized with High-Capacity cDNA Reverse Transcription Kits (Applied Biosystems) according to manufacturers' protocol. RT-PCR was performed with specific primers and KAPA SYBR FAST qPCR Kit (KAPA Biosystems) according to manufacturer's protocol.

Gene expressions were analyzed using GAPDH as a reference gene and normalized to controls using the $2^{-\Delta\Delta CT}$ method (30).

Isolation of mouse primary peritoneal macrophages

Mouse primary peritoneal macrophages were isolated following a protocol published by Fortier and Falk (31). Briefly, 1 ml of 3% Brewer thioglycollate medium was administered via intraperitoneal injection. Donor mice were euthanized 5 days after injection by CO2 asphyxiation and abdominal skins were retracted. 10 ml of harvest medium (DMEM with 5% FBS) per mouse was injected intraperitoneally using a 20 G needle and peritoneal fluid was withdrawn into the same syringe slowly. Cells were seeded in 12-well plates at a density of 4.5×10^5/well and grown to confluent before use.

Results

Host CD73 promotes anti-inflammatory immune responses to GB.

We have previously shown that GB pathogenesis is hindered in a host environment lacking CD73, and this leads to a reduction in GB size and invasiveness (28). Because of the potent anti-inflammatory properties of extracellular adenosine, we hypothesized that host CD73 also contributed to promoting GB pathogenesis by attenuating the anti-GB immune response. To test this, we intracranially implanted mouse GL261 glioma cells or saline (sham) into C57BL/6 wild-type (WT) and $CD73^{-/-}$ mice and collected their brain tissues after 3 weeks to determine whether anti-GB immune responses were altered in the CNS. We found that GBs were highly infiltrated by $CD45^{+}$ leukocytes in both WT and $CD73^{-/-}$ mice (**Fig. 3.1A**). However, brain cytokine mRNA profiles from GB-bearing WT and $CD73^{-/-}$ mice were drastically different. The inflammatory cytokine TNF-α was significantly upregulated in GB-bearing $CD73^{-/-}$ mice compared with the TNF-α level in GB-bearing WT mice (**Fig. 3.1C**). A similar trend was also observed in inflammatory cytokine IL-1β, which was increased in GB-bearing $CD73^{-/-}$ mice compared with GB-bearing WT mice (**Fig. 3.1D**). Conversely, the anti-inflammatory cytokine IL-10 was significantly downregulated in GB-bearing $CD73^{-/-}$ mice compared with GB-bearing WT mice (**Fig. 3.1E**). This suggested that although a similar number of leukocytes infiltrated GB in WT and $CD73^{-/-}$ mice, leukocytes with different phenotypes were recruited to the tumor site in the absence of host CD73. They generated a different cytokine profile in GB-bearing $CD73^{-/-}$ mice, which had increased inflammatory cytokines, compared with the cytokine profile in GB-bearing WT mice. This also suggested that host CD73 promoted an anti-inflammatory immune response to GB. Because regulatory T (Treg) cells are one of the main producers of IL-10 and are often found infiltrating GB, we next quantified the

mRNA level of Treg cell transcription factor Foxp3 in the brains of GB-bearing WT and CD73$^{-/-}$ mice. We found that unlike GBs in WT mice, which had a significant increase in Foxp3 level, the Foxp3 level in GB-bearing CD73$^{-/-}$ mice was similar to sham mice (**Fig. 3.1F**). This indicated that there was a reduction in Treg cell recruitment in GB-bearing CD73$^{-/-}$ mice and suggested that the reduction of Treg cells contributed to the decreased IL-10 level in GB-bearing CD73$^{-/-}$ mice. These findings suggest that host CD73 plays a critical role in inhibiting the inflammatory response to GB, promoting Treg cell recruitment to GB.

Figure 3.1

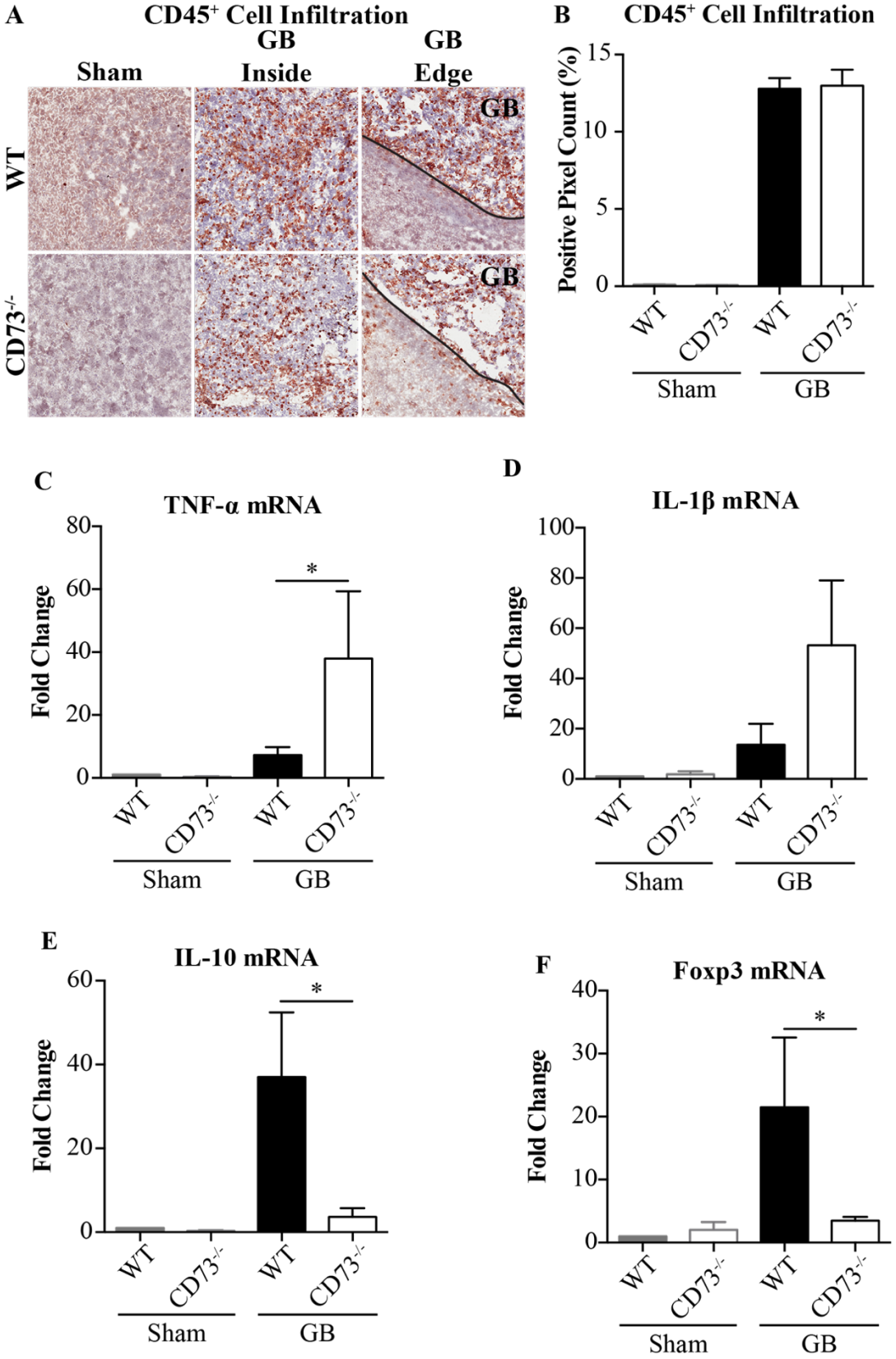
A
CD45+ Cell Infiltration
Sham
GB Inside
GB Edge
WT
CD73-/-
GB
GB
B
CD45+ Cell Infiltration
Positive Pixel Count (%)
15
10
5
0
WT
CD73-/-
WT
CD73-/-
Sham
GB
C
TNF-α mRNA
Fold Change
80
60
40
20
0
*
WT
CD73-/-
WT
CD73-/-
Sham
GB
D
IL-1β mRNA
Fold Change
100
80
60
40
20
0
WT
CD73-/-
WT
CD73-/-
Sham
GB
E
IL-10 mRNA
Fold Change
60
40
20
0
*
WT
CD73-/-
WT
CD73-/-
Sham
GB
F
Foxp3 mRNA
Fold Change
40
30
20
10
0
*
WT
CD73-/-
WT
CD73-/-
Sham
GB

Figure 3.1. Host CD73 attenuates the anti-GB inflammatory immune response. A, Immunohistochemistry staining of CD45 (brown) on frozen brain sections from GB- or sham-implanted WT and CD73 mice, 3 weeks after implantation (n = 3 – 4 per group for GB-bearing mice and n = 1 per group for sham). Solid lines indicate GB border. **B**, Quantification of CD45-positive signal from (**A**) by positive pixel count (n = 3 – 4 per group for GB-bearing mice and n = 1 per group for sham). **C**, **D**, **E**, **F**, Real time-PCR quantification of TNF-α (**C**), IL-1β (**D**), IL-10 (**E**), and Foxp3 (**F**) mRNA levels from GB- or sham-implanted WT or $CD73^{-/-}$ mice, 3 weeks after implantation (n = 3 – 5 per group for GB-bearing mice and n = 2 per group for sham). Data represent mean ± SEM. *P ≤ 0.05, **P ≤ 0.01, ***P ≤ 0.001 (Student's two-tailed t-test).

Host CD73 promotes alternatively activated macrophages (M2) polarization in GB.

GB-infiltrating microglia and macrophages are highly abundant compared with other GB-infiltrating leukocytes, and they constitute up to 30% of tumor mass (32–34). Because CD73 regulates microglia activation and microglia in $CD73^{-/-}$ mice are more activated even under basal conditions (35, 36), we wanted to elucidate whether microglia and macrophages contributed to the altered cytokine profile seen in GB-bearing $CD73^{-/-}$ mice. We stained brain sections from GB-bearing WT and $CD73^{-/-}$ mice for the microglia and macrophage marker Iba1 and found that there was a significant decrease in Iba1 expression in GBs in $CD73^{-/-}$ mice (**Fig. 3.2A and B**). This indicated that there were less GB-infiltrating microglia and macrophages in $CD73^{-/-}$ mice and suggested that host CD73 promoted microglia and macrophage infiltration in GB. Because tumor-associated microglia and macrophages are anti-inflammatory in GB and support GB pathogenesis (37), we stained GB brain sections with Iba1 and alternatively activated (M2) macrophage marker CD206 to test whether this was the case in both GB-bearing WT and $CD73^{-/-}$ mice. We found that GB-infiltrating microglia and macrophages in WT mice highly expressed the M2 marker CD206, whereas GB-infiltrating microglia and macrophages in $CD73^{-/-}$ mice had significantly reduced CD206 expression (**Fig. 3.2C and D**). This suggests that microglia and macrophages in GB-bearing $CD73^{-/-}$ mice are classically activated (M1), pro-inflammatory, and tumor suppressive. To investigate whether microglia and macrophages in GB-bearing $CD73^{-/-}$ were more pro-inflammatory, we measured arginase and iNOS mRNA levels in brain tissues. We found that, compared with sham mice, GB-bearing WT mice had a 100-fold increase in arginase levels and a decrease in iNOS levels (**Fig. 3.2E and F**). However, the arginase level in GB-bearing $CD73^{-/-}$ mice was similar to that of sham-implanted

mice, and iNOS was significantly increased in GB-bearing CD73$^{-/-}$ mice (**Fig. 3.2E and F**). This indicates that host CD73 promotes M2 polarization of microglia and macrophages in GB while in the absence of host CD73, GB-infiltrating microglia and macrophages are pro-inflammatory and M1 polarized.

We further investigated whether this increased pro-inflammatory response to GB in CD73$^{-/-}$ mice was because CD73$^{-/-}$ microglia and macrophages were intrinsically more pro-inflammatory. We isolated macrophages from WT and CD73$^{-/-}$ mice, stimulated them with LPS, and measured pro-inflammatory cytokine IL-1β mRNA levels. We found that CD73$^{-/-}$ macrophages had increased IL-1β levels compared to WT macrophages (**Fig. 3.2G**), suggesting that the lack of CD73 expression on macrophages made them intrinsically more pro-inflammatory. When we co-cultured mouse MGPP3 glioma cells with macrophages and treated them with LPS, we found that CD73$^{-/-}$ macrophages still responded stronger to the LPS treatment and had increased IL-1β levels compared to WT macrophages under the same conditions (**Fig. 3.2G**). However, compared with non-cocultured macrophages, both WT and CD73$^{-/-}$ macrophages co-cultured with MGPP3 had reduced IL-1β levels (**Fig. 3.2G**). This indicates that co-culturing with glioma cells attenuated the immune response of both WT and CD73$^{-/-}$ macrophages against LPS. However, CD73$^{-/-}$ macrophages still initiated a stronger inflammatory response even in the presence of glioma cells, suggesting that they were intrinsically more pro-inflammatory than WT macrophages. This suggests that CD73$^{-/-}$ macrophages induced a stronger inflammatory response even in the GB microenvironment.

Figure 3.2

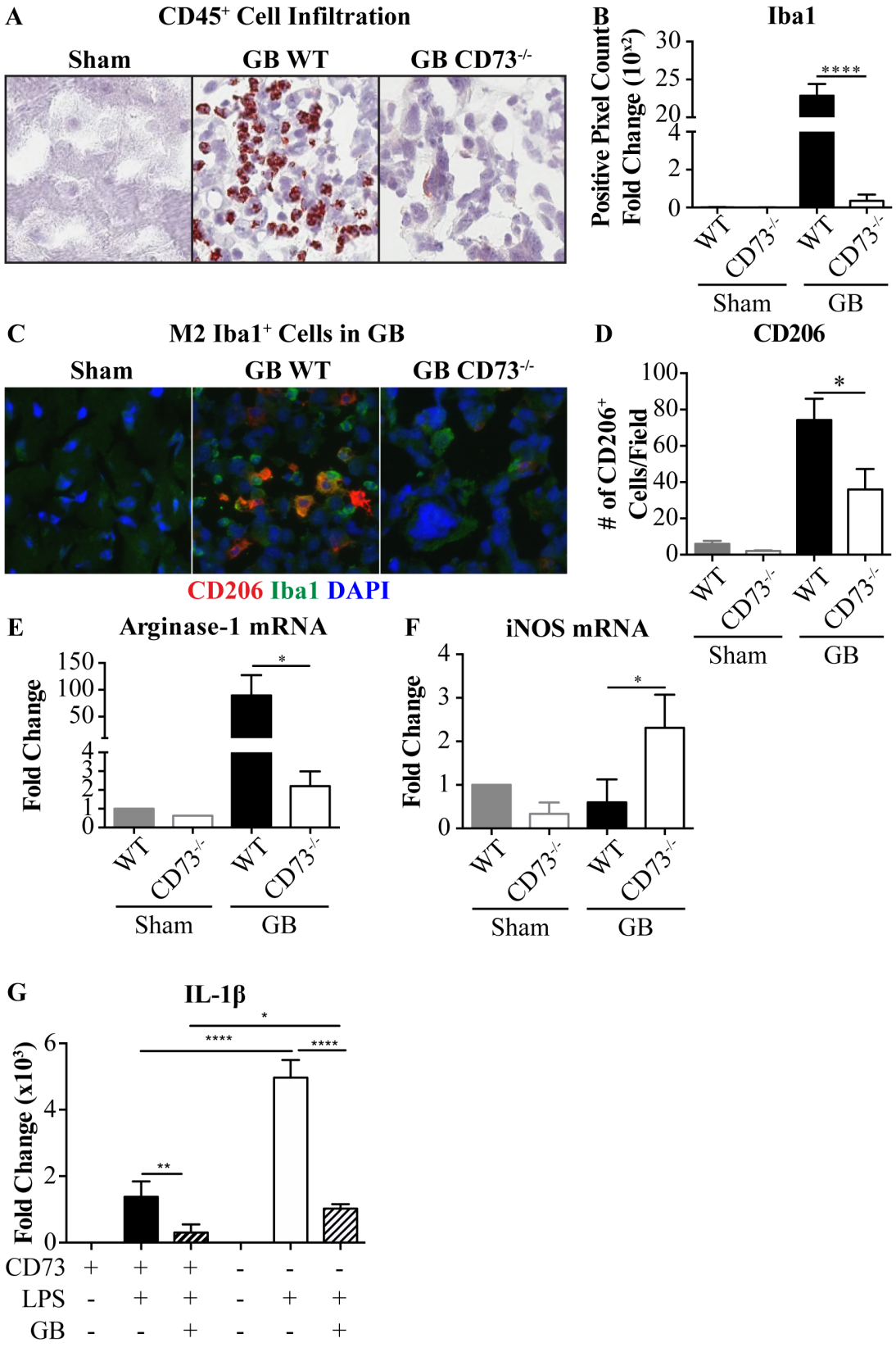
A
CD45+ Cell Infiltration
Sham
GB WT
GB CD73-/-
B
Iba1
Positive Pixel Count Fold Change (10x2)
****
WT
CD73-/-
Sham
GB
C
M2 Iba1+ Cells in GB
CD206 Iba1 DAPI
D
CD206
# of CD206+ Cells/Field
*
E
Arginase-1 mRNA
Fold Change
F
iNOS mRNA
G
IL-1β
Fold Change (x10³)
CD73
LPS
GB

Figure 3.2. CD73 on macrophages intrinsically promotes an anti-inflammatory M2 phenotype in GB immune microenvironment. **A**, Immunohistochemistry staining of Iba1 (brown) on frozen brain sections from GB- or sham-implanted WT and CD73 mice, 3 weeks after implantation (n = 3 per group for GB-bearing mice and n = 1 per group for sham). **B**, Quantification of Iba1 positive signal from (**A**) by positive pixel count (n = 3 per group for GB-bearing mice and n = 1 per group for sham). **C**, Immunofluorescent staining of Iba1 (green), CD206 (red), and cell nuclei (blue) on frozen brain sections from GB- or sham-implanted WT or $CD73^{-/-}$ mice, 3 weeks after implantation (n = 7 – 9 per group for GB-bearing mice and n = 3 – 4 per group for sham). **D**, CD206 staining was quantified by counting the number of positively stained cell per microscopic field from 3 representative microscopic fields per sample (n = 7 – 9 per group for GB-bearing mice and n = 3 – 4 per group for sham). **E**, **F**, Real time-PCR quantification of arginase-1 (**E**) (n = 3 per group for GB-bearing mice and n = 1 for sham) and iNOS (**F**) (n = 4 – 5 for GB-bearing mice and n = 1 – 2 for sham) brain mRNA levels from GB- or sham-implanted WT or $CD73^{-/-}$ mice, 3 weeks after implantation. **G**, Real time-PCR quantification of IL-1β mRNA levels from WT or $CD73^{-/-}$ macrophages co-cultured with GL261 cells and treated with LPS or controls (n = 3-4 per group). Data represent mean ± SEM. *P ≤ 0.05, **P ≤ 0.01, ***P ≤ 0.001 (Student's two-tailed t-test).

Host CD73 inhibits cytotoxic T cell infiltration in GB.

Besides microglia and macrophages, we investigated whether cytotoxic T cells responded to GB differently in $CD73^{-/-}$ mice compared with WT mice. We hypothesized that more cytotoxic $CD8^{+}$ T cells infiltrated GBs in $CD73^{-/-}$ mice compared to GBs in WT mice. Indeed, we observed increased tumor-infiltrating $CD8^{+}$ T cells in GB-bearing $CD73^{-/-}$ mice compared with GB-bearing WT mice (**Fig. 3.3A and B**). Additionally, these tumor-infiltrating $CD8^{+}$ T cells expressed the T cell activation marker CD44 (**Fig. 3.3A**), indicating that they are cytotoxic effector T cells. This suggests that host CD73 inhibits cytotoxic $CD8^{+}$ T cell response to GB.

Figure 3.3

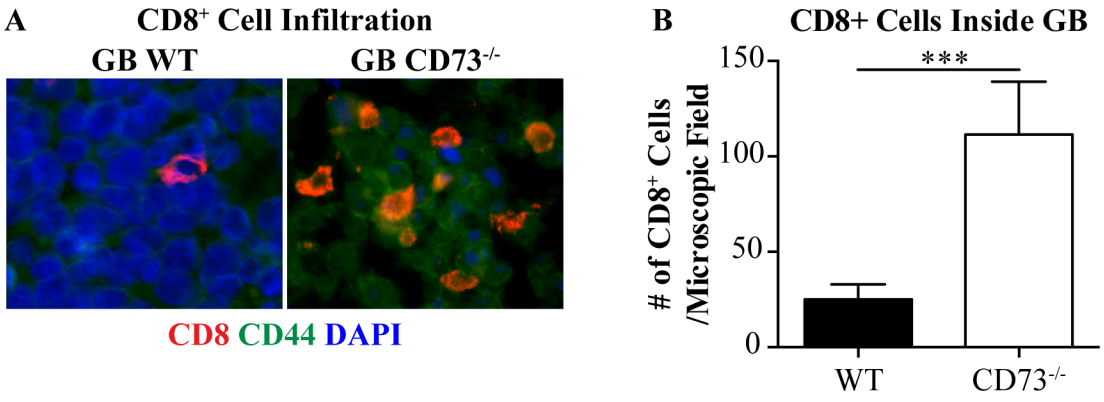

Figure 3.3. Host CD73 inhibits cytotoxic T cell infiltration in GB. A, Immunofluorescent staining of CD44 (green), CD8 (red), and cell nuclei (blue) on frozen brain sections from GB- or sham-implanted WT or $CD73^{-/-}$ mice, 3 weeks after implantation (n = 4 – 7 per group for GB-bearing mice and n = 3 per group for sham). **B**, CD8 staining was quantified by counting the number of positively stained cells per microscopic field from 3 representative microscopic fields per sample (n = 4 – 7 per group for GB-bearing mice and n = 3 per group for sham). Data represent mean ± SEM. *P ≤ 0.05, **P ≤ 0.01, ***P ≤ 0.001 (Student's two-tailed t-test).

CD73 promotes leukocyte entry into the brain parenchyma by permeating the glia limitans barrier.

The increased pro-inflammatory response in GB-bearing $CD73^{-/-}$ mice compared with GB-bearing WT mice led us to hypothesize that Treg cell recruitment to the site of GB was inhibited in $CD73^{-/-}$ mice. To test this hypothesis, we first analyzed mRNA levels of the the macrophage-derived chemokine CCL22 in the brain tissues of GB-bearing mice. CCL22 is mostly produced by M2 microglia and macrophages, and it promotes Treg cell recruitment (38). We found a decrease in CCL22 levels in GB-bearing $CD73^{-/-}$ mice compared with GB-bearing WT mice (**Fig. 3.4A)**. This suggested that CD73 promoted CCL22 production in GB-bearing WT mice. We also found a decrease in mRNA levels of the Treg cell chemokine receptor CCR4 in GB-bearing $CD73^{-/-}$ mice (**Fig. 3.4B**). Treg cells are recruited to the brain by sensing the microglia/macrophage-generated CCL22 concentration gradient through their chemokine receptor CCR4. Thus, a reduction in both CCL22 and CCR4 in GB-bearing $CD73^{-/-}$ mice suggests that the lack of host CD73 leads to reduced CCL22 secretion, and thereby decreases Treg cell recruitment in GB-bearing $CD73^{-/-}$ mice (**Fig. 3.1F**).

To investigate whether CD73 regulated other leukocyte recruitment pathways in GB-bearing mice, we next quantified leukocytes' ability to cross the blood-brain barrier (BBB) and the glia limitans layer to enter the brain parenchyma in GB (**Fig. 3.4C**). We stained brain sections from GB-bearing WT and $CD73^{-/-}$ mice and found that in GB-bearing $CD73^{-/-}$ mice, significantly more $CD45^{+}$ leukocytes were trapped in the perivascular space and were not able to cross the glia limitans barrier (**Fig. 3.4D and E**). Conversely, $CD45^{+}$ leukocytes in GB-bearing WT mice were able to pass the glia limitans layer and enter the brain parenchyma (**Fig. 3.4D**). This suggests that CD73

promotes leukocyte recruitment to the GB brain parenchyma by regulating their ability to cross the glia limitans barrier.

Figure 3.4

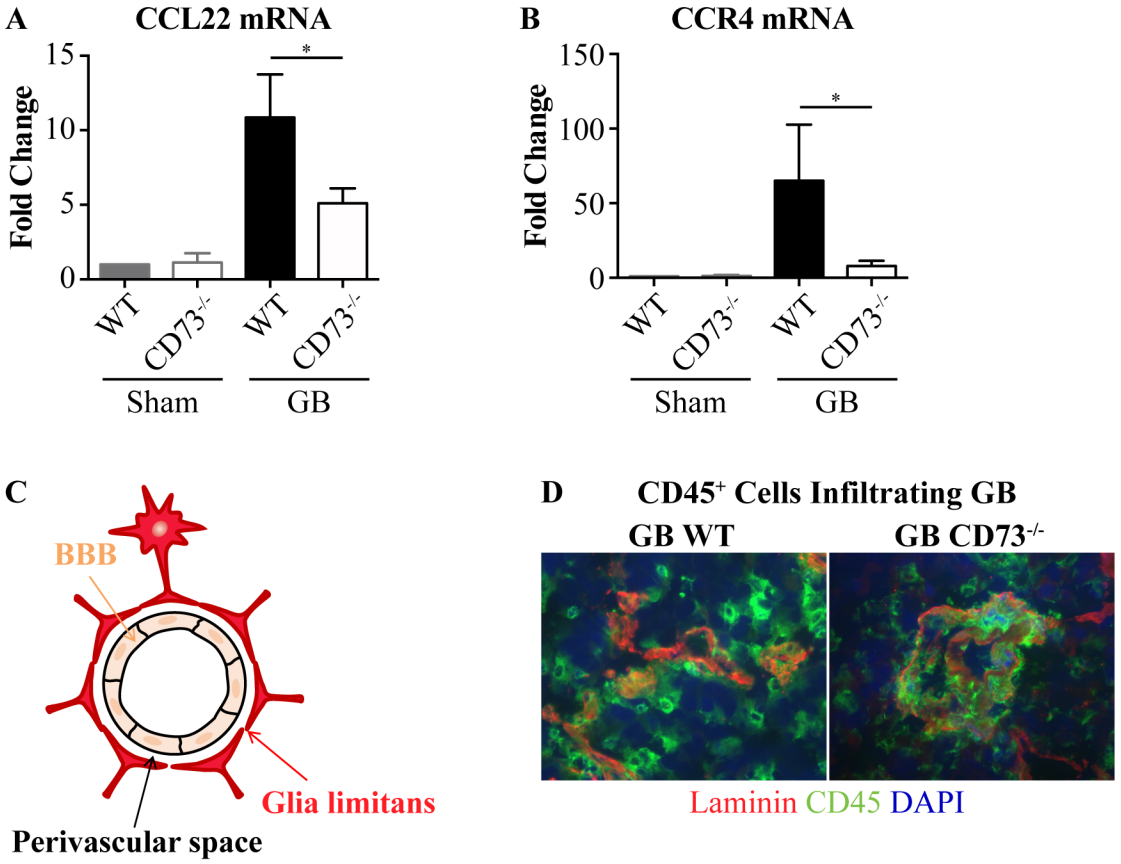
A
CCL22 mRNA
Fold Change
15
10
5
0
*
WT
CD73-/-
WT
CD73-/-
Sham
GB
B
CCR4 mRNA
Fold Change
150
100
50
0
*
WT
CD73-/-
WT
CD73-/-
Sham
GB
C
BBB
Glia limitans
Perivascular space
D
CD45+ Cells Infiltrating GB
GB WT
GB CD73-/-
Laminin CD45 DAPI
E
CD45+ Cells Trapped in the Perivascular Space
# of CD45+ Cells in the Perivascular Space/Microscopic Field
40
30
20
10
0
*
WT
CD73-/-

Figure 3.4. CD73 promotes leukocyte entry into the brain parenchyma by opening the glia limitans barrier. A, **B**, Real time-PCR quantification of CCL22 (**A**) (n = 5 for GB-bearing mice and n = 2 for sham) and CCR4 (**B**) (n = 5 for GB-bearing mice and n = 2 for sham) mRNA expression from brains of GB- or sham-implanted WT or $CD73^{-/-}$ mice, 3 weeks after implantation. **C**, Drawings demonstrating the blood-brain barrier (BBB), the glia limitans layer, and the perivascular space. **D**, Immunofluorescent staining of CD45 (green), laminin (red), and cell nuclei (blue) on frozen brain sections from GB- or sham-implanted WT or $CD73^{-/-}$ mice, 3 weeks after implantation (n = 3 – 4 for GB-bearing mice and n = 2 for sham). **E**, CD45 staining was quantified by counting the number of positively stained cells per microscopic field from 1 representative microscopic field per sample (n = 4 – 5 per group for GB-bearing mice and n = 3 per group for sham). Data represent mean ± SEM. *P ≤ 0.05, **P ≤ 0.01, ***P ≤ 0.001 (Student's two-tailed t-test).

Discussion

In this report, we found that the absence of host CD73 resulted in an increased inflammatory host immune response to GB, including reduced Treg cell recruitment, increased pro-inflammatory cytokines, and decreased anti-inflammatory cytokines. Increased cytotoxic T cell infiltration was also observed in GB-bearing $CD73^{-/-}$ mice. $CD73^{-/-}$ microglia and macrophages in GB-bearing $CD73^{-/-}$ mice adopted an M1 phenotype, which was the opposite of what was normally seen in GB immune microenvironments. We also demonstrated that $CD73^{-/-}$ macrophages were intrinsically more pro-inflammatory, as they mounted a stronger inflammatory response upon LPS treatment, and their response remained higher than that of WT macrophages even when they were co-cultured with GB cells. This shows that host CD73 promots M2 polarization in microglia and macrophages (**Figure 3.5A and D**).

Tumor-associated microglia and macrophages are critical in the anti-tumor immune response. They are two of the main producers of CCL22, which is a major chemokine that recruits Treg cells. Studies have shown that Treg cells isolated from GB patients have increased CCR4 than those from healthy controls (39). Blocking CCR4 with antibodies inhibited Treg cell migration (39). Therefore, this suggests that M1 polarization of microglia and macrophages in GB-bearing $CD73^{-/-}$ mice leads to the reduction of Treg cell recruitment because CCL22 is produced mostly by M2 microglia/macrophages (**Figure 3.5B and E**). Reduced Treg cells in the GB immune microenvironment in $CD73^{-/-}$ mice further increase the pro-inflammatory response to GB in $CD73^{-/-}$ mice.

Although a similar number of GB-infiltrating $CD45^{+}$ leukocytes were observed in WT and $CD73^{-/-}$ mice, more $CD45^{+}$ leukocytes were trapped in the perivascular space

of GB-bearing CD73$^{-/-}$ mice. This indicates that host CD73 promotes passage of leukocytes across the glia limitans barrier and entering the brain parenchyma (**Figure 3.5C and F**). GB releases factors, including M-CSF, TGFβ, PGE, IL-1, IL-10 and FGL2, to attenuate the immune response (40). Therefore, it was interesting to find that the immune responses mounted against GB in CD73$^{-/-}$ mice were not attenuated, unlike the anti-inflammatory immune responses found in GB-bearing WT mice. It is plausible that the glia limitans barrier in the GB-bearing CD73$^{-/-}$ mice partly prevented factors secreted by GB to attenuate the leukocytes trapped inside the perivascular space, allowing them to maintain their anti-GB, inflammatory properties.

Although CD73 plays an important role in regulating GB pathogenesis, the host immune response also contributes greatly to tumor development. We have shown in this report that CD73$^{-/-}$ mice mounted a much stronger inflammatory response against GB than WT mice expressing CD73. This suggested that the overall increased inflammation in the GB microenvironment in GB-bearing CD73$^{-/-}$ mice contributed to the GB size reduction. However, GB still developed in CD73$^{-/-}$ mice and was still aggressive and life threatening in the CD73$^{-/-}$ mice. This suggests that removing host CD73 and extracellular adenosine is not sufficient to completely inhibit GB growth. However, because of CD73's prominent role in regulating GB pathogenesis and the host anti-GB immune response, targeting the CD73/adenosine axis has great potential to improve GB treatment and prolong patients' life span when combined with other treatments.

Figure 3.5

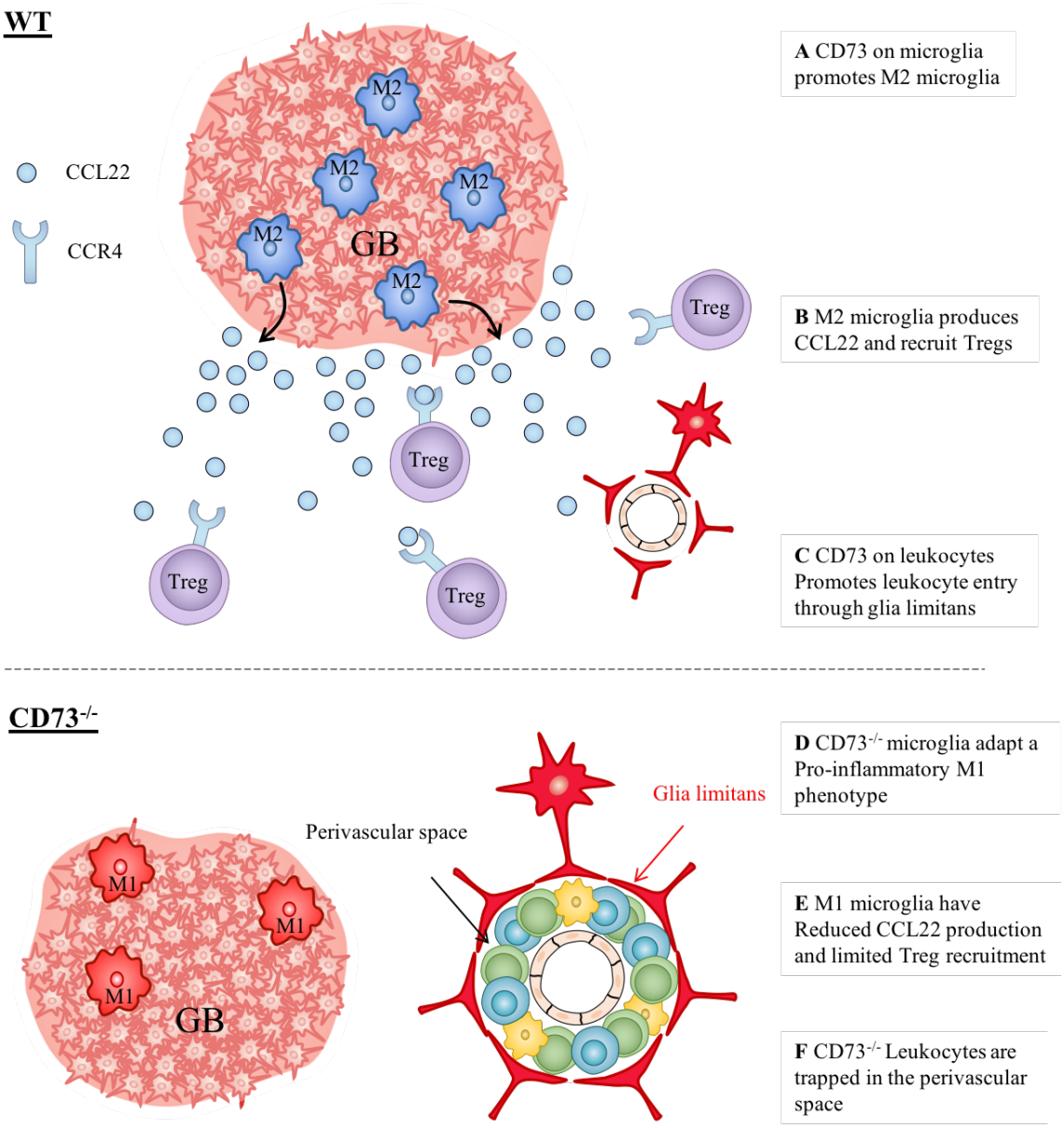
WT
CCL22
CCR4
M2
M2
M2
M2
M2
GB
Treg
Treg
Treg
Treg
A CD73 on microglia promotes M2 microglia
B M2 microglia produces CCL22 and recruit Tregs
C CD73 on leukocytes Promotes leukocyte entry through glia limitans
CD73-/-
M1
M1
M1
GB
Perivascular space
Glia limitans
D CD73-/- microglia adapt a Pro-inflammatory M1 phenotype
E M1 microglia have Reduced CCL22 production and limited Treg recruitment
F CD73-/- Leukocytes are trapped in the perivascular space

Figure 3.5. Working model describing how CD73 regulates the tumor immune microenvironment in GB. A, CD73 on microglia promotes an M2 microglia phenotype in the GB microenvironment. **B**, M2 microglia produce CCL22 and recruit Treg cells to the GB site, further attenuating the inflammatory response in the GB microenvironment. **C**, CD73 on leukocytes promotes entry to the brain parenchyma. **D**, $CD73^{-/-}$ microglia are intrinsically more pro-inflammatory and adapt an M1 microglia phenotype in the GB microenvironment. **E**, $CD73^{-/-}$ M1 microglia reduce their production of CCL22 and result in limited Treg cell recruitment, allowing the inflammatory response to continue. **F**, $CD73^{-/-}$ leukocytes are trapped in the perivascular space and cannot enter the brain parenchyma. The glia limitans layer shields them from factors secreted by GB and allows them to maintain their inflammatory state.

REFERENCES

1. Panjehpour M, Karami Tehrani F, Karami M (2003) The role of adenosine A3 receptors in cytotoxicity of the breast cancer cell lines. *Physiol Pharmacol* 7(2):115–122.

2. Haskó G, Linden J, Cronstein B, Pacher P (2008) Adenosine receptors: Therapeutic aspects for inflammatory and immune diseases. *Nat Rev Drug Discov* 7(9):759–770.

3. Bakker WW, et al. (2007) Plasma hemopexin activity in pregnancy and preeclampsia. *Hypertens Pregnancy* 26(2):227–239.

4. Crane JK, Naeher TM, Choudhari SS, Giroux EM (2005) Two pathways for ATP release from host cells in enteropathogenic Escherichia coli infection. *Am J Physiol Gastrointest Liver Physiol* 289(3):G407–G417.

5. Mizumoto N, et al. (2002) CD39 is the dominant Langerhans cell-associated ecto-NTPDase: Modulatory roles in inflammation and immune responsiveness. *Nat Med* 8(4):358–365.

6. Gerasimovskaya E, et al. (2002) Extracellular ATP is an autocrine/paracrine regulator of hypoxia-induced adventitial fibroblast growth: Signaling through extracellular signal-regulated kinase-1/2 and the Egr-1 transcription factor. *J Biol Chem* 277(47):44638–44650.

7. Ayna G, et al. (2012) ATP release from dying autophagic cells and their phagocytosis are crucial for inflammasome activation in macrophages. *PLoS One* 7(6):e40069.

8. Faas MM, Sáez T, de Vos P (2017) Extracellular ATP and adenosine: The Yin and Yang in immune responses? *Mol Aspects Med* 55:9–19.

9. Kronlage M, et al. (2010) Autocrine Purinergic Receptor Signaling Is Essential for Macrophage Chemotaxis. *Sci Signal* 3(132):ra55.

10. Iwata M, et al. (2016) Psychological stress activates the inflammasome via release of adenosine triphosphate and stimulation of the purinergic type 2X7 receptor. *Biol Psychiatry* 80(1):12–22.

11. Axtell RA, Sandborg RR, Smolen JE, Ward PA, Boxer LA (1990) Exposure of human neutrophils to exogenous nucleotides causes elevation in intracellular calcium, transmembrane calcium fluxes, and an alteration of a cytosolic factor resulting in enhanced superoxide production in response to FMLP and arachidonic acid. *Blood* 75(6):1324–1332.

12. Haskó G, et al. (2000) Adenosine inhibits IL-12 and TNF-α production via

adenosine A2a receptor-dependent and independent mechanisms. *FASEB J* 14(13):2065–2074.

13. Koscso B, et al. (2012) Adenosine Augments IL-10 Production by Microglial Cells through an A2B Adenosine Receptor-Mediated Process. *J Immunol* 188(1):445–453.

14. Koroskenyi K, et al. (2011) Involvement of Adenosine A2A Receptors in Engulfment-Dependent Apoptotic Cell Suppression of Inflammation. *J Immunol* 186(12):7144–7155.

15. Bouma MG, van den Wildenberg FA, Buurman WA (1996) Adenosine inhibits cytokine release and expression of adhesion molecules by activated human endothelial cells. *Am J Physiol* 270(2 Pt 1):C522-9.

16. Montesinos MC, et al. (2002) Adenosine promotes wound healing and mediates angiogenesis in response to tissue injury via occupancy of A2Areceptors. *Am J Pathol* 160(6):2009–2018.

17. Klabunde RE (1983) Dipyridamole inhibition of adenosine metabolism in human blood. *Eur J Pharmacol* 93(1–2):21–26.

18. Möser GH, Schrader J, Deussen A (1989) Turnover of adenosine in plasma of human and dog blood. *Am J Physiol* 256(4 Pt 1):C799–C806.

19. Xu S, et al. (2013) Synergy between the ectoenzymes CD39 and CD73 contributes to adenosinergic immunosuppression in human malignant gliomas. *Neuro Oncol* 15(9):1160–1172.

20. Stella J, et al. (2010) Differential ectonucleotidase expression in human bladder cancer. *URO* 28(3):260–267.

21. Wang L, et al. (2008) Ecto-5'-nucleotidase promotes invasion, migration and adhesion of human breast cancer cells. *J Cancer Res Clin Oncol* 134(3):365–372.

22. Wu R, et al. (2016) Effects of CD73 on human colorectal cancer cell growth in vivo and in vitro. *Oncology* 35(3):1750–1756.

23. Fukuda K, et al. (2004) Differential gene expression profiles of radioresistant oesophageal cancer cell lines established by continuous fractionated irradiation. *Br J Cancer* 91(8):1543–1550.

24. Sadej R, Spychala J, Skladanowski AC (2006) Ecto-5'-nucleotidase (eN, CD73) is coexpressed with metastasis promoting antigens in human melanoma cells. *Nucleosides Nucleotides Nucleic Acids* 25(9–11):1119–1123.

25. Turcotte M, et al. (2015) CD73 Is Associated with Poor Prognosis in High-Grade Serous Ovarian Cancer. *Cancer Res* 75(21):4494–4503.

26. Hastie C, et al. (2005) Combined affinity labelling and mass spectrometry analysis of differential cell surface protein expression in normal and prostate cancer cells. *Oncogene* 24(38):5905–5913.

27. Kondo T, Nakazawa T, Murata SI, Katoh R (2006) Expression of CD73 and its ecto-5'-nucleotidase activity are elevated in papillary thyroid carcinomas. *Histopathology* 48(5):612–614.

28. Yan A, et al. (2019) CD73 promotes glioblastoma pathogenesis and enhances its chemoresistance via A2B adenosine receptor signaling. *J Neurosci*.

29. Thompson LF, et al. (2004) Crucial role for ecto-5'-nucleotidase (CD73) in vascular leakage during hypoxia. *J Exp Med* 200(11):1395–1405.

30. Livak KJ, Schmittgen TD (2001) Analysis of Relative Gene Expression Data Using Real-Time Quantitative PCR and the 2(-Delta Delta C(T)) Method. *Methods* 25(4):402–408.

31. Fortier A, Falk L (2001) Isolation of Murine Macrophages. *Curr Protoc Immunol* Chapter 14:Unit 14.1.

32. Dello Russo C, et al. (2017) Exploiting Microglial Functions for the Treatment of Glioblastoma. *Curr Cancer Drug Targets* 17(3):267–281.

33. Charles NA, Holland EC, Gilbertson R, Glass R, Kettenmann H (2012) The brain tumor microenvironment. *Glia* 60(3):502–514.

34. Chen Z, Hambardzumyan D (2018) Immune Microenvironment in Glioblastoma Subtypes. *Front Immunol* 9:1004.

35. Matyash M, Zabiegalov O, Wendt S, Matyash V, Kettenmann H (2017) The adenosine generating enzymes CD39/CD73 control microglial processes ramification in the mouse brain. *PLoS One* 12(4):1–27.

36. Sperlágh B, Illes P (2007) Purinergic modulation of microglial cell activation. *Purinergic Signal* 3(1–2):117–127.

37. Roesch S, Rapp C, Dettling S, Herold-Mende C (2018) When Immune Cells Turn Bad — Tumor-Associated Microglia/Macrophages in Glioma. *Int J Mol Sci* 19(2):436.

38. Sun J, et al. (2016) Fucoidan inhibits CCL22 production through NF-κB pathway in M2 macrophages: a potential therapeutic strategy for cancer. *Sci Rep* 6:35855.

39. Jordan JT, et al. (2008) Preferential migration of regulatory T cells mediated by glioma-secreted chemokines can be blocked with chemotherapy. *Cancer Immunol Immunother* 57(1):123–131.

40. Nduom EK, Weller M, Heimberger AB (2015) Immunosuppressive mechanisms

in glioblastoma. *Neuro Oncol* 17(July):vii9-vii14.

CHAPTER 4

Summary, Conclusions, and Future Directions

Previous studies have shown that CD73 is overexpressed in multiple cancer cell lines and patient biopsy samples, including GB (1). Because CD73-generated extracellular adenosine is a strong anti-inflammatory molecule that signals through the A_{2A} AR on leukocytes to attenuate inflammation, it is used by cancer cells to promote tumor immune evasion (2). The ongoing interest in CD73 and adenosine lies in determining the role of CD73 and adenosine in specific cancers. This information can potentially allow us to target CD73 and/or adenosine signaling to improve cancer treatments. It has been shown that CD73 promotes breast cancer angiogenesis (3), proliferation, and metastasis (4, 5) and is associated with a worse diagnosis for patients with triple negative breast cancer (6). CD73 expression is also associated with reduced overall survival among patients and used as a poor prognosis biomarker in gastric cancer, colorectal cancer, and gallbladder cancer (7–10). However, it is still unclear how CD73 and adenosine contribute to GB pathogenesis.

In this dissertation, we demonstrated that CD73 promoted GB pathogenesis through multiple pathways. We found that CD73 was expressed on both the human and the mouse GB cell lines. When we implanted mouse GB cells in WT and $CD73^{-/-}$ mice, GB-CD73 was increased in $CD73^{-/-}$ mice compared with WT mice. This suggests that host CD73 plays a critical role in GB pathogenesis and that GB-CD73 and host CD73 had overlapping roles in GB pathogenesis. Additionally, we found that GB size and invasiveness were both decreased in $CD73^{-/-}$ mice. To test whether host CD73 promoted GB invasiveness, we generated the CD73-FLK mouse model by enforcing CD73 expression on endothelial cells in $CD73^{-/-}$ mice under the control of the *Flk-1* promoter. This allowed us to determine whether having limited host CD73 in the environment initiated GB cells to migrate from their point of implantation to gain access to the host CD73, making GB more invasive. Indeed, we found that GB was the most invasive in

CD73-FLK mice compared with GBs in CD73$^{-/-}$ and WT mice. Furthermore, GB-bearing CD73-FLK mice had a significantly reduced survival time compared to GB-bearing CD73$^{-/-}$ mice. Overall, these findings demonstrate that host CD73 promotes GB invasiveness, and that the absence of host CD73 prolongs the survival time in GB-bearing mice. In future studies, we would like to determine whether inhibiting CD73 activity using the CD73 inhibitor α,β-methylene ADP (meADP) or blocking CD73 with anti-CD73 antibodies prolongs survival in GB-bearing WT mice. If CD73 is promoting GB pathogenesis through its enzymatic activity, meADP or anti-CD73 antibody treatment will reduce GB growth and invasiveness and prolong GB-bearing mice survival.

To determine how the absence of host CD73 resulted in reduced GB growth, we analyzed whether GB angiogenesis was altered in CD73$^{-/-}$ mice. We showed that GB vessel density was significantly decreased in CD73$^{-/-}$ mice compared with WT mice, with an increase in intravascular proliferation. Furthermore, more glomeruloid vessels were found in GB-bearing CD73$^{-/-}$ mice. Because CD73 has been shown to regulate tumor angiogenesis through VEGF (11, 12), we first quantified VEFG expression in GB-bearing CD73$^{-/-}$ and WT mice. We showed that VEGF expression was upregulated in GB-bearing CD73$^{-/-}$ mice compared with GB-bearing WT mice. Because VEGF promotes endothelial cell proliferation (13, 14), this increased VEGF likely contributed to the increased intravascular proliferation observed in GB-bearing CD73$^{-/-}$ mice. To investigate why GB in CD73$^{-/-}$ had decreased vessel density despite the upregulated VEGF, we hypothesized that endothelial cells in GB-bearing CD73$^{-/-}$ mice had reduced migratory ability and that the mother vessels were not able to divide into smaller vessels, resulting in the formation of glomeruloid vessels. Therefore, we quantified the α-dystroglycan expression in GB-bearing mice. α-dystroglycan is a membrane receptor

that tethers endothelial cells to the basement membranes of vessels and limits endothelial cell migration (15, 16). We found that α-dystroglycan expression was increased in GB vessels in $CD73^{-/-}$ mice compared with those in WT mice. Increased α-dystroglycan suggests that GB endothelial cells in $CD73^{-/-}$ mice are bound to the basement membrane more tightly and resulted in the formation of glomeruloid vessels . This then suggests that host CD73 limits GB endothelial cell tethering to the extracellular matrix (ECM), which promotes mother vessels to divide and increased GB vessel density. In the absence of host CD73, increased VEGF and α-dystroglycan expression promote glomeruloid vessel formation.

Because both angiogenesis and GB invasion requires remodeling of the ECM, we next investigated the MMP activity in GB-bearing mice. MMP2 and MMP9 are both associated with GB (17, 18), and we found that MMP9 was mostly expressed along the tumor edge, while MMP2 mostly surrounded the GB vasculature. We also showed that, compared with GB-bearing WT mice, MMP activity in GB-bearing $CD73^{-/-}$ mice was decreased overall. Because α-dystroglycan digestion by MMP and remodeling of the ECM are essential steps for tumor angiogenesis, this reduction in MMP activity in GB-bearing $CD73^{-/-}$ mice potentially hindered GB angiogenesis. Furthermore, we also found the MMP9 inhibitor TIMP1 increased in GB-bearing $CD73^{-/-}$ mice, with reduced expression of TIMP1 in GB-bearing CD73-FLK mice. MMP9 expression was also increased along the tumor edge in GB-bearing CD73-FLK mice. This demonstrated a positive correlation between MMP9 activity and GB invasiveness. Overall, our findings suggest that host CD73 upregulates MMP activity in GB to promote GB angiogenesis and invasiveness. A possible future study is to identify whether MMP2 and MMP9 are generated by GB cells or by host cells in GB-bearing mice. Because it was not GB-CD73 but host CD73 that promoted MMP activity in GB-bearing mice, we hypothesize

that the host cells in the tumor microenvironment are the main producers of MMPs. A future goal will be to implant WT GB in MMP2 knockout and MMP9 knockout mice and measure GB angiogenesis, invasiveness, and MMP activity in these mice. If the host cells are the main MMP producers in GB-bearing mice, we expect to see reduced GB angiogenesis in MMP2$^{-/-}$ mice and decreased GB invasiveness in MMP9$^{-/-}$ mice at levels similar to GBs in the CD73$^{-/-}$ mice. If GB cells are the main MMP producers, GB angiogenesis and invasiveness should not be affected in MMP2$^{-/-}$ or MMP9$^{-/-}$ mice.

To elucidate whether CD73 regulates MMPs through adenosine receptor signaling, we quantified ARs expression in GB-bearing mice. We found that A_{2B} AR expression was highly upregulated in GB compared with other ARs. A_{2B} AR expression in the CNS is normally very low under physiological conditions and is only upregulated during pathological conditions (19–21). Therefore, the high A_{2B} AR expression we observed in GB suggested that it was involved in GB pathogenesis. We next investigated whether A_{2B} AR signaling was involved in regulating MMP activity. We found that A_{2B} AR signaling in GL261 mouse GB cells increased MMP2 mRNA levels, while inhibition of the A_{2B} AR decreased GL261 MMP activity. This indicated that the increased GB-CD73 in GB-bearing CD73$^{-/-}$ mice induced MMP2 expression through A_{2B} AR signaling. However, in the absence of host CD73, the overall MMP activity was decreased. This suggested that host CD73 was the main regulator of MMP activity. Host CD73 upregulated MMP9 and inhibited TIMP1 expression to promote GB invasiveness. In the absence of host CD73, GB-CD73 increased MMP2 expression but was not able to increase the overall MMP activity in GB. This indicated that increased GB-CD73 in GB-bearing CD73$^{-/-}$ mice could not fully compensate for the lack of host CD73.

Because we previously found that AR signaling regulated MDR transporters on the BBB, we next investigated whether A_{2B} AR signaling regulated MDR transporters

in GB. We showed that both P-gp and MRP1 were upregulated in GB-bearing mice, and their expression were significantly higher in GB-bearing CD73$^{-/-}$ mice than in GB-bearing WT mice. We also demonstrated that inhibiting A_{2B} AR signaling downregulated P-gp and MRP1 expression on GB cells, increased P-gp substrate Rho-123 uptake, and increased TMZ-induced cell death. We therefore concluded that A_{2B} AR signaling promoted GB chemoresistance by upregulating MDR transporters on GB. In a future experiment, we would like to knockout the A_{2B} AR in GL261-luciferase GB cells and test if A_{2B} AR$^{-/-}$ GB is be more sensitive to TMZ treatment. We will implant A_{2B} AR$^{-/-}$ GB and WT GB into WT mice and allow the tumor to develop for 2 weeks before TMZ treatment. This will allow us to monitor GB size in real-time through the luciferase activity on GB and quantify TMZ efficacy in A_{2B} AR$^{-/-}$ GB and WT GB-bearing mice. Because the A_{2B} AR regulates MDR transporters on GB, we expect to see increased TMZ sensitivity and prolonged survival in TMZ-treated mice with A_{2B} AR$^{-/-}$ GB compared with WT GB.

Because adenosine signaling through the A_{2A} AR has been shown to attenuate the immune response in cancer (2), we next investigated whether the anti-tumor immune response was stronger in the GB-bearing CD73$^{-/-}$ mice. We found a similar number of CD45^{+} tumor-infiltrating leukocytes in GB-bearing WT and CD73$^{-/-}$ mice. However, the cytokine profile in GB-bearing CD73$^{-/-}$ mice was very different from GB-bearing WT mice. We found an increase in pro-inflammatory cytokines TNF-α and IL-1β in GB-bearing CD73$^{-/-}$ mice compared with GB-bearing WT mice. Conversely, the anti-inflammatory cytokine IL-10 was significantly higher in GB-bearing WT mice compared with GB-bearing CD73$^{-/-}$ mice. Additionally, we found that, unlike GB-bearing mice, microglia and macrophages in GB-bearing CD73$^{-/-}$ mice had a pro-inflammatory phenotype. They had reduced CD206 and arginase-1 expression and

increased iNOS expression. We demonstrated that CD73$^{-/-}$ macrophages were intrinsically more pro-inflammatory compared with WT macrophages. Furthermore, we showed that GB-bearing CD73$^{-/-}$ mice had more activated CD8^{+} T cell infiltration and reduced Treg cell infiltration compared to GB-bearing WT mice. Overall, we demonstrated that host CD73 attenuated the anti-GB immune response. To elucidate whether this increased inflammatory response in GB-bearing CD73$^{-/-}$ mice is a direct result of the lack of CD73 on GB-infiltrating leukocytes, we propose implanting GB in bone marrow chimeric mice generated from CD73$^{-/-}$ and WT mice as a future study. We will transfer bone marrow from WT mice into irradiated CD73$^{-/-}$ and WT mice, and bone marrow from CD73$^{-/-}$ mice into irradiated WT mice and CD73$^{-/-}$ mice. The chimeric mice will be allowed to reconstitute for 45 days before GB implantation. Three weeks after GB implantation, we will analyze the cytokine profiles, the GB-infiltrating immune cell types, and their phenotype in the GB-bearing chimeric mice. We expect chimeric mice with CD73$^{-/-}$ bone marrow donors to have a stronger inflammatory response to GB, and we also expect chimeric mice with WT bone marrow donors to have an anti-inflammatory immune response. This is because Treg cells highly infiltrate the tumor and elicit some of their immune-attenuating functions through their surface CD73 expression (22). In the absence of CD73 expression on Treg cells, their immune-attenuating functions may be reduced. Additionally, because we found that CD73$^{-/-}$ macrophages were intrinsically more proinflammatory, chimeric mice with CD73$^{-/-}$ bone marrow donors may elicit a stronger inflammatory response.

The dramatic difference in the immune profiles between GB-bearing WT mice and GB-bearing CD73$^{-/-}$ mice led us to investigate whether Treg recruitment in GB-bearing CD73$^{-/-}$ mice was inhibited. We found that the macrophage-secreted Treg cell recruitment cytokine CCL22 and its receptor CCR4 were decreased in GB-bearing

$CD73^{-/-}$ mice compared with GB-bearing WT mice. In addition, leukocytes were trapped in the perivascular space and blocked by the glia limitans layer in GB-bearing $CD73^{-/-}$ mice. Therefore, we proposed that the more pro-inflammatory $CD73^{-/-}$ macrophages and microglia had reduced CCL22 production. This led to decreased Treg cell recruitment in GB-bearing $CD73^{-/-}$ mice and an overall increase in the anti-tumor inflammatory response. Additionally, an increase in leukocytes trapped in the perivascular space indicated that CD73 was required for leukocyte entry into the brain parenchyma. In future studies, we will identify the leukocytes trapped in the perivascular space in the GB-bearing $CD73^{-/-}$ mice and compare them with leukocytes that exited the glia limitans layer. Because GB-bearing $CD73^{-/-}$ mice elicited a stronger anti-tumor immune response, we hypothesize that leukocytes trapped in the perivascular space may be physically blocked from GB-secreted factors and thus able to better maintain their anti-tumor properties. We will separate leukocytes trapped in the perivascular space from leukocytes in the brain parenchyma through laser microdissection and identify their phenotype through flow cytometry. We expect to see more pro-inflammatory leukocytes, including M1 macrophages and cytotoxic T cells, inside the perivascular space compared with leukocytes in the brain parenchyma.

In sum, we demonstrated that CD73 and adenosine signaling are key modulators of GB pathogenesis and the anti-GB immune response. We showed that host CD73 promoted GB angiogenesis and invasiveness through the regulation of MMP activity, which critically impacted GB growth and GB-bearing mice survival time. We also showed that A_{2B} AR signaling promoted GB chemoresistance by upregulating the MDR transporters P-gp and MRP1 on GB cells. Inhibition of A_{2B} AR signaling effectively increased TMZ-induced GB cell death in vitro. Additionally, we demonstrated that host CD73 modulated the anti-GB immune response by attenuating inflammation, increasing

GB-infiltrating Treg cells, and polarizing microglia and macrophages into an anti-inflammatory phenotype. Therefore, when targeting CD73 and adenosine as a potential treatment for GB patients, it has to be taken into account that CD73 and adenosine signaling have a multi-faceted influence on GB pathogenesis and host anti-GB immune responses. Overall, our findings demonstrate that inhibition or blockade of CD73 and/or extracellular adenosine signaling pathway present great potentials for future GB therapeutic interventions.

REFERENCES

1. Gao Z, Dong K, Zhang H (2014) The Roles of CD73 in Cancer. *Biomed Res Int* 2014:460654.

2. Young A, et al. (2016) Co-inhibition of CD73 and A2AR Adenosine Signaling Improves Anti-tumor Immune Responses. *Cancer Cell* 30(3):391–403.

3. Allard B, et al. (2014) Anti-CD73 therapy impairs tumor angiogenesis. *Int J Cancer* 134(6):1466–1473.

4. Yu J, et al. (2018) Extracellular 5'-nucleotidase (CD73) promotes human breast cancer cells growth through AKT/GSK-3β/β-catenin/cyclinD1 signaling pathway. *Int J Cancer* 142(5):959–967.

5. Terp MG, et al. (2013) Anti-Human CD73 Monoclonal Antibody Inhibits Metastasis Formation in Human Breast Cancer by Inducing Clustering and Internalization of CD73 Expressed on the Surface of Cancer Cells. *J Immunol* 191(8):4165–4173.

6. Loi S, et al. (2013) CD73 promotes anthracycline resistance and poor prognosis in triple negative breast cancer. *PNAS* 110(27):11091–11096.

7. Lu X, et al. (2013) Expression and clinical significance of CD73 and hypoxia-inducible factor-1α in gastric carcinoma. *World J Gastroenterol* 19(12):1912–1918.

8. Liu NAN, Fang X (2012) CD73 as a Novel Prognostic Biomarker for Human Colorectal Cancer. *J Surg Oncol* 106(7):918–919.

9. Wu X, He X, Chen Y, Yuan R, Zeng Y (2012) High Expression of CD73 as a Poor Prognostic Biomarker in Human Colorectal Cancer. *J Surg Oncol* 106(2):130–137.

10. Xiong L, Wen Y, Miao X, Yang Z (2014) NT5E and FcGBP as key regulators of TGF-1-induced epithelial–mesenchymal transition (EMT) are associated with tumor progression and survival of patients with gallbladder cancer. *Cell Tissue Res* 355(2):365–374.

11. Ghalamfarsa G, et al. (2018) Anti-angiogenic effects of CD73-specific siRNA-loaded nanoparticles in breast cancer-bearing mice. *J Cell Physiol* 233(10):7165–7177.

12. Allard B, et al. (2014) Anti-CD73 therapy impairs tumor angiogenesis. *Int J Cancer* 134(6):1466–1473.

13. Bernatchez PN, Soker S, Sirois MG (1999) Vascular endothelial growth factor

effect on endothelial cell proliferation, migration, and platelet-activating factor synthesis is Flk-1-dependent. *J Biol Chem* 274(43):31047–31054.

14. Wang S, et al. (2008) Control of endothelial cell proliferation and migration by VEGF signaling to histone deacetylase 7. *PNAS* 105(22):7738–7743.

15. Hosokawa H, Ninomiya H, Kitamura Y, Fujiwara K, Masaki T (2002) Vascular endothelial cells that express dystroglycan are involved in angiogenesis. *J Cell Sci* 115:1487–1496.

16. Gee SH, et al. (1993) Laminin-binding protein 120 from brain is closely related to the dystrophin-associated glycoprotein, dystroglycan, and binds with high affinity to the major heparin binding domain of laminin. *J Biol Chem* 268(20):14972–14980.

17. Wang M, Wang T, Liu S, Yoshida D, Teramoto A (2003) The expression of matrix metalloproteinase-2 and-9 in human gliomas of different pathological grades. *Brain Tumor Pathol* 20(2):65–72.

18. Du R, et al. (2008) Matrix metalloproteinase-2 regulates vascular patterning and growth affecting tumor cell survival and invasion in GBM. *Neuro Oncol* 10(3):254–264.

19. Mundd SJ, Kelly E (1998) Evidence for Co-Expression and Desensitization of A2a and A2b Adenosine Receptors in NGl08-15 Cells. *Science* 55:595–603.

20. Haskó G, Csóka B, Németh ZH, Vizi ES, Pacher P (2009) A2B adenosine receptors in immunity and inflammation. *Trends Immunol* 30(6):263–270.

21. Aherne CM, Kewley EM, Eltzschig HK (2011) The resurgence of A2B adenosine receptor signaling. *Biochim Biophys Acta* 1808(5):1329–1339.

22. Haskó G, Linden J, Cronstein B, Pacher P (2008) Adenosine receptors: Therapeutic aspects for inflammatory and immune diseases. *Nat Rev Drug Discov* 7(9):759–770.

APPENDIX

SUMMARY OF ADDITIONAL PUBLICATIONS:

Non-alcoholic fatty liver disease induces signs of Alzheimer's disease (AD) in wildtype mice and accelerates pathological signs of AD in an AD model

and

Toxoplasma gondii alters NMDAR signaling and induces signs of Alzheimer's disease in wild-type, C57BL/6 mice

Alzheimer's disease (AD) is an irreversible and progressive neurodegenerative disease that leads to declined cognitive function, loss of memory, and eventually the inability to carry out daily tasks (1). The major neuropathological hallmarks of AD include senile amyloid plaques composed of β-amyloid (Aβ) protein and intracellular neurofibrillary tangles comprised of hyperphosphorylated tau protein aggregates (1). Current treatments for AD only reduce the symptoms and no cure is available. Common risk factors associated with AD include advanced age, environmental stressors, and genetic factors (2, 3). Additionally, consumption of a high-fat diet, obesity, and cholesterol-uptake receptors involved in cholesterol metabolism, such as low-density lipoprotein receptor-related protein 1 (LRP1) and apoliprotein-E (ApoE), are important risk factors contributing to the prevalence of AD (4–7). We therefore investigated non-alcoholic fatty liver disease (NAFLD)-induced liver inflammation in the pathogenesis of AD in C57/BL6 wild-type (WT) and AD transgenic mouse model (APP-Tg) mice.

We found that, during the acute phase of NAFLD, both WT and APP-Tg mice developed significant liver inflammation and pathology that coincided with increased numbers of activated microglial cells in the brain, increased inflammatory cytokine profile, and increased expression of toll-like receptors (8). Chronic NAFLD induced advanced pathological signs of AD in both WT and APP-Tg mice, and also induced neuronal apoptosis (8). We observed decreased brain expression of LRP-1, which is involved in β-amyloid clearance, in both WT and APP-Tg mice after 1 year of being on the HFD (8). Removal of mice from HFD during acute NAFLD reversed liver pathology, decreased signs of activated microglial cells and neuro-inflammation, and decreased β-amyloid plaque load (8). Our findings indicate that chronic inflammation outside of the CNS is sufficient to induce neurodegeneration and advanced pathological signs of AD in WT mice.

In addition to chronic inflammation induced by NAFLD, Toxoplasma gondii (T. gondii), which directly infects the CNS, has also been implicated as a contributor to Parkinson's disease, schizophrenia, obsessive compulsive disorder, and Tourette syndrome (9). However, little is known about the impact of T. gondii infection on neuronal cells. We infected male and female WT mice with 10 T. gondii ME49 cysts and assessed whether infection led to behavioral and anatomical effects. We show that T. gondii infection induced two major hallmarks of AD in the brains of both male and female WT mice: Aβ immunoreactivity and hyperphosphorylated Tau (10). Infected male and female mice showed significant neuronal death, loss of N-methyl-D-aspartate receptor (NMDAR) expression, and loss of olfactory sensory neurons (10). T. gondii infection also caused anxiety-like behavior, altered recognition of social novelty, altered spatial memory, and reduced olfactory sensitivity (10). This last finding was exclusive to male mice, as infected females showed intact olfactory sensitivity (10). These findings indicate that T gondii infection induces advanced pathological signs of AD in WT mice. Together, these two studies demonstrated that inflammation both in and outside of the CNS have significant neurodegenerative effects in the CNS that lead to advanced pathological signs of AD.

REFERENCES

1. Serrano-pozo A, Frosch MP, Masliah E, Hyman BT (2011) Neuropathological Alterations in Alzheimer Disease. *Cold Spring Harb Perspect Med* 1(1):a006189a006189.

2. Benilova I, Karran E, De Strooper B (2012) The toxic Aβ oligomer and Alzheimer's disease: an emperor in need of clothes. *Nat Neurosci* 15(3):349–57.

3. Suh J, et al. (2013) ADAM10 Missense Mutations Potentiate β-Amyloid Accumulation by Impairing Prodomain Chaperone Function. *Neuron* 80(2):385–401.

4. Puglielli L, Tanzi RE, Kovacs DM (2003) Alzheimer 's disease: the cholesterol connection. *Nat Neurosci* 6(5):345–351.

5. Canevari L, Clark JB (2007) Alzheimer's Disease and Cholesterol: The Fat Connection. *Neurochem Res* 32(4–5):739–750.

6. Proitsi P, et al. (2015) Plasma lipidomics analysis finds long chain cholesteryl esters to be associated with Alzheimer's disease. *Transl Psychiatry* 5(1):e494.

7. Ghareeb DA, Hafez HS, Hussien HM, Kabapy NF (2011) Non-alcoholic fatty liver induces insulin resistance and metabolic disorders with development of brain damage and dysfunction. *Metab Brain Dis* 26(4):253–267.

8. Kim DG, et al. (2016) Non-alcoholic fatty liver disease induces signs of Alzheimer's disease (AD) in wild-type mice and accelerates pathological signs of AD in an AD model. *J Neuroinflammation* 13(1):1.

9. Mcconkey GA, Martin HL, Bristow GC, Webster JP (2013) Toxoplasma gondii infection and behaviour - Location, location, location? *J Exp Biol* 216(Pt 1):113–119.

10. Torres L, et al. (2018) Toxoplasma gondii alters NMDAR signaling and induces signs of Alzheimer's disease in wild-type, C57BL/6 mice. *J Neuroinflammation* 15(1):1–19.